รายงานวิจัยฉบับสมบูรณ์

โครงการ “การศึกษาบทบาทของวิตามินดี 3 ในรูปแอ๊คทีฟฟอร์ม [1α,25$(OH)_2D_3$] ต่อการควบคุมการทำงานของเซลล์ต้นกำเนิดของกล้ามเนื้อลาย, การสังเคราะห์โปรตีน และการทำงานของกล้ามเนื้อในขณะฟื้นฟูสภาพจากการบาดเจ็บ”

โดย ผศ.ดร. รัชกฤต ศรีเกื้อ

ธันวาคม 2558

สัญญาเลขที่ MRG5680061

รายงานวิจัยฉบับสมบูรณ์

โครงการ “การศึกษาบทบาทของวิตามินดี 3 ในรูปแอ๊คทีฟฟอร์ม [1α,25$(OH)_2D_3$] ต่อการควบคุมการทำงานของเซลล์ต้นกำเนิดของกล้ามเนื้อลาย, การสังเคราะห์โปรตีน และการทำงานของกล้ามเนื้อในขณะฟื้นฟูสภาพจากการบาดเจ็บ”

ผศ.ดร. รัชกฤต ศรีเกื้อ มหาวิทยาลัยมหิดล

สนับสนุนโดยสำนักงานกองทุนสนับสนุนการวิจัย

บทคัดย่อ

Project Code : MRG5680061

Project Title : การศึกษาบทบาทของวิตามินดี 3 ในรูปแอ๊คทีฟฟอร์ม [1α,25$(OH)_2D_3$] ต่อการควบคุมการทำงานของเซลล์ต้นกำเนิดของกล้ามเนื้อลาย, การสังเคราะห์โปรตีน และการทำงานของกล้ามเนื้อในขณะฟื้นฟูสภาพจากการบาดเจ็บ

Investigator : ผศ.ดร. รัชกฤต ศรีเกื้อ มหาวิทยาลัยมหิดล

E-mail Address : ratchakrit.sri@mahidol.ac.th

Project Period : 2 ปี (ได้รับการอนุมัติขยายระยะเวลาโครงการเพิ่มอีก 6 เดือน)

การค้นพบตัวรับสัญญาณการทำงานของวิตามินดี 3 (VDR) ในกล้ามเนื้อลายที่กำลังฟื้นฟูสภาพเมื่อไม่นานมานี้ ทำให้เกิดคำถามเกี่ยวกับบทบาทของวิตามินดี 3 ว่ามีความเกี่ยวข้องกับการฟื้นฟูสภาพของกล้ามเนื้อลายอย่างไร เพื่อศึกษาถึงบทบาทของวิตามินดี 3 ต่อกระบวนการดังกล่าว กล้ามเนื้อลายบริเวณหน้าแข้ง (tibialis anterior) ของหนูเมาส์เพศผู้ สายพันธุ์ C57BL/6 อายุ 10 สัปดาห์ ได้ถูกทำให้บาดเจ็บด้วย 1.2% $BaCl_2$ หลังจากนั้นวิตามินดี 3 ในรูปแอ๊คทีฟฟอร์ม [1α,25$(OH)_2D_3$] ได้ถูกฉีดเข้ากล้ามเนื้อลายที่มีการบาดเจ็บในขณะฟื้นฟูสภาพ (วันที่ 4-7 ภายหลังการบาดเจ็บ) โดยใช้ความเข้มข้น 2 ระดับในการศึกษา ได้แก่ 1 µg/kg ต่อน้ำหนักกล้ามเนื้อหรือน้ำหนักตัวของสัตว์ทดลอง ตัวอย่างกล้ามเนื้อสำหรับการวิเคราะห์ได้ถูกเก็บภายหลังจากการบาดเจ็บเป็นระยะเวลา 8 วัน เพื่อศึกษาการเปลี่ยนแปลงของโปรตีนที่เกี่ยวข้องกับเมแทบอลิซึมของวิตามินดี 3 (VDR, CYP24A1 และ CYP27B1), การทำงานของเซลล์ต้นกำเนิดของกล้ามเนื้อลายและการสร้างเส้นใยกล้ามเนื้อลายขึ้นมาใหม่ (myogenin และ EbMHC), กระบวนการสังเคราะห์โปรตีน (Akt, p70 S6K1, 4E-BP1 และ myostatin), ชนิดของเส้นใยกล้ามเนื้อลาย (fast MHC และ slow MHC), ปริมาณเนื้อเยื่อเกี่ยวพัน (vimentin) และปริมาณหลอดเลือด (CD31) ซึ่งปัจจัยทั้งหมดส่งผลต่อการทำงานของกล้ามเนื้อลายในขณะฟื้นฟูสภาพจากการบาดเจ็บ จากการศึกษาพบว่าการฉีด 1α,25$(OH)_2D_3$ เข้าไปที่กล้ามเนื้อลายที่กำลังฟื้นฟูสภาพสามารถเพิ่มการแสดงออกของ VDR ได้ทั้ง 2 ความเข้มข้นที่ทดสอบ โดยการเพิ่มขึ้นของโปรตีน CYP24A1 และ vimentin รวมถึงการลดลงของโปรตีน myogenin และ EbMHC ถูกพบเฉพาะเมื่อได้รับ 1α,25$(OH)_2D_3$ ที่ความเข้มข้นต่อน้ำหนักตัวของสัตว์ทดลองเท่านั้น ซึ่งผลด้านการยับยั้งโปรตีน myogenin และ EbMHC ได้ถูกยืนยันด้วยการทดสอบในหลอดทดลองกับเซลล์กล้ามเนื้อลายเพาะเลี้ยง (C2C12 myotubes) อย่างไรก็ตามไม่พบการเปลี่ยนแปลงของโปรตีน CYP27B1, Akt, p70 S6K1, 4E-BP1, myostatin, fast MHC, slow MHC หรือ CD31 แต่อย่างใดในทั้ง 2 ความเข้มข้นที่ทดสอบ จากผลการวิจัยข้างต้นสามารถสรุปได้ว่าการทำงานของ 1α,25$(OH)_2D_3$ ต่อกระบวนการฟื้นฟูสภาพของกล้ามเนื้อลายขึ้นอยู่กับระดับความเข้มข้น โดยความเข้มข้นที่ระดับ 1 µg/kg ต่อน้ำหนักตัวของสัตว์ทดลองนั้นสามารถส่งผลยับยั้งการทำงานของเซลล์ต้นกำเนิดของกล้ามเนื้อลายและการสร้างเส้นใยกล้ามเนื้อลายขึ้นมาใหม่ รวมถึงส่งผลให้เกิดการสร้างเนื้อเยื่อเกี่ยวพันที่มากกว่าปกติ อย่างไรก็ตามการได้รับ 1α,25$(OH)_2D_3$ ไม่มีผลต่อกระบวนการสังเคราะห์โปรตีน, ชนิดของเส้นใยกล้ามเนื้อลาย และการปริมาณของหลอดเลือดที่สร้างขึ้นมาใหม่แต่อย่างใด

คำสืบค้น : วิตามินดี 3, การฟื้นฟูสภาพของกล้ามเนื้อลาย, การฉีดสารเข้ากล้ามเนื้อลาย, การเกิดพังผืด, การสร้างหลอดเลือด

Abstract

Project Code : MRG5680061

Project Title : An investigation on the effect of bioactive form of vitamin D_3 [1α,25$(OH)_2D_3$] on the regulation of satellite cell activity, protein synthesis, and muscle function during muscle regeneration

Investigator : Asst. Prof. Dr. Ratchakrit Srikuea (Mahidol University)

E-mail Address : ratchakrit.sri@mahidol.ac.th

Project Period : 2 years (6 months extension was approved)

The recent discovery of the vitamin D receptor (VDR) in regenerating muscle raises the question regarding the action of vitamin D_3 on skeletal muscle regeneration. To investigate the action of vitamin D_3 on this process, tibialis anterior (TA) muscle of male C57BL/6 mice (10 week of age) was injected with 1.2% $BaCl_2$ to induce extensive muscle injury. The bioactive form of vitamin D3 [1α,25$(OH)_2D_3$] was administered daily via intramuscular injections during regenerative phase (day 4-7 post-injury). Two doses of 1α,25$(OH)_2D_3$ at 1 μg/kg muscle wet weight (MW) and mouse body weight (BW) were investigated. Muscle samples were collected on day 8 post-injury to examine proteins related to vitamin D_3 metabolism (VDR, CYP24A1, and CYP27B1), satellite cell differentiation and regenerative muscle fiber formation (myogenin and EbMHC), protein synthesis signaling (Akt, p70 S6K1, 4E-BP1, and myostatin), fiber type composition (fast and slow MHCs), fibrous formation (vimentin), and angiogenesis (CD31). Administration of 1α,25$(OH)_2D_3$ at MW and BW doses increased VDR in regenerative muscle. Increased CYP24A1 and vimentin expression accompany decreased myogenin and EbMHC expression at the BW dose of 1α,25$(OH)_2D_3$. The suppressive effect of 1α,25$(OH)_2D_3$ on myogenin and EbMHC expression was confirmed in C2C12 myotubes. However, there was no change in CYP27B1, Akt, p70 S6K1, 4E-BP1, myostatin, fast and slow MHCs, or CD31 expression at any dose investigated. Taken together, there was a dose-dependent effect of 1α,25$(OH)_2D_3$ on skeletal muscle regeneration. Administration of 1α,25$(OH)_2D_3$ at BW dose resulted in decreased satellite cell differentiation, delayed regenerative muscle fiber formation, and increased muscular fibrosis. However, protein synthesis signaling, fiber type composition, and angiogenesis were not affected by 1α,25$(OH)_2D_3$ administration.

Keywords : vitamin D_3, muscle regeneration, intramuscular injection, muscular fibrosis, angiogenesis

Executive Summary

Vitamin D_3 is a pleiotropic hormone that has a broad range of physiological functions. Besides regulation of calcium homeostasis, various studies reported an action of the bioactive form of vitamin D_3 [$1\alpha,25(OH)_2D_3$] on noncalcemic functions, i.e. controlling cell proliferation, differentiation, and apoptosis. The action of $1\alpha,25(OH)_2D_3$ requires binding to the vitamin D receptor (VDR) in order to initiate downstream cascades and modulate gene transcription. Besides regulation of calcemic genes, myogenic and muscle phenotypic genes can be modulated in responses to $1\alpha,25(OH)_2D_3$. Moreover, two major enzymes regulating vitamin D_3 metabolism, CYP27B1 and CYP24A1, were expressed in skeletal muscle cells. Expression of the VDR and vitamin D_3 metabolizing enzymes in skeletal muscle cells suggest the possible local regulation of vitamin D_3 on this extrarenal tissue. Recently, substantial VDR protein expression in regenerative muscle was discovered that in contrast to the barely detectable level in normal muscle. This finding raised a major question regarding to the potential role of $1\alpha,25(OH)_2D_3$ on the regulation of skeletal muscle regenerative capacity.

Skeletal muscle regeneration is a self-repairing process following muscle injury. This process involves the activity of resident skeletal muscle stem cells (satellite cells) that are located between the basement membrane and basal lamina of muscle fibers. The efficiency of the regenerative process requires sufficient myoblast-derived satellite cell number, effectiveness of myoblast fusion and differentiation, and a rapid increase in the rate of protein synthesis. In addition, connective tissue formation and angiogenesis act as contributing factors to determine skeletal muscle regenerative capacity. Excess connective tissue formation (fibrous formation) and defect of revascularization after muscle injury can delay regenerative process. Unfortunately, an investigation on the direct action of $1\alpha,25(OH)_2D_3$ on during skeletal muscle regeneration has not been demonstrated. Therefore, the aim of this study was designed to test the direct effects of $1\alpha,25(OH)_2D_3$ on regenerative capacity, muscular fibrosis, and angiogenesis during skeletal muscle regeneration.

In this study, tibialis anterior muscle of adult male C57BL/6 mice (10 weeks of age) were injected intramuscularly with 1.2% $BaCl_2$ to induce extensive muscle injury. Intramuscular injection of two different doses of $1\alpha,25(OH)_2D_3$ (1 μg/kg relative to muscle wet weight and mouse body weight) at regenerative phase was investigated to test the dose

dependent effects of 1α,25$(OH)_2D_3$ on skeletal muscle regeneration. Muscle samples were collected to examine proteins related to vitamin D_3 metabolism, satellite cell differentiation and regenerative muscle fiber formation, protein synthesis signaling, fiber type composition, fibrous formation, and angiogenesis. The expression levels of protein investigated were examined by immunohistochemistry and Western blot analysis. Regenerative muscle fiber size was determined by histochemical analysis. The effects of 1α,25$(OH)_2D_3$ on the expression of vitamin D_3 regulating enzyme, skeletal muscle cell differentiation, and myotube formation were confirmed *in vitro* study with mouse muscle cell line (C2C12).

The results demonstrated that administration of 1α,25$(OH)_2D_3$ increase VDR protein expression in regenerative muscle. However, increased vitamin D_3 catabolizing enzyme (CYP24A1), decreased satellite cell differentiation, delayed regenerative muscle fiber formation, and increased muscular fibrosis were evident only 1α,25$(OH)_2D_3$ was administrated at mouse body weight dose. Furthermore, protein synthesis signaling, fiber type composition, and angiogenesis were not affected by 1α,25$(OH)_2D_3$ administration at any dose investigated. These finding suggest there was a dose-dependent effect of 1α,25$(OH)_2D_3$ on skeletal muscle regeneration. The novelty of this work is the finding of non-calcemic functions of 1α,25$(OH)_2D_3$ on regenerative capacity and muscular fibrosis during skeletal muscle regeneration. The results of the present study provide a significant contribution to the field regarding knowledge of the physiological functions of the bioactive form of vitamin D_3 and vitamin D_3 metabolizing enzymes on the regenerative process of skeletal muscle.

Research Contents

Introduction

Vitamin D_3 (cholecalciferol) is a steroid hormone that is essential for calcium homeostasis (Lips, 2006). Furthermore, a broad range of physiological non-calcemic functions of vitamin D_3 have been reported i.e., controlling cell proliferation, differentiation, and apoptosis (Samuel and Sitrin, 2008). The metabolism of vitamin D_3 from precursor to its bioactive form to initiate its action on the target tissue requires multiple steps. Briefly, synthesis of vitamin D_3 occurs in the skin after the vitamin D_3 precursor (7-dehydrocholesterol) is exposed to sun light to form cholecalciferol. Cholecalciferol is hydroxylated in the liver to form 25(OH)D_3 (calcidiol). 25(OH)D_3 is further hydroxylated via 1-α hydroxylase, a cytochrome P450 containing-hydroxylase encoded by *cyp27b1* gene, in the kidney to produce the bioactive form of vitamin D3, 1α,25$(OH)_2D_3$ (calcitriol). The concentration of 1α,25$(OH)_2D_3$ is regulated by the action of the vitamin D_3 catabolizing enzyme, which is encoded by *cyp24a1* gene, to convert 1α,25$(OH)_2D_3$ to the inactive metabolite calcitroic acid (Reviewed: Prosser and Jones, 2004).

The action of 1α,25$(OH)_2D_3$ requires binding to the vitamin D receptor (VDR) in order to initiate downstream cascades and modulate gene transcription. VDR is localized as a nuclear receptor and acts as a transcription factor that recognizes cognate vitamin D response elements (VDREs) in more than 3,000 target genes in the mouse genome (Wang *et al*., 2005). In addition to calcemic regulatory genes, myogenic regulatory genes (Myf5, MyoD, myogenin, and myostatin) (Endo *et al*., 2003; Garcia *et al*., 2011; Girgis *et al*., 2014a) and muscle phenotypic genes (myosin heavy chain; MHC isoform) (Endo *et al*., 2003; Garcia *et al*., 2011; Okuno *et al*., 2012) were modulated in responses to 1α,25$(OH)_2D_3$ treatment. The action of 1α,25$(OH)_2D_3$ on skeletal muscle cells and tissue was supported by the presence of VDR protein in a mouse muscle cell line (C2C12) (Garcia *et al*. 2011; Srikuea *et al*., 2012; Girgis *et al*., 2014a), rodent skeletal muscle (Endo *et al*., 2003; Srikuea *et al*., 2012; Stratos *et al*., 2013; Makanae *et al*., 2015), human primary myoblasts (Pojednic *et al*., 2015a; Olsson *et al*., 2015), and human skeletal muscle (Bischoff *et al*., 2001; Bischoff-Ferrari *et al*., 2004; Pojednic *et al*., 2015b). Moreover, two major enzymes regulating vitamin D_3 metabolism, CYP27B1 and CYP24A1, were also expressed in C2C12 cells and mouse primary myotubes

(Girgis *et al*., 2014b). Taken together, expression of the VDR and vitamin D_3 metabolizing enzymes in skeletal muscle suggest the possible local regulation of vitamin D_3 on this extrarenal tissue.

The presence of VDR protein in regenerative muscle, as demonstrated by immunohistochemistry (Srikuea *et al*., 2012) and Western blot analysis (Stratos *et al*., 2013), raised a major question regarding to the potential role of $1\alpha,25(OH)_2D_3$ on the regulation of skeletal muscle regenerative capacity. Skeletal muscle regeneration is a self-repairing process following muscle injury. This process involves the activity of resident skeletal muscle stem cells (satellite cells) that are located between the basement membrane and basal lamina of muscle fibers (Mauro, 1961). Satellite cells are unipotent and can differentiate to form muscle fibers in addition to self-renewal (Relaix and Zammit, 2012). Under normal conditions, satellite cells are quiescent but can become active, proliferating and differentiating after injury to repair damaged muscle fibers or generate new muscle fibers (Hawke and Garry, 2001). After activation, satellite cells express transcription factors that can be used to identify the stages of their activity, i.e. MyoD, Myf5, Myf6 (activation, proliferation, and differentiation) and myogenin (differentiation) (Shi and Garry, 2006). Currently, the satellite cell population can be determined by the expression of specific transcription factor; Pax7 (Seale *et al*., 2000). The central nuclei derived from satellite cell fusion in regenerating muscle fibers are a hallmark of muscle regeneration. These newly formed muscle fibers after muscle injury can be characterized by the expression of embryonic myosin heavy chain (EbMHC) (Melcon *et al*., 2006).

The efficiency of the regenerative process requires sufficient myoblast-derived satellite cell number, effectiveness of myoblast fusion and differentiation, and a rapid increase in the rate of protein synthesis. The suppressive effects of $1\alpha,25(OH)_2D_3$ on myogenic cells have been reported in various studies on myoblast proliferation (Garcia *et al*. 2011; Srikuea *et al*., 2012; Girgis *et al*., 2014a) and myotube formation (Garcia *et al*. 2011; Girgis *et al*., 2014a). Although its effect leads to a decrease in myotube number, an increase in myotube size in vitro has been reported (Garcia *et al*. 2011; Girgis *et al*., 2014a). In addition, treatment with $1\alpha,25(OH)_2D_3$ in combination with insulin and leucine increased the phosphorylation of Akt/mTOR pathway suggesting an anabolic effect in skeletal muscle cells (Salles *et al*., 2013). An impaired muscle fiber regenerative response occurs when mTOR is inhibited after muscle

injury (Ge *et al*., 2009); however, the direct effect of $1\alpha,25(OH)_2D_3$ on Akt/mTOR pathway activation in regenerative muscle has not been investigated. Only one investigation reported an effect of vitamin D_3 on muscle regeneration using a crush injury model (Stratos *et al*., 2013). Administration of activated 7-dehydrocholesterol via subcutaneous administration to the rats immediately after contusion induced-muscle injury leads to partial restoration of muscle function. However, VDR protein expression and satellite cell activity did not changes in response to activated 7-dehydrocholesterol administration. Furthermore, an investigation on the direct action of the bioactive form of vitamin D_3, $1\alpha,25(OH)_2D_3$, on skeletal muscle regeneration has not been investigated.

Connective tissue formation and angiogenesis act as contributing factors to determine skeletal muscle regenerative capacity. Increased fibroblast proliferation and collagen production after activated 7-dehydrocholesterol administration has been demonstrated (Stratos *et al*., 2013). However, a single dose of activated 7-dehydrocholesterol immediately after muscle injury leads to an increased serum $25(OH)D_3$ that suppressed $1\alpha,25(OH)_2D_3$ serum level. This leaves the direct action of $1\alpha,25(OH)_2D_3$ on regulation of connective tissue formation/muscular fibrosis in regenerative muscle still unanswered. Moreover, the effect of $1\alpha,25(OH)_2D_3$ on pro-angiogenic growth factors and angiogenic inhibition was recently discovered (Garcia *et al*., 2013). Treatment of $1\alpha,25(OH)_2D_3$ to C2C12 myoblasts increased vascular endothelial growth factor A (VEGF-A) and fibroblast growth factor-1 (FGF-1) while suppressing FGF-2 and tissue inhibitor of matrix metalloproteinases-3 (TIMP-3). However, this study was conducted *in vitro* demonstrating a need to clarify $1\alpha,25(OH)_2D_3$ action on angiogenesis during skeletal muscle regeneration *in vivo*.

Objectives

The aim of this study was designed to test the direct effects of $1\alpha,25(OH)_2D_3$ on regenerative capacity, muscular fibrosis, and angiogenesis during skeletal muscle regeneration.

Research Methodology

Adult male C57BL/6 mice were obtained from the National Laboratory Animal Centre, Salaya, Nakhon Pathom, Thailand. All animal procedures were performed in accordance with institutional guidelines for the care and use of laboratory animals as approved by the Ethics Committee on the Use of Experimental Animals, Faculty of Science, Mahidol University, Thailand (Protocol no. MUSC56-005-267).

$BaCl_2$-induced muscle injury

C57BL/6 mice (10 weeks of age) were anesthetized by inhalation with isoflurane gas prior injury induction. Left and right tibialis anterior (TA) muscles were injected intramuscularly with 50 µl of 1.2% $BaCl_2$ dissolved in sterile PBS to induce extensive muscle injury. Mouse TA muscle was illustrated in Fig. 1.

Fig. 1 Mouse TA muscle in this study. The location of TA muscle that was injected with 1.2% $BaCl_2$ solution to induce extensive muscle injury (arrow).

Intramuscular 1α,25$(OH)_2D_3$ administration

Mice were randomly assigned in to one of three groups (n=6/group): control group, injury + 1α,25$(OH)_2D_3$ (dose 1 µg/kg relative to TA muscle wet weight; MW) group, and injury + 1α,25$(OH)_2D_3$ (dose 1 µg/kg relative to mouse body weight; BW) group. Two doses of 1α,25$(OH)_2D_3$ were used in this study to determine the dose dependent effect of 1α,25$(OH)_2D_3$ on skeletal muscle regenerative capacity, muscular fibrosis, and angiogenesis. 1α,25$(OH)_2D_3$ (Cayman Chemical Inc., 71820) was administered daily via intramuscular injection to the left injured TA muscle on days 4-7 post-injury (Fig. 2). The right injured TA served as contralateral injured muscle and was administrated a vehicle treatment. The

administration period of 1α,25(OH)$_2$D$_3$ represents the phase of muscle regeneration that involves satellite cell differentiation, rapid increases in protein synthesis, regenerative muscle fiber formation, extracellular matrix remodeling, and revascularization.

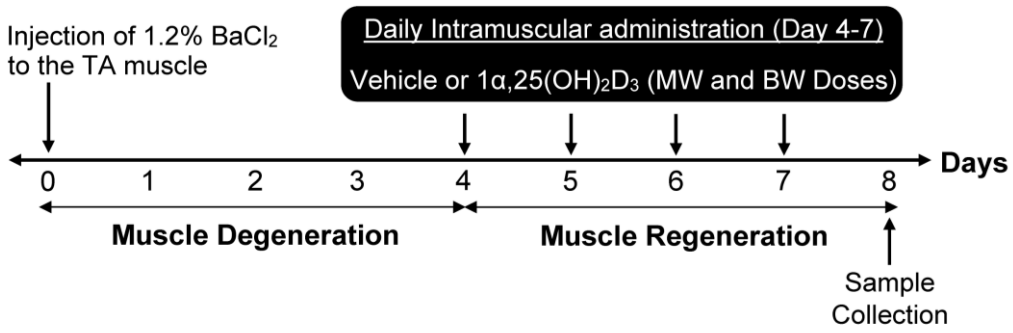

Fig. 2 Experimental diagram of intramuscular administration of vehicle and 1α,25(OH)$_2$D$_3$ during skeletal muscle regeneration. Vehicle and 1α,25(OH)$_2$D$_3$ at MW and BW doses were administered daily via intramuscular injections during day 4 to 7 post-injury. This administration period represents the regenerative phase.

Muscle wet weight/body weight ratio

On day 8 post-injury, injured TA muscles from either vehicle- or 1α,25(OH)$_2$D$_3$-administrated were dissected and weighed using digital weight scale to within ± 0.001 mg (Mettler Toledo, MS204S). Immediately after dissection, excess fluid was removed with filter paper. TA muscle wet weight (mg) was measured, normalized to mouse body weight (g), and recorded as muscle wet weight to body weight ratio.

Western blot analysis

Muscle samples were homogenized in ice-cold homogenizing buffer containing 50 mM Tris pH 7.5, 150 mM NaCl, 1 mM EDTA, 1% Triton X-100 supplemented with protease inhibitor cocktail (Sigma, P8340) (1:100) and phosphatase inhibitor cocktail (Calbiochem, 524625) (1:100). Muscle homogenates were centrifuged at 1,500 g for 10 min at 4^{o}C to separate cytosolic and myofibrillar fractions. The cytosolic fraction was further centrifuged at 10,000 g for 10 min at 4^{o}C and the supernatant portion was collected. To remove debris in myofibrillar fraction, pellets were suspended in the same ice-cold homogenizing buffer and centrifuged at 1,500 g for 10 min × 3 (4°C). Thereafter, the insoluble pellet was re-suspended with 0.5 M NaOH in 50 mM Tris-HCl, pH 7.5. Protein concentrations were determined by BCA

assay in triplicate measurements. Under a reducing condition, 40 µg of cytosolic protein and 10 µg myofibrillar protein fractions containing sample buffer solution were denatured by heating at 60^{o}C for 10 min. The protein samples were loaded into SDS-polyacrylamide gel (5% stacking and 8-10% separating gels), and then transferred to a PVDF membrane (Millipore, IPVH-00010). The membrane was blocked with 5% non-fat milk (Bio-Rad, 1706404XTU), and probed with primary antibodies. The cytosolic proteins were incubated overnight with the following primary antibodies; VDR (D-6) (Santa Cruz Biotechnology sc-13133, 1:200), CYP24A1 (Santa Cruz Biotechnology SC-66851, 1:200), CYP27B1 (Santa Cruz Biotechnology SC-67261, 1:200), myogenin (Santa Cruz Biotechnology SC-12732, 1:200), myostatin (Santa Cruz Biotechnology SC-393335, 1:200), vimentin (Santa Cruz Biotechnology SC-32322, 1:200), CD31 (Abcam ab28364, 1:500), phospho-p70 S6K1 Thr389 (Cell signaling 9206, 1:1,000), p70 S6K1 (Cell signaling 2708, 1:1,000), phospho-4E-BP1 (Cell signaling 9451, 1:1,000), 4E-BP1 (Cell signaling 9644, 1:1,000), phospho-Akt Ser473 (Cell signaling 4060, 1:1,000), and Akt Ser473 (Cell signaling 2967, 1:2,000). However, the myofibrillar protein were incubated with the following primary antibodies including fast MHC (Abcam ab91506, 1:2,000), slow MHC (Abcam ab11083, 1:2,000), and EbMHC (Santa Cruz Biotechnology SC-53091, 1:500). Particularly, fast MHC and slow MHC antibodies also applied with cytosolic protein fraction to determine soluble pool of MHCs. Thereafter, the membrane was incubated with appropriate horseradish peroxidase (HRP) conjugated secondary antibodies. Protein bands were visualized with chemiluminescence HRP detection reagent (Millipore, WBLUR0100) and exposed to CL-XPosure film (Thermo Scientific, PIE34090). Band density was analyzed with ImageJ software version 1.44p [National Institutes of Health (NIH), Bethesda, MD]. Cytosolic protein expression was normalized to GAPDH (Millipore AB2302, 1:5,000), except phospho-p70 S6K1 Thr389, phospho-4E-BP1, and phospho-Akt Ser473 which were normalized to their total proteins. Myofibrillar protein expression was normalized with amount of loading protein as determined by Ponceau S staining.

Histological analysis

The frozen muscle samples were sectioned at 10 µm thickness with cryostat (Leica, Model CM1850). To determine cross-sectional area (CSA) of regenerative muscle fibers, the muscle sections were stained with hematoxylin and eosin to visualize the presence of central

nucleated regenerative muscle fibers that represents the hallmark of muscle regeneration. Representative images were taken at 200× magnification with Olympus microscope BX53 (Olympus, Japan). Six images were randomly captured using cellSens Dimension version 1.81 software (Olympus, Japan) for quantitative analysis. Regenerative muscle fiber CSA was quantified using ImageJ software version 1.44p as illustrated in Fig. 3.

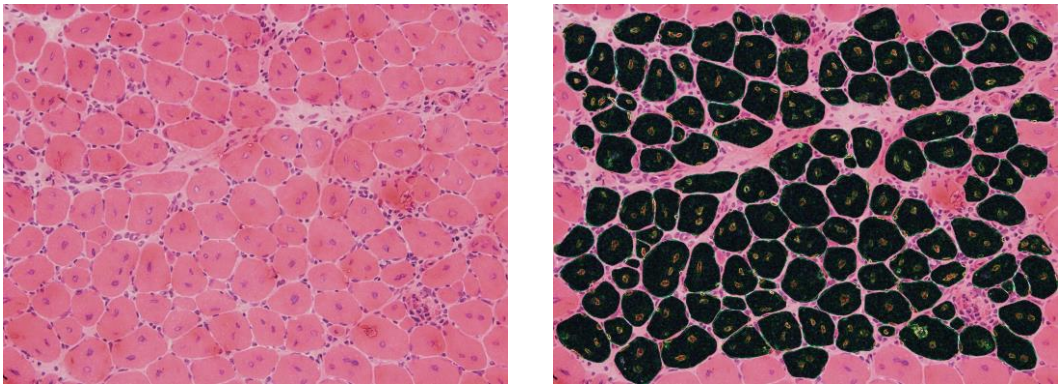

Original Captured Image **Analyzed Image**

Fig. 3 Representative images of regenerative muscle fiber CSA that was quantified with ImageJ software. Individual regenerative muscle fiber with the presence of central nuclei was manually quantified as demonstrated by the dark contour. Left and right images represent original captured image and analyzed image, respectively.

Immunohistochemical analysis

The serial sections at 10 μm thickness were used to investigate the changes of VDR, CYP24A1, CYP27B1, ATP synthase (complex V) subunit alpha (OxPhos) (Invitrogen, 1IV13-45-9240), Pax7 (R&D systems MAB1675), myogenin, EbMHC, fast MHC, slow MHC, vimentin, and CD31 protein expression using immunofluorescence staining. All subsequent steps were performed at room temperature except as noted. Briefly, VDR, CYP24A1, CYP27B1, ATP synthase (complex V) subunit alpha (OxPhos), Pax7, myogenin, and vimentin-stained sections were pre-fixed with 4% paraformaldehyde (PFA) from 10 min. In contrast, CD31-stained sections were pre-fixed with ice-cold acetone for 10 min while fast MHC, slow MHC, and EbMHC-stained section were unfixed at this step. For nuclear localization proteins (VDR, Pax7, and myogenin), the sections were permeabilized with 0.5% Triton X-100 for 5 min. Then, the sections were blocked with mouse IgG blocking reagent

(Vector Labs, MKB-2213) for 1 h followed with 10% normal goat serum (Invitrogen, PCN5000) for 1 h. Primary antibodies were incubated overnight at 4^{o}C and dilution used for immunohistochemical analysis were listed as follows: mouse monoclonal VDR (D-6) (1:50), rabbit polyclonal VDR (H-81) (1:50), rabbit polyclonal CYP24A1 (1:50), rabbit polyclonal CYP27B1 (1:50), mouse monoclonal ATP synthase (complex V) subunit alpha (OxPhos) (1:200), mouse monoclonal myogenin (1:50), rabbit polyclonal fast MHC (1:1,000), mouse monoclonal slow MHC (1:2,000), mouse monoclonal EbMHC (1:100), mouse monoclonal vimentin (1:100), and rabbit polyclonal CD31 (1:100). Rabbit polyclonal laminin antibody (Sigma L9393, 1:400) was used to visualize regenerative muscle fiber structure. Thereafter, the sections were incubated with goat anti-mouse Alexa 568 (Invitrogen A-11004, 1:500) and goat anti-rabbit Alexa 488 (Invitrogen A-11008, 1:500) for 1 h in the dark. Fast MHC, slow MHC, and EbMHC-stained sections were post-fixed with 4% PFA for 10 min. All stained sections were mounted with anti-fade containing DAPI (Vector Labs, H-1200). Representative images were taken at 100×, 200×, or 400× magnification with Olympus microscope BX53 (Olympus, Japan). Six to eight images were randomly captured at 200× magnification using cellSens Dimension version 1.81 software (Olympus, Japan) for quantitative analysis. Myogenin-positive nuclei counting and quantitative expression analysis of EbMHC, vimentin, and CD31 protein were performed using ImageJ software version 1.44p.

Cell Culture

The C2C12 mouse muscle cell line (Source: The American Type Culture Collection, CRL-1772) was used in this study. This cell line has been widely used to test the myogenic differentiation capacity that represents satellite cell differentiation during skeletal muscle regeneration *in vivo*. Briefly, C2C12 myoblasts were cultured with growth medium (DMEM + 10% fetal bovine serum) in 6-well plate at a starting density 5×10^4 cells/well. When cell density reached approximately 70% confluency, growth medium was replaced with differentiation medium (DMEM + 2% horse serum) to activate cell fusion and differentiation to form myotubes. At this step, differentiation medium was supplemented with $1\alpha,25(OH)_2D_3$ at final concentrations of 0.1, 1, and 10 nM and refreshed daily for 4 days to test the direct effect of $1\alpha,25(OH)_2D_3$ on myogenic cell differentiation and myotube formation. The changes of myogenin and EbMHC protein expression was investigated with immunocytochemistry. In another set of experiment, C2C12 myoblasts were seeded at density 2.5×10^4 cells/well and

cultured with growth medium in 12-well plate for 24 h. Thereafter, cells were treated with 1α,25$(OH)_2D_3$ at final concentration 10 nM for 24 h to determine VDR and CYP24A1 protein expression and localization. The mitochondrial compartment of the treated C2C12 myoblasts was localized with ATP synthase (complex V) subunit alpha (OxPhos).

Immunocytochemistry

Briefly, cells were fixed with 4% PFA for 10 min and permeabilized with 0.1% Triton X-100 for 5 min. The permeabilization step was performed specifically for nuclear localization protein staining (VDR and myogenin proteins). Cells were blocked with 10% normal goat serum for 30 min and incubated with primary antibodies as follows: VDR (D-6) (1:100), CYP24A1 (1:100), ATP synthase (complex V) subunit alpha (OxPhos) (1:200), myogenin (1:100), EbMHC (1:200) for 1 h. Cells were incubated simultaneously with goat anti-mouse Alexa 568 (1:500) and goat anti-rabbit Alexa 488 (1:500) for 1 h in the dark. Nuclei were counterstained with DAPI (Invitrogen, 1:1,000) for 5 min and a temporary mounting medium (20% PBS + 80% glycerol) was applied. Representative images were captured at either 100× or 200× magnification with Olympus microscope IX83 (Olympus, Japan). Images for quantitative analysis were randomly captured at 100× magnification. The quantitative analysis of myogenin positive nuclei and EbMHC protein expression was performed using cellSens Dimension version 1.81 software. Semi-automated cell counting and semi-automated area of expression functions of cellSens Dimension version 1.81 software for determination of myogenin positive nuclei and EbMHC protein expression were illustrated in Fig. 4.

A

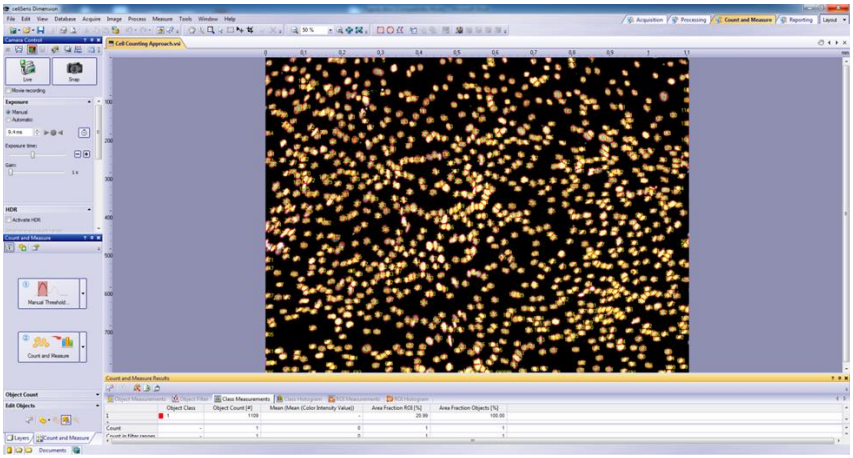

B

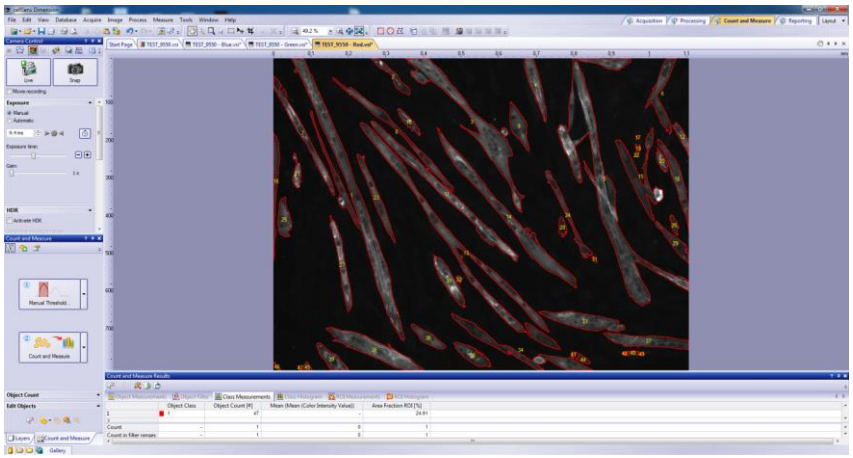

Fig. 4 Representative images of semi-automated cell counting and semi-automated area of expression functions of cellSens Dimension version 1.81 software. (A) Semi-automated cell counting for determination of myogenin positive nuclei per total cell number (DAPI positive nuclei) in an image (B) Semi-automated area of expression for analysis of EbMHC area of expression as demonstrated by the red contour.

Statistical Analysis

Data are presented as mean and standard error of the mean (mean ± SEM). Normal distribution and homogeneity of variance were determined using Shapiro-Wilk test and Levene's test, respectively. Significant differences among groups were analyzed with either one-way ANOVA with Tukey's post hoc test or Kruskal-Wallis with Dunn's multiple comparison test where appropriate. Data are analyzed with SPSS version 18.0.0, and the level of statistical significance was set with α level of $p<0.05$.

Results

Effect of consecutive intramuscular administrations on muscle wet weight to body weight ratio

Muscle wet weight to body weight ratio was determined to evaluate whether consecutive intramuscular administration of either vehicle or 1α,25$(OH)_2D_3$ at both MW and BW doses during the regenerative phase (day 4-7 post-injury) has an effect on muscle edema that may impact skeletal muscle regenerative capacity. The results demonstrated that the TA muscle wet weight to mouse body weight ratio significantly decreased during skeletal muscle regeneration in vehicle-administrated (1.54±0.05 mg/g BW), 1α,25$(OH)_2D_3$ administrated at MW dose (1.58±0.02 mg/g BW) and BW dose (1.57±0.08 mg/g BW) compared to control group (1.81±0.02 mg/g BW) (p<0.05) (Fig. 5). Irrespective of treatment (vehicle- or 1α,25$(OH)_2D_3$-administration), the muscle wet weight to body weight ratios were not significant different. These data suggest that muscle edema was not apparent after consecutive intramuscular administration of either vehicle or 1α,25$(OH)_2D_3$ at both MW and BW doses during skeletal muscle regeneration.

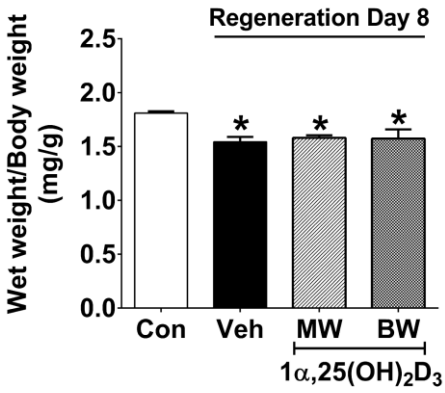

Fig. 5 Muscle wet weight to body weight ratio. TA muscle wet weight was normalized to mouse body weight and plotted as control, vehicle-administrated, and 1α,25$(OH)_2D_3$ MW and BW doses administrated groups (n=6/group), *p<0.05 compared to control group. 1α,25$(OH)_2D_3$ (MW) and (BW) represent dose at 1 μg/kg relative to TA muscle wet weight and mouse body weight, respectively.

VDR protein was expressed in regenerative muscle fibers and satellite cells

To determine if skeletal muscle regenerative capacity could be modulated by 1α,25$(OH)_2D_3$, VDR protein expression in regenerative muscle fibers and satellite cells was verified using the highly sensitive VDR antibody, VDR (D-6) (Wang *et al*., 2012). The results demonstrated that regenerative muscle fibers expressed VDR protein as determined by immunostaining with the mouse VDR (D-6) antibody (Fig. 6A). Since regenerative muscle fiber formation is depended on the function of satellite cells, we further determined whether satellite cells are a target of 1α,25$(OH)_2D_3$ in regenerative muscle. Counterstaining with both mouse Pax7 antibody and a rabbit VDR (H-81) antibody that was previously reported to detect VDR protein expression in regenerative muscle fibers (Srikuea *et al*., 2012) was performed (Fig. 6B). The results revealed that in addition to regenerating muscle fibers, satellite cells also expressed VDR protein. Furthermore, the specificity of VDR staining in regenerative muscle with rabbit VDR (H-81) antibody was verified with mouse VDR (D-6) antibody (Fig. 6C).

Intramuscular administration of 1α,25$(OH)_2D_3$ during muscle regeneration increased VDR protein expression

Since VDR protein was expressed in regenerating muscle fibers and satellite cells, this suggests a possible role of 1α,25$(OH)_2D_3$ in regulating muscle regenerative capacity. Therefore, intramuscular administration of 1α,25$(OH)_2D_3$ during skeletal muscle regeneration was investigated. Two relative doses of 1α,25$(OH)_2D_3$ (1 μg/kg relative to TA muscle wet weight (MW) and mouse body weight (BW)) were administrated for 4 consecutive days during days 4-7 post-injury (regenerative phase). Western blot analysis using VDR (D-6) antibody revealed that VDR protein was expressed at a barely detectable level in control compared to regenerative muscle (Fig. 6D). VDR protein expression was significantly increased 5.6±1.7-fold during muscle regeneration in vehicle-administrated group (p<0.05) and further increased in response to 1α,25$(OH)_2D_3$ administration at MW dose (8.1±2.2-fold) and BW dose (9.9±3.1-fold) (p<0.01) when compared to control group (Fig. 6D; two set of samples were illustrated). These results suggest that intramuscular administration of 1α,25$(OH)_2D_3$ during muscle regeneration enhanced VDR protein expression in regenerative muscle.

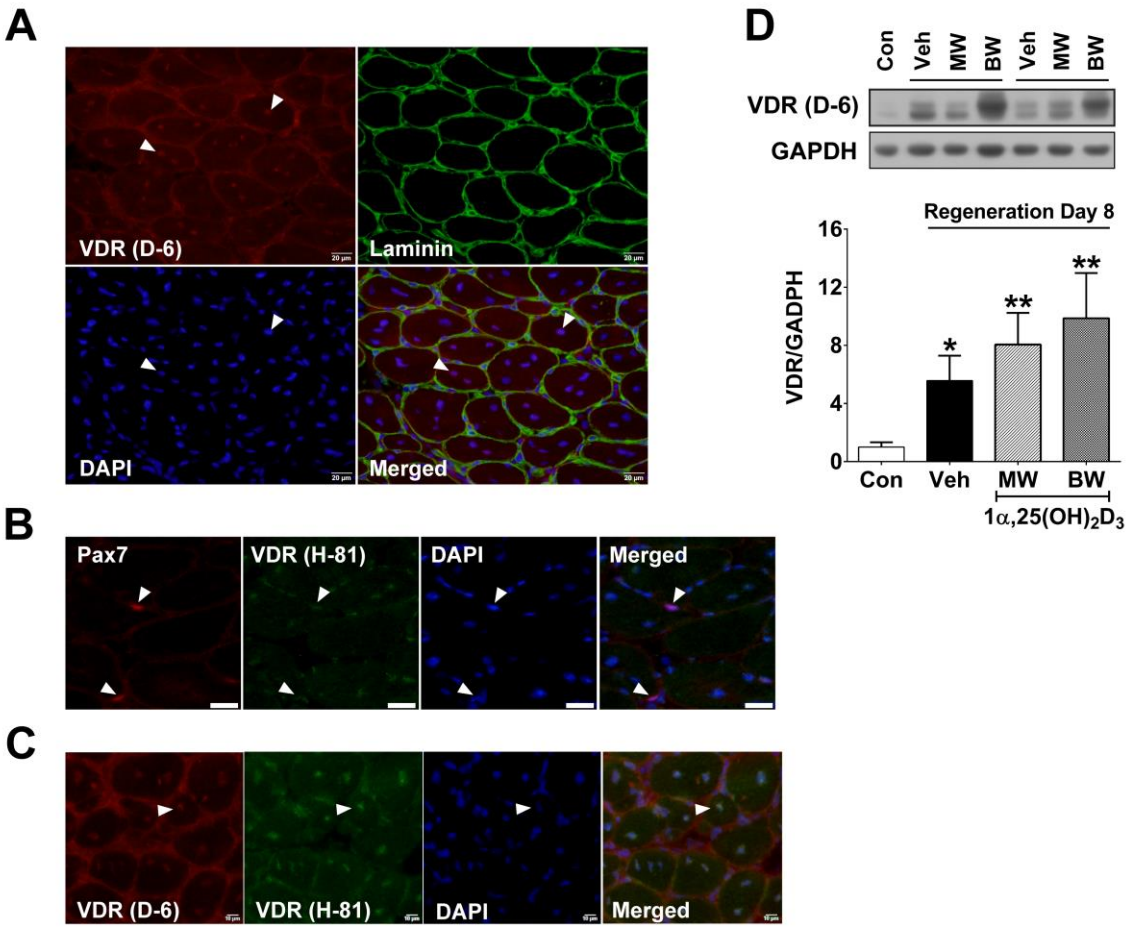

Fig. 6 Localization of VDR protein in regenerative muscle and the response to intramuscular administration of 1α,25(OH)$_2$D$_3$. (A) Expression of VDR protein in central nuclei of regenerative muscle fibers using VDR (D-6) antibody, arrows indicate VDR-positive nuclei. Representative images were captured at 400× magnification with scale bars 20 μm. (B) VDR protein was expressed and localized in the nucleus of satellite cells (Pax7 positive nuclei) as determined by co-localization of VDR (H-81) and Pax7 proteins (arrows). (C) The specificity of VDR (D-6) vs. VDR (H-81) to detected VDR protein in regenerative muscle was verified. Representative images of B-C were captured at 200× magnification (cropped) with scale bars 20 μm and 10 μm, respectively. (D) Western blot analysis revealed VDR protein expression in control, vehicle-administrated, and 1α,25(OH)$_2$D$_3$ at MW and BW doses administrated groups. GAPDH was used as a loading control. *p<0.05, **p<0.01 compared to control group (n=6/group). 1α,25(OH)$_2$D$_3$ (MW) and (BW) represent dose at 1 μg/kg relative to TA muscle wet weight and mouse body weight, respectively.

Intramuscular administration of 1α,25(OH)$_2$D$_3$ during muscle regeneration increased CYP24A1 but not CYP27B1 protein expression

To understand the regulation of vitamin D$_3$ during skeletal muscle regeneration, the effect of intramuscular administration of 1α,25(OH)$_2$D$_3$ on alterations in vitamin D$_3$ metabolizing enzymes in regenerative muscle was investigated. It is known that 1α,25(OH)$_2$D$_3$ concentration is regulated by two vitamin D$_3$ regulating enzymes, including CYP24A1 and CYP27B1. In general, excess 1α,25(OH)$_2$D$_3$ can be converted to its catabolite form 1α,24,25(OH)$_2$D$_3$ via CYP24A1 enzyme in which 1α,24,25(OH)$_2$D$_3$ is less active and has a lower affinity for VDR binding. In contrast, CYP27B1 functions to increase 1α,25(OH)$_2$D$_3$ synthesis from 25(OH)D$_3$ in both renal and extrarenal tissue. In the present study, Western blot analysis revealed that administration of 1α,25(OH)$_2$D$_3$ at BW dose significantly increased CYP24A1 protein expression by 1.5±0.2-fold compared to control group (p<0.05) while no significant difference was detected at MW dose (Fig 7A). Immunohistochemical analysis revealed that CYP24A1 protein was expressed in regenerative muscle and its localization was present at both regenerative muscle fibers and the extracellular matrix. Interestingly, CYP24A1 protein was co-localized with VDR protein in the central nuclei of regenerative muscle fibers (Fig. 7B). This result suggests the possible local regulation of 1α,25(OH)$_2$D$_3$ during skeletal muscle regeneration to regulate the concentration of 1α,25(OH)$_2$D$_3$. The specific nuclear localization of CYP24A1 protein in regenerative muscle fibers was further clarified in mouse C2C12 myoblasts. Results clearly demonstrate that CYP24A1 is mainly expressed in the nuclei of myoblasts which co-localized with VDR protein after 1α,25(OH)$_2$D$_3$ treatment (Fig. 7C; upper panel). Furthermore, CYP24A1 protein was expressed at low levels in mitochondrial compartment as determined by counterstaining with ATP synthase (complex V) subunit alpha (OxPhos) to show mitochondrial localization (Fig. 7C; lower panel). In contrast to CYP24A1, CYP27B1 protein expression was not changed in response to either vehicle or 1α,25(OH)$_2$D$_3$ administration at MW and BW doses (Fig. 7D). In addition, CYP27B1 protein was expressed mainly in mitochondrial compartment of the regenerative muscle fibers and extracellular matrix (Fig. 7E).

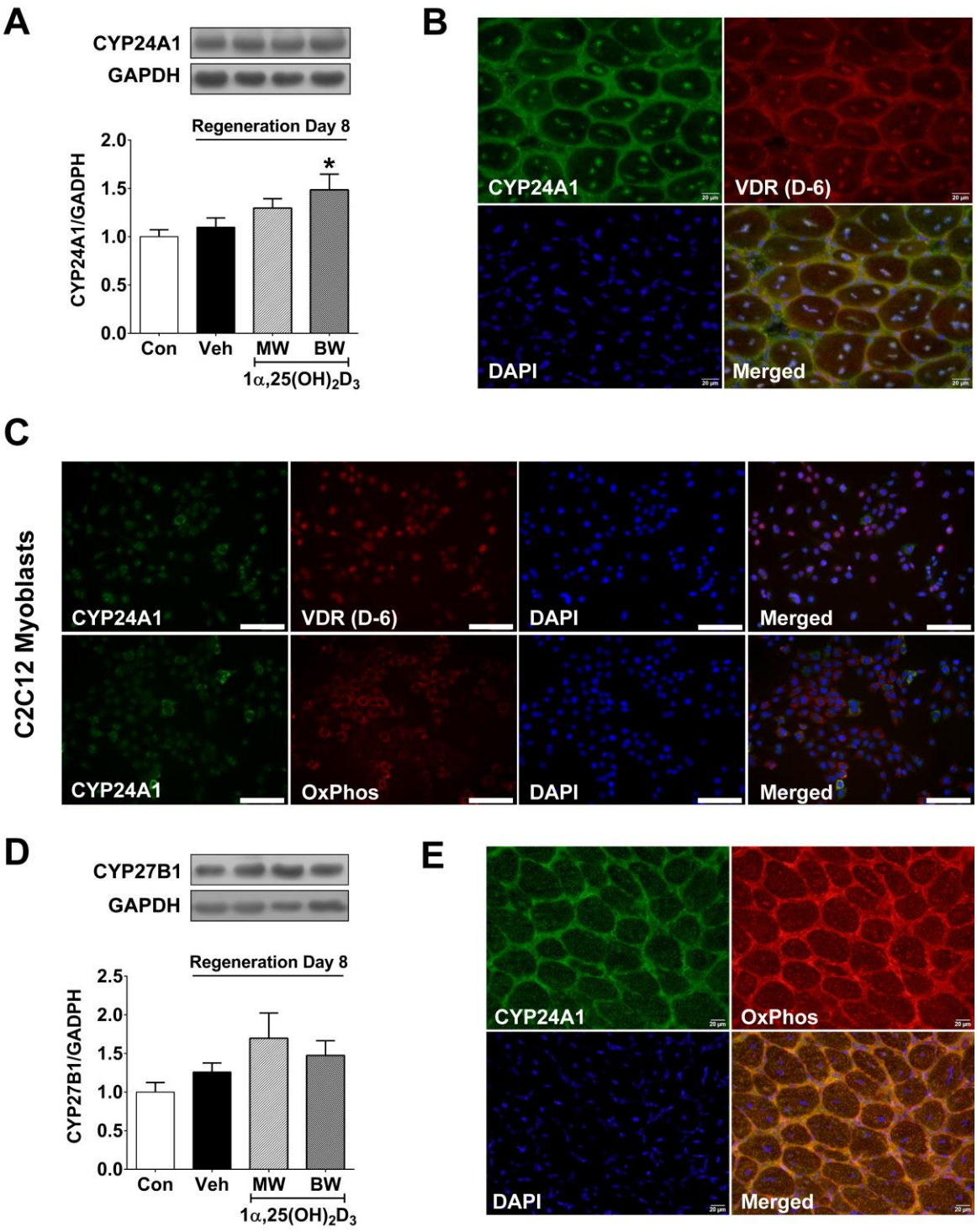

Fig. 7 Expression of vitamin D_3 metabolizing enzymes in response to intramuscular administration of $1\alpha,25(OH)_2D_3$. (A) Western blot analysis revealed CYP24A1 protein expression in control, vehicle-administrated, and $1\alpha,25(OH)_2D_3$ at MW and BW doses administrated groups, *p<0.05 compared to control group (n=6/group). GAPDH was used as a loading control. (B) CYP24A1 protein is localized in regenerative muscle fibers and the extracellular matrix compartment. Co-localization of CYP24A1 and VDR proteins was

detected in central nuclei of regenerative muscle fibers. Representative images were captured at 400× magnification with scale bars 20 μm. (C) CYP24A1 protein was expressed predominantly in the nucleus of C2C12 myoblasts and co-localized with VDR after 1α,25$(OH)_2D_3$ treatment at 10 nM for 24 h. Barely overlapping with ATP synthase (complex V) subunit alpha (OxPhos) was detected in C2C12 myoblasts under the same experimental condition. Representative images were captured at 200× magnification with scale bars 100 μm. (D) Western blot analysis revealed CYP27B1 protein expression in control, vehicle-administrated, and at MW and BW doses administrated groups (n=6/group). GAPDH was used as a loading control. (E) CYP27B1 protein is predominantly localized in the mitochondrial compartment of regenerative muscle fibers (OxPhos positive-stained) and the extracellular matrix. Representative images were captured at 200× magnification (cropped) with scale bars 20 μm. 1α,25$(OH)_2D_3$ (MW) and (BW) represent dose at 1 μg/kg relative to TA muscle wet weight and mouse body weight, respectively.

Skeletal muscle regenerative capacity in responses to intramuscular administration of 1α,25$(OH)_2D_3$

- **Decreased regenerative muscle fiber CSA**

H&E-stained sections illustrated the presence of small regenerative muscle fibers in 1α,25$(OH)_2D_3$ administrated groups at both MW and BW doses compared to control group (Fig. 8A). The number of regenerative muscle fiber size <600 μm^2 significantly increased in 1α,25$(OH)_2D_3$ administration at BW dose compared to vehicle group (49±10 fibers vs. 251±53 fibers, p<0.01) (Fig. 8B). To support this notion, the CSA histogram revealed a leftward shift of regenerative muscle fiber CSA size <600 μm^2 in 1α,25$(OH)_2D_3$ administration at BW dose compared to vehicle group (Fig. 8C).

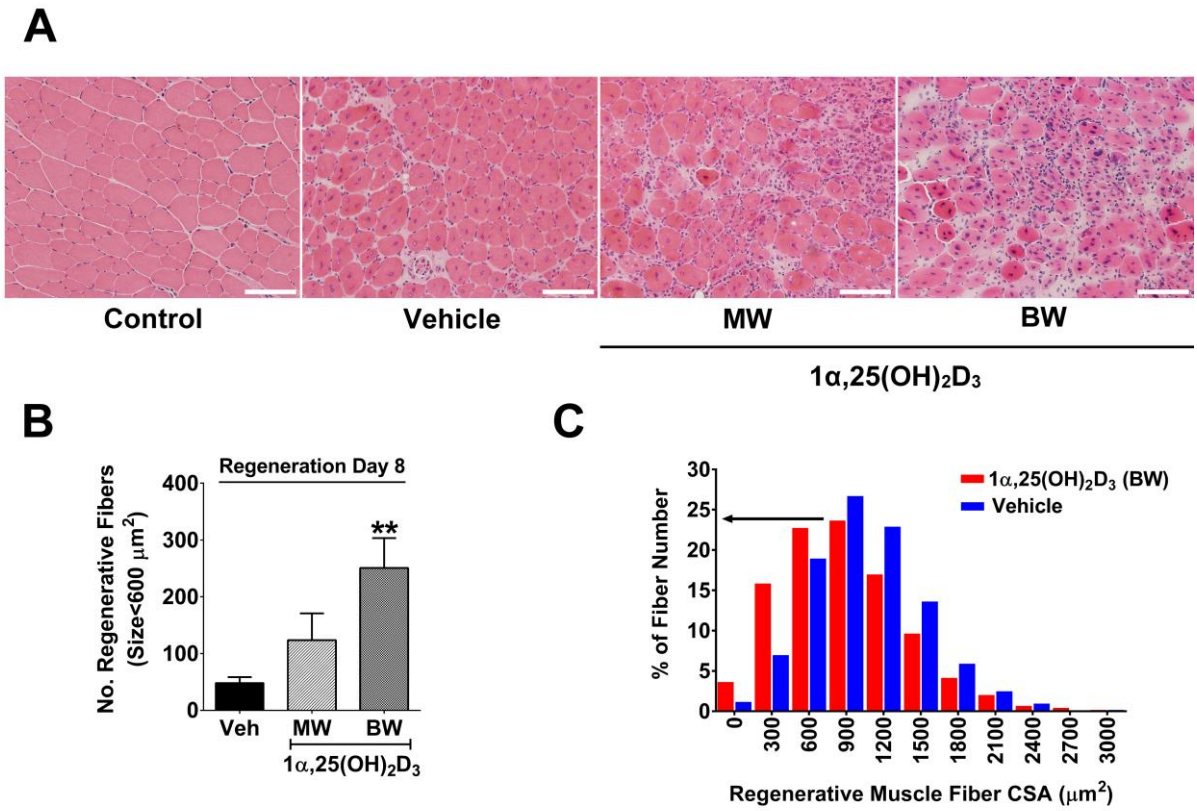

Fig. 8 Regenerative muscle fiber size in response to in response to intramuscular administration of 1α,25(OH)$_2$D$_3$. (A) Representative H&E-stained sections from control, vehicle-administrated, and 1α,25(OH)$_2$D$_3$ at MW and BW doses administrated groups. Small regenerative muscle fibers were observed in 1α,25(OH)$_2$D$_3$ at MW and BW doses administrated groups compared to vehicle-administrated group. Representative images were captured at 200× magnification with scale bars 100 μm. (B) The average number of regenerative muscle fibers size <600 μm^2 compared between control, vehicle-administrated, and 1α,25(OH)$_2$D$_3$ at MW and BW doses administrated groups. Six images were randomly captured using cellSens Dimension version 1.81 software (Olympus, Japan) for quantitative analysis. ***p*<0.01 compared to vehicle-administrated group (n=6/group). (C) CSA histogram revealed a leftward shift of regenerative muscle fiber size <600 μm^2 in 1α,25(OH)$_2$D$_3$ at BW dose administrated compared to vehicle-administrated groups. The total number of measured fibers was 3,936 fibers for vehicle-administrated group and 4,979 fibers for 1α,25(OH)$_2$D$_3$ at BW dose group (n=6/group). 1α,25(OH)$_2$D$_3$ (MW) and (BW) represent dose at 1 μg/kg relative to TA muscle wet weight and mouse body weight, respectively.

- **Decreased satellite cell differentiation and regenerative muscle fiber formation**

Following the observation of increased number of regenerative muscle fibers <600 μm^2, we investigated the expression level of proteins related to satellite cell differentiation (myogenin) that are required for developing nascent myotubes during skeletal muscle regeneration. Myogenin positive nuclear localization in regenerative muscle fibers was illustrated in Fig. 9A (arrows). The qualitative expression of myogenin positive nuclei in control, vehicle-, and 1α,25$(OH)_2D_3$- administrated groups at MW and BW doses were demonstrated in Fig. 9B. The quantitative analysis from immunohistochemical staining revealed a significant decrease in myogenin positive nuclei/field during skeletal muscle regeneration in 1α,25$(OH)_2D_3$-administrated group at BW dose compared to vehicle-administrated group (8±1 vs. 14±2 positive nuclei/field) (p<0.05) (Fig. 9C). This result was confirmed by Western blot analysis with a suppressive of myogenin protein expression after 1α,25$(OH)_2D_3$ administration at BW dose (Fig. 9D). In addition, results from the *in vitro* study of C2C12 myotubes (Fig. 9E) supported *in vivo* results that myogenin protein expression was significantly decreased to 59.6±3.5% after 1α,25$(OH)_2D_3$ treatment at high dose (10 nM) compared to vehicle-treated (p<0.05) (Fig. 9F).

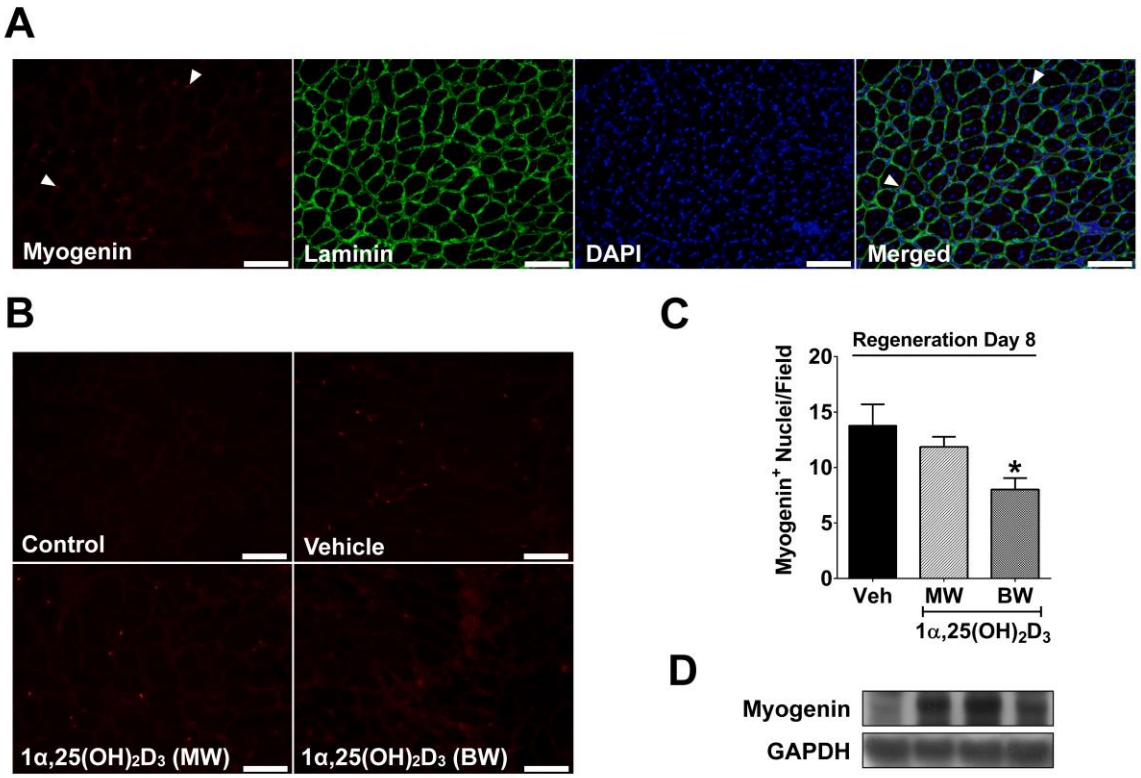

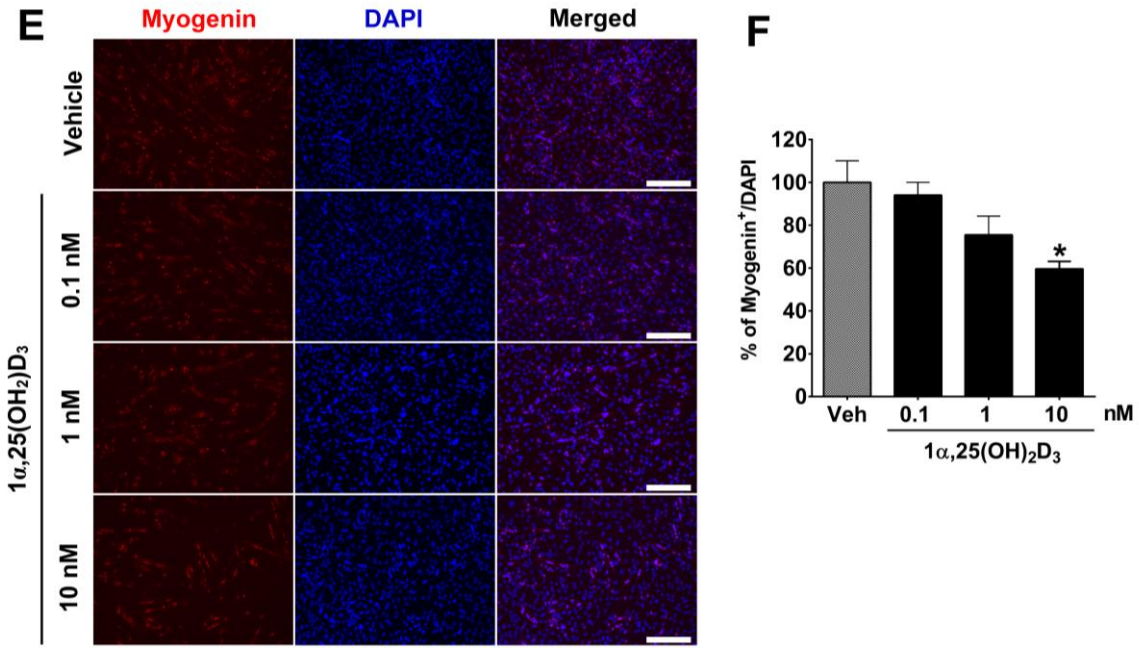

Fig. 9 Myogenin protein expression in responses to 1α,25(OH)$_2$D$_3$ administration *in vivo* and *in vitro*. (A) Differentiated satellite cells were identified as myogenin-positive nuclei (arrows). Laminin was counterstained for visualization of regenerative muscle fibers and DAPI was stained for nuclear localization. (B) Representative images of myogenin positive nuclei in control, vehicle-administrated, and 1α,25(OH)$_2$D$_3$ at MW and BW doses administrated groups. Images of panels A-B were captured at 200× magnification with scale bars 100 μm. (C) Quantitative analysis of myogenin positive nuclei in vehicle-administrated and 1α,25(OH)$_2$D$_3$ at MW and BW doses administrated groups (n=6/group). *p<0.05 compared to vehicle-administrated group. (D) Western blot analysis revealed myogenin protein expression in control, vehicle-administrated, and 1α,25(OH)$_2$D$_3$ at MW and BW doses administrated groups. GAPDH was used as a loading control. 1α,25(OH)$_2$D$_3$ (MW) and (BW) represent dose at 1 μg/kg relative to TA muscle wet weight and mouse body weight, respectively. (E) Representative images of myogenin-positive nuclei in C2C12 myotubes that were treated with 1α,25(OH)$_2$D$_3$ at 0.1, 1, and 10 nM compared to vehicle-treated group. Images of panel E were captured at 100× magnification with scale bars 200 μm. (F) Quantitative analysis of myogenin-positive nuclei in control, vehicle-treated, and 1α,25(OH)$_2$D$_3$ at 0.1, 1, and 10 nM treated groups. Six images were used for counting the number of myogenin positive nuclei. *p<0.05 compared to vehicle-treated group (n= 3 replicate experiments).

To further clarify that the suppression of satellite cell differentiation led to an impaired in skeletal muscle regeneration, we examined EbMHC protein expression that is required for de novo fiber formation. EbMHC protein localization and expression in regenerative muscle fibers was illustrated in Fig. 10A (arrows). Qualitative expression of EbMHC protein in control, vehicle-, and 1α,25$(OH)_2D_3$- administrated groups at MW and BW doses were demonstrated in Fig. 10B. EbMHC protein expression was significantly suppressed after intramuscular administration of 1α,25$(OH)_2D_3$ at BW dose compared to vehicle-administrated as determined by quantitative expression analysis (3.9±1.1vs. 8.6±1.7%) (p<0.05) (Fig. 10C). These results were confirmed by Western blot analysis that demonstrate a suppressive effect on EbMHC protein expression after 1α,25$(OH)_2D_3$ administration at BW dose (Fig. 10D). Furthermore, treatment of C2C12 myotubes with 1α,25$(OH)_2D_3$ led to a dose-dependent suppression of EbMHC protein expression (Fig. 10E-F). The quantitative analysis revealed significantly decreased EbMHC protein expression to 42.4±1.9% after C2C12 myotubes were treated with 10 nM 1α,25$(OH)_2D_3$ compared to the vehicle-treated group (p<0.001) (Fig. 10F). Taken together, these data suggest that intramuscular administration of 1α,25$(OH)_2D_3$ at BW dose led to impaired muscle regenerative capacity via suppression of satellite cell differentiation and EbMHC protein expression.

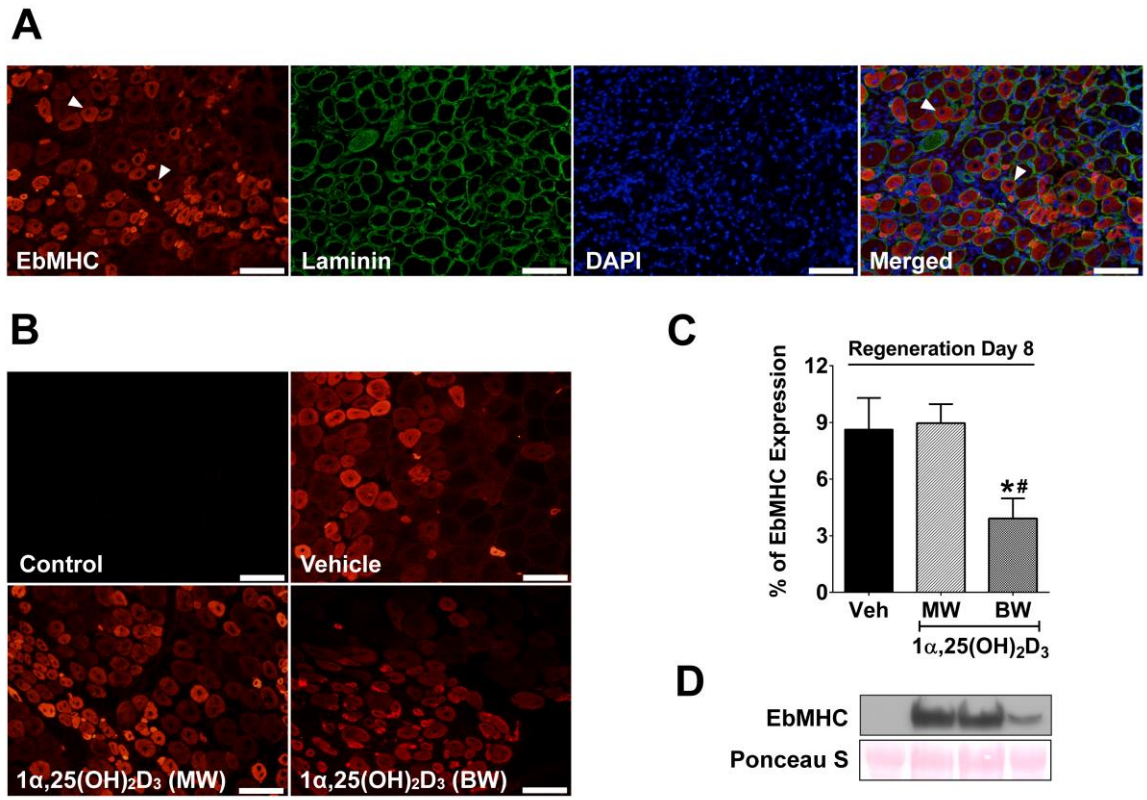

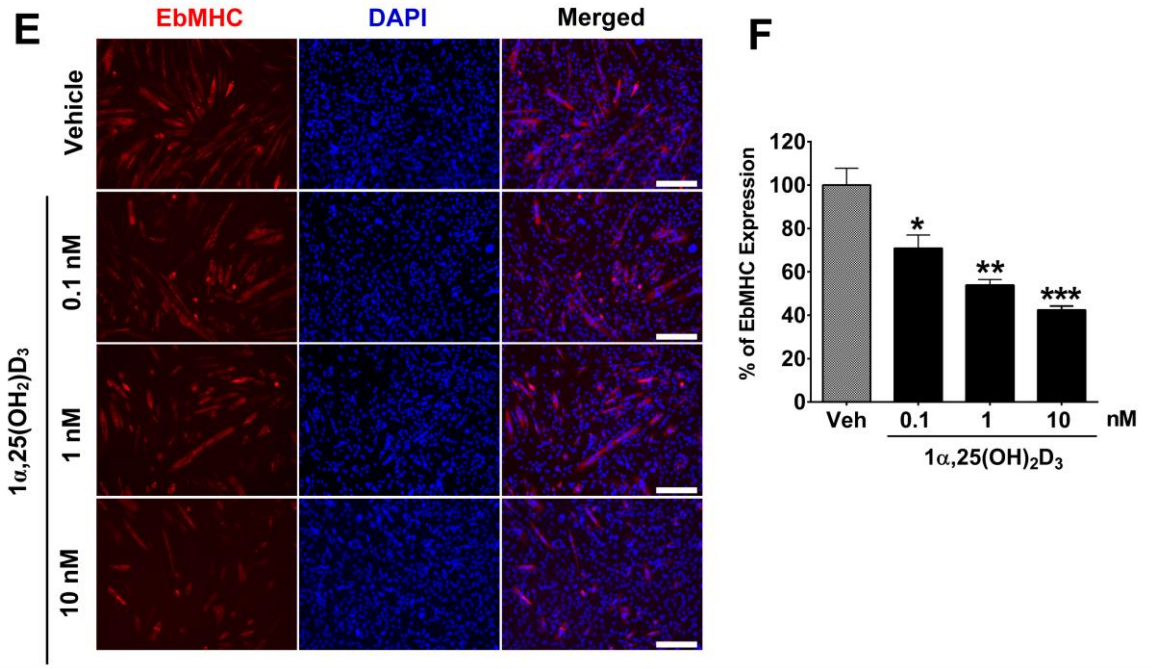

Fig. 10 EbMHC protein expression in responses to 1α,25(OH)$_2$D$_3$ administration *in vivo* and *in vitro*. (A) Newly formed regenerative muscle fibers were identified by the expression of EbMHC (arrows). Laminin was counterstained for visualization of regenerative muscle fibers and DAPI was stained for nuclear localization. (B) Representative of EbMHC-positive fibers in control, vehicle-administrated, and 1α,25(OH)$_2$D$_3$ at MW and BW doses administrated groups. Images of panels A-B were captured at 200× magnification with scale bars 100 μm. (C) Quantitative analysis on the percentage of EbMHC protein expression in vehicle-administrated and 1α,25(OH)$_2$D$_3$ at MW and BW doses administrated groups (n=6/group). *p<0.05, $^{\#}p$<0.05 compared to vehicle-administrated and 1α,25(OH)$_2$D$_3$ at MW dose administrated groups, respectively. (D) Western blot analysis revealed EbMHC protein expression in control, vehicle-administrated, and 1α,25(OH)$_2$D$_3$ at MW and BW doses administrated groups. Ponceau S was used as a loading control. (E) Representative images of EbMHC protein expression in C2C12 myotubes that were treated with 1α,25(OH)$_2$D$_3$ at 0.1, 1, and 10 nM compared to vehicle-treated group. Images of panel E were captured at 100× magnification with scale bars 200 μm. (F) Quantitative analysis of EbMHC protein expression in control, vehicle-treated, and 1α,25(OH)$_2$D$_3$ at 0.1, 1, and 10 nM treated groups. Twenty-five images were used for analysis of EbMHC area of expression. *p<0.05, **p<0.01, ***p<0.001 compared to vehicle-treated group (n= 3 replicate experiments).

- **No change in regenerative muscle protein synthesis and myostatin expression**

To determine whether 1α,25$(OH)_2D_3$ affects muscle protein synthesis during skeletal muscle regeneration, its effect on the expression of p70 S6K1, 4E-BP1, and Akt that represent a major protein synthesis pathway in skeletal muscle tissue was examined. Western blot analysis demonstrated that phosphorylated protein/total protein levels of p70 S6K1 (Fig. 11A), 4E-BP1 (Fig. 11B), and Akt (Fig. 11C) were not significantly different in either administered condition (vehicle- or 1α,25$(OH)_2D_3$-administration). To support this notion, there was also no difference in expression of mature myostatin protein compared between vehicle- and 1α,25$(OH)_2D_3$ administrated groups (Fig. 11D). These results suggest that an impairment of regenerative muscle capacity originated from the suppression of satellite cell differentiation and regenerative muscle fiber formation rather than decreased muscle protein synthesis.

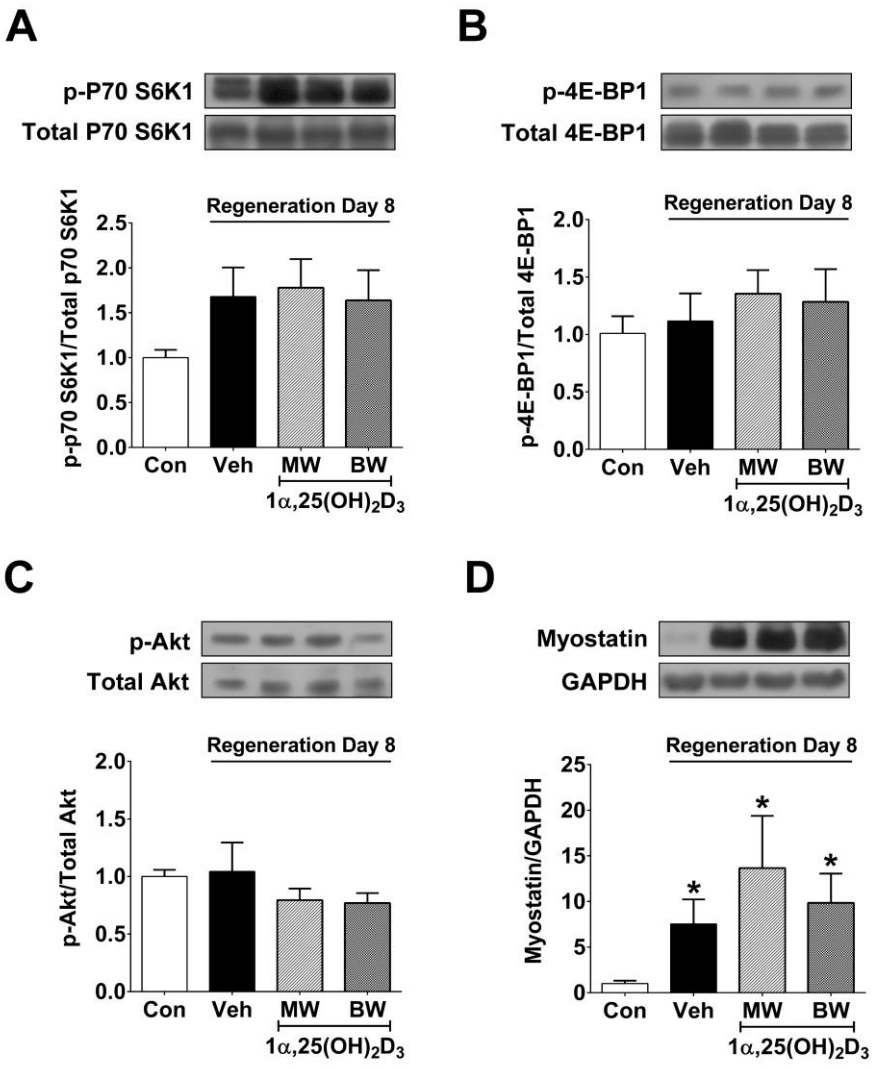

Fig. 11 Muscle protein synthesis signaling in response to intramuscular administration of 1α,25(OH)$_2$D$_3$. Western blot analysis of (A) phospho-p70 s6K1 and total p70 s6K1 (B) phospho-4E-BP1 and total 4E-BP1 (C) phospho-Akt and total Akt and (D) myostatin protein expression in control, vehicle-administrated, and 1α,25(OH)$_2$D$_3$ at MW and BW doses administrated groups. GAPDH was used as a loading control for myostatin protein expression. *p<0.05 compared to control group (n=6/group). 1α,25(OH)$_2$D$_3$ (MW) and (BW) represent dose at 1 μg/kg relative to TA muscle wet weight and mouse body weight, respectively.

- **No fiber type transition**

Recent studies in cell culture provided evidence that 1α,25(OH)$_2$D$_3$ treatment induced increased type II muscle fibers (Okuno *et al*., 2012). However, whether intramuscular administration of 1α,25(OH)$_2$D$_3$ could alter regenerative muscle fiber phenotype is currently unknown. The fiber type distribution of mouse TA muscle between control and regenerative muscle were illustrated in Fig. 12A. The expression of fast fibers was higher than slow fibers in both normal and regenerative TA muscles. The results demonstrated no significant increase in fast fiber phenotype in any administrated doses of 1α,25(OH)$_2$D$_3$ in both myofibrillar (Fig. 12B) and supernatant protein fractions (Fig. 12C). In contrast, there was a tend to increase slow MHC in regenerative muscle after administration of 1α,25(OH)$_2$D$_3$ at BW dose in myofibrillar protein fraction (Fig. 12B). However, slow MHC protein expression was almost undetectable in supernatant protein fraction (Fig. 12C).

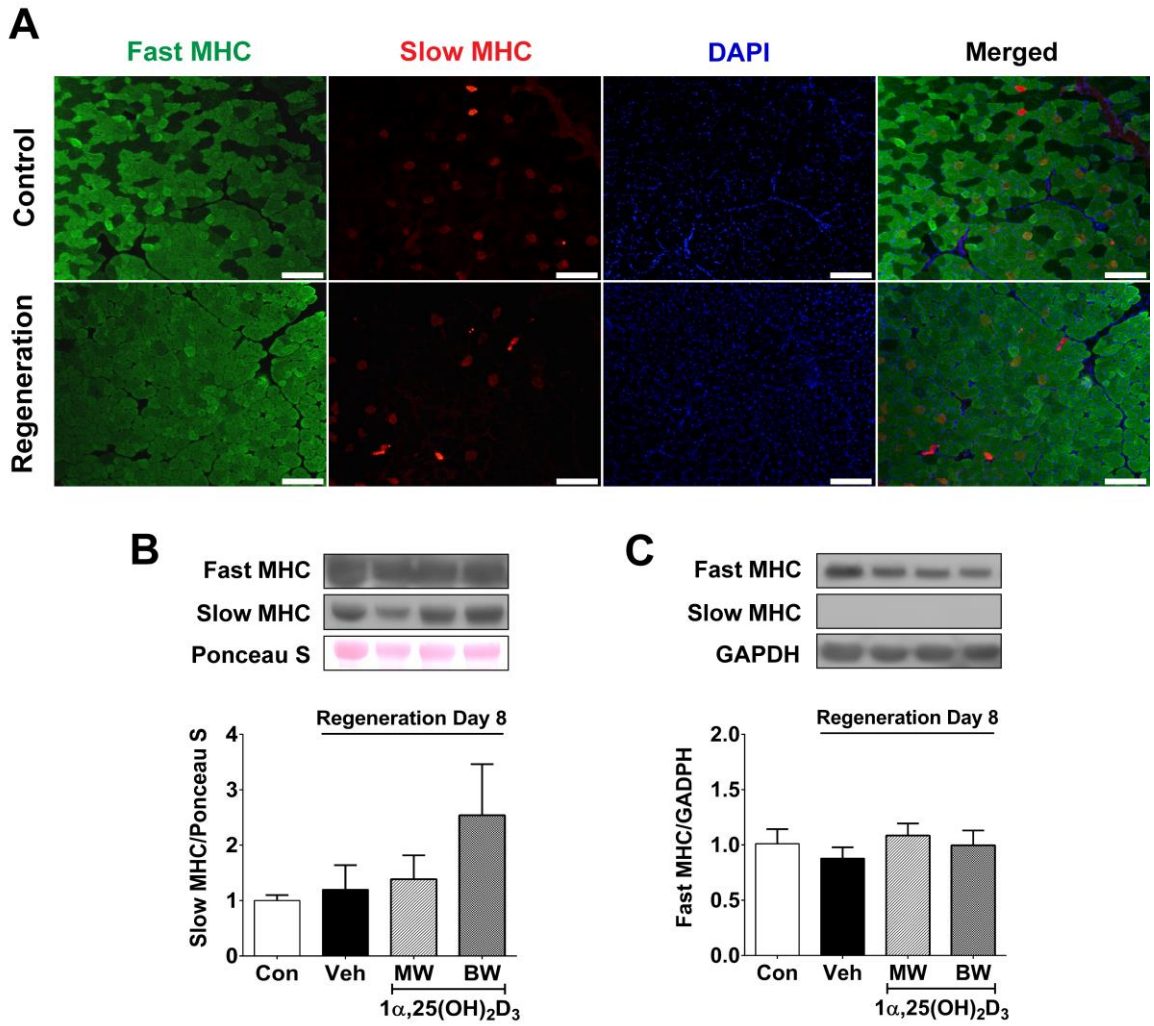

Fig. 12 Fast MHC and slow MHC protein expression in responses to intramuscular administration of 1α,25(OH)$_2$D$_3$. (A) Representative images for identification of fast MHC and slow MHC protein expression in control and regenerative muscles. Fast MHC was illustrated in green and slow MHC was illustrated in red, DAPI was stained for nuclear localization. Merged image shown in the right panel. Images were captured at 100× magnification with scale bars 200 μm. (B) Western blot analysis from myofibrillar protein fraction revealed fast MHC and slow MHC protein expression in control, vehicle-administrated, and 1α,25(OH)$_2$D$_3$ at MW and BW doses administrated groups (n=6/group). (C) Western blot analysis from cytosolic protein fraction revealed fast MHC and slow MHC protein expression in control, vehicle-administrated, and 1α,25(OH)$_2$D$_3$ at MW and BW doses administrated groups (n=6/group). Ponceau S and GAPDH were used as loading control for myofibrillar and cytosolic protein expression, respectively. 1α,25(OH)$_2$D$_3$ (MW) and (BW) represent dose at 1 μg/kg relative to TA muscle wet weight and mouse body weight, respectively.

- **Increased connective tissue formation**

Extracellular matrix remodeling is an essential factor during skeletal muscle regeneration to provide the connective tissue support. Delayed muscle regeneration could lead to an increase in fibrous tissue formation. Connective tissue formation was significantly increased during skeletal muscle regeneration and further increased when 1α,25$(OH)_2D_3$ at BW dose was intramuscularly administered as determined by vimentin protein expression (a marker of muscular fibrosis) (Fig. 13A). Quantitative analysis revealed an approximate 4-fold increase in vimentin protein expression during skeletal muscle regeneration compared to control. Moreover, vimentin protein expression was significantly increased after 1α,25$(OH)_2D_3$ administration at BW dose compared to vehicle group (18.7±2.6% vs. 12.6±1.0%) (p<0.05) (Fig. 13B). The expressions of vimentin protein in control and regenerative muscle with either vehicle or 1α,25$(OH)_2D_3$ administrated was confirmed with Western blot analysis (Fig. 13C).

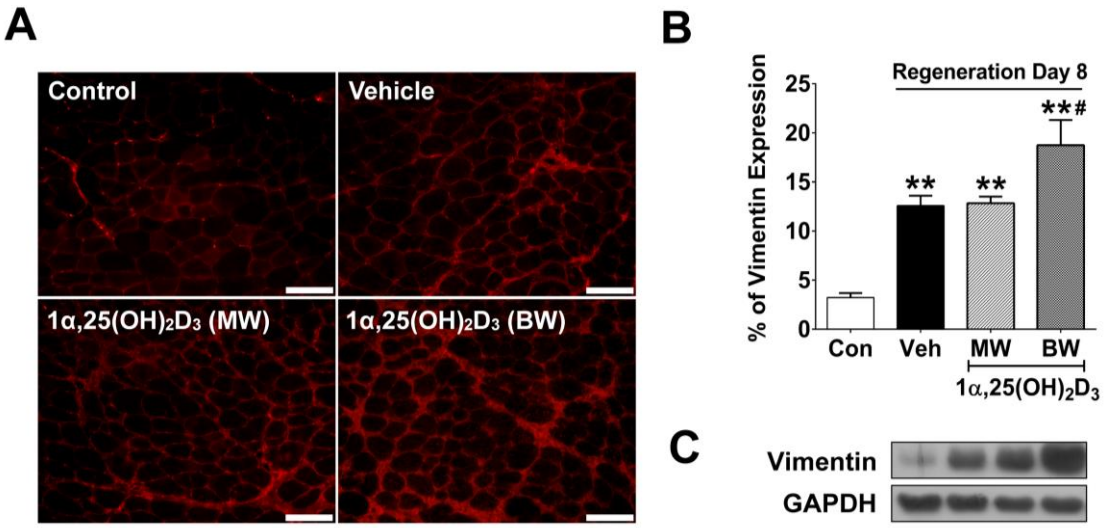

Fig. 13 Connective tissue formation in responses to 1α,25$(OH)_2D_3$ administration. (A) Representative images of vimentin protein expression in control, vehicle-administrated, and 1α,25$(OH)_2D_3$ at MW and BW doses administrated groups. (B) Quantitative analysis on the percentage of vimentin protein expression in control, vehicle-administrated, and 1α,25$(OH)_2D_3$ at MW and BW doses administrated groups. (C) Western blot analysis revealed vimentin protein expression in control, vehicle-administrated, and 1α,25$(OH)_2D_3$ at MW and BW doses administrated groups (n=6/group). GAPDH was used as a loading control. **p<0.01 compared to control group; $^{\#}p$<0.05 compared to vehicle and 1α,25$(OH)_2D_3$ at MW dose administrated groups.

- **No change of capillary density**

Revascularization is required during skeletal muscle regeneration to deliver nutrients and oxygen supply for functional recovery. Immunostaining of CD31, an endothelial cell marker that used to determine angiogenesis was illustrated in Fig. 14A. In control muscle, the percentage of CD31 area expression was approximately 3.1±0.2% and increased to 4.3±0.2%, 4.5±0.2%, and 4.5±0.5% during skeletal muscle regeneration after administrations of vehicle and 1α,25$(OH)_2D_3$ at MW and BW doses, respectively. However, there was no significant difference between vehicle- and 1α,25$(OH)_2D_3$-administrated groups (Fig. 14B). CD31 protein expression in control, vehicle- and 1α,25$(OH)_2D_3$-administrated groups was confirmed with Western blot analysis (Fig. 14C).

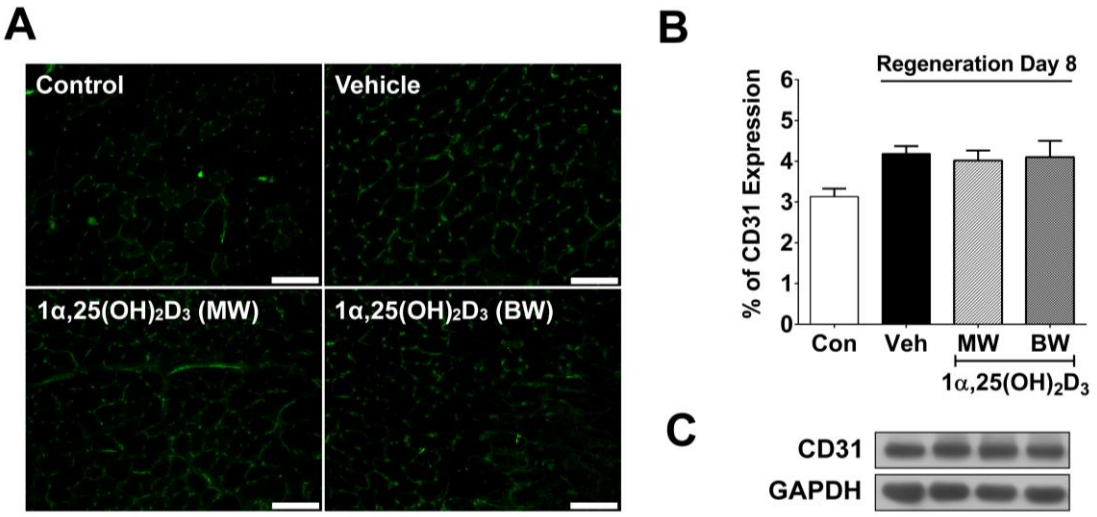

Fig. 14 Angiogenesis in responses to 1α,25$(OH)_2D_3$ administration. (A) Representative images of CD31 protein expression in control, vehicle-administrated, and 1α,25$(OH)_2D_3$ at MW and BW doses administrated groups. (B) Quantitative analysis on the percentage of CD31 protein expression in control, vehicle-administrated, and 1α,25$(OH)_2D_3$ at MW and BW doses administrated groups. (C) Western blot analysis revealed CD31 protein expression in control, vehicle-administrated, and 1α,25$(OH)_2D_3$ at MW and BW doses administrated groups (n=6/group). GAPDH was used as a loading control. Images of panels A and D were captured at 200× magnification with scale bars 100 μm. 1α,25$(OH)_2D_3$ (MW) and (BW) represent dose at 1 μg/kg relative to TA muscle wet weight and mouse body weight, respectively.

Discussion

In the present study, the action of the bioactive form of vitamin D_3 [$1\alpha,25(OH)_2D_3$] via intramuscular administration during skeletal muscle regeneration was investigated. The significant findings are: 1) regenerative muscle expressed VDR and vitamin D_3 metabolizing enzyme (CYP24A1 and CYP27B1) proteins which suggest the local metabolism of vitamin D_3 in skeletal muscle during regenerative process; 2) an increased VDR protein expression in regenerative muscle after intramuscular administration of $1\alpha,25(OH)_2D_3$ was verified with VDR (D-6) antibody. This antibody was reported as highly sensitive antibody to detect VDR protein expression in skeletal muscle tissue; 3) intramuscular administration of $1\alpha,25(OH)_2D_3$ at MW and BW doses into regenerative muscle had a dose-dependent effect on skeletal muscle regenerative capacity and muscular fibrosis but not angiogenesis.

Expression of VDR protein is currently under debated and contradictory results have been reported in normal skeletal muscle. Western blot analysis using VDR (D-6), which has the highest sensitivity to VDR, to verify VDR protein expression was undetectable (Wang and Deluca, 2011) and detectable (Girgis *et al*., 2014b) in whole muscle lysate. Moreover, VDR protein was expressed in normal skeletal muscle with immunohistochemistry using VDR (D-6) antibody (Girgis *et al*., 2014b), but this evidence has not been reported in the other investigations (Reviewed: Wang *et al*., 2012). Although, VDR protein was barely detectable in normal skeletal muscle, it was substantially expressed and localized in regenerative muscle fibers during skeletal muscle regeneration using VDR (H-81) antibody (Srikuea *et al*., 2012). In this study, VDR protein was detected to express during skeletal muscle regeneration using highly sensitive VDR (D-6) antibody (Wang *et al*., 2010). Both VDR (D-6) and VDR (H-81) antibodies were raised against identical amino acids 344-424 of VDR of human origin, except the host species of VDR (D-6) was mouse monoclonal and VDR (H-81) was rabbit polyclonal. The specificity of VDR (H-81) was verified with VDR (D-6) antibody on its ability to detect VDR protein in regenerative muscle using immunohistochemical analysis. The results confirmed the expression of VDR protein in the central nuclei of regenerative muscle fibers can be detected with both VDR (H-81) and VDR (D-6) antibodies.

Skeletal muscle regeneration is the self-repairing process after muscle injury in which the regenerative capacity relies on the function of satellite cells (Hawke and Garry, 2001). However, whether endogenous VDR protein is expressed in satellite cells is currently unknown. The result shown that satellite cells expressed VDR protein during skeletal muscle regeneration as demonstrated by the co-localization of Pax7 and VDR proteins. This finding suggests the possible direct action of vitamin D_3 on myogenesis during the regenerative process and further extends the knowledge on VDR protein expression in regenerative muscle (Srikuea *et al*., 2012). To support this notion, the presence of endogenous VDR protein expression was reported in the nucleus of C2C12 myoblasts (Garcia *et al*. 2011; Srikuea *et al*., 2012; Girgis *et al*., 2014a) and primary myotubes isolated from skeletal muscle fibers (Girgis *et al*., 2014b) suggesting satellite cells could be the source of VDR after skeletal muscle injury.

The intramuscular administration of $1\alpha,25(OH)_2D_3$ was performed in this study to verify the direct action of $1\alpha,25(OH)_2D_3$ at the injured site. The beneficial effect of intramuscular administration of the bioactive form of vitamin D_3 was the ability to control the concentration of $1\alpha,25(OH)_2D_3$ at the administered site, maximize the interaction of $1\alpha,25(OH)_2D_3$ to its receptor, and reduce the undesired systemic effect to the other tissues. In this study, two doses of $1\alpha,25(OH)_2D_3$ with consecutive administration during skeletal muscle regeneration were investigated to clarify the dose dependent effect of $1\alpha,25(OH)_2D_3$. The results demonstrated that intramuscular administration of $1\alpha,25(OH)_2D_3$ at both MW and BW doses significantly increase VDR protein expression in regenerative muscle. The effective dose which increased VDR protein expression was similar to the systemic dose (1 μg/kg BW) that is used to investigate calcemic function of $1\alpha,25(OH)_2D_3$ in the duodenum (a vitamin D_3 sensitive tissue) (Khuituan *et al*., 2012). However, VDR protein expression was slightly increased (1.8-fold) in the BW dose administration compared to MW dose. This result raised the possibility that regenerative muscle has a local control of vitamin D_3 metabolism to regulate the response to high concentration of $1\alpha,25(OH)_2D_3$.

In vitro study in C2C12 cells revealed that when the cells were treated with $1\alpha,25(OH)_2D_3$, CYP24A1 mRNA expression was significantly increased as a dose dependent manner in response to $1\alpha,25(OH)_2D_3$ treatments (Girgis *et al*., 2014b). In the current

investigation, CYP24A1 protein expression was increased after 1α,25$(OH)_2D_3$ was administrated at BW dose suggesting the local regulation of 1α,25$(OH)_2D_3$ concentration *in vivo*. The increase in CYP24A1 possibly decreased the toxicity of high concentration of 1α,25$(OH)_2D_3$ to regenerative muscle. Besides CY24A1 protein expression, the expression level of CYP27B1 protein was investigated, a vitamin D_3 regulating enzyme, which was previously reported to be expressed in regenerative muscle (Srikuea *et al*., 2012). 1α,25$(OH)_2D_3$ administration at both MW and BW doses did not change CYP27B1 protein level. This result could imply that the regulation of this enzyme was less affected by 1α,25$(OH)_2D_3$ concentration *in vivo*. In contrast, the regulation of CYP27B1 protein was dependent on the level of 25$(OH)D_3$ as demonstrated by luciferase reporter assays studied in both C2C12 myoblasts (Girgis *et al*., 2014a) and primary myotubes (Girgis *et al*., 2014b).

Impairments in muscle regenerative capacity were demonstrated after 1α,25$(OH)_2D_3$ administration at BW dose as CSA analysis revealed an significant increase in regenerating muscle fibers with a size <600 μm^2. This suppressive effect of 1α,25$(OH)_2D_3$ on skeletal muscle regeneration could involve either decrease satellite cell differentiation that led to impaired regenerative muscle fiber formation or suppression of protein synthesis signaling in regenerative muscle. Here, administration of 1α,25$(OH)_2D_3$ at BW dose induced a significant decrease in proteins related to satellite cell differentiation (myogenin) and regenerative muscle fiber formation (EbMHC) during skeletal muscle regeneration. Suppression of these two proteins after 1α,25$(OH)_2D_3$ treatment in C2C12 myotubes *in vitro* supported the finding *in vivo*. These data suggest that satellite cell differentiation and regenerative muscle formation could be impaired after high concentrations of 1α,25$(OH)_2D_3$ are administered. However, the major pathway of skeletal muscle protein synthesis was not affected by 1α,25$(OH)_2D_3$ administration. Phosphorylation of Akt, P70 S6K1, and 4E-BP1 proteins relative to their total protein expressions were not altered. Moreover, myostatin protein expression during skeletal muscle regeneration was not influenced by 1α,25$(OH)_2D_3$ administration. Taken together, these results suggest that 1α,25$(OH)_2D_3$ could interfere with the process of muscle stem cell differentiation that leads to impaired regenerative muscle fiber formation rather than suppressing protein synthesis signaling in regenerative muscle.

Although mouse TA muscle is a majority of fast muscle fibers (>99%) (Bloemberg and Quadrilatero, 2012), a tend to increase slow MHC protein expression with no significant change of fast MHC when compared between 1α,25$(OH)_2D_3$ administrated at BW dose and vehicle-administrated was observed. These data are in contrast to the study by Okuno *et al*. (2012) in which they demonstrate an increase in fast MHC in differentiated C2C12 myoblasts after 1 nM of 1α,25$(OH)_2D_3$ treatment. This discrepancy may rely on the aspect that differentiated C2C12 myoblasts in cultured do not contain all the characteristics of regenerating muscle fibers. Moreover, lacking nerve innovation and interaction between growth factors during the regenerative phase are limitations in an investigation of fiber type transition in the culture system. Therefore, this limitations may lead to the differential response of fiber type transition after 1α,25$(OH)_2D_3$ administration *in vivo* vs. *in vitro* studies.

Full recovery of skeletal muscle regeneration requires the balance between regenerating muscle fibers and connective tissue formation where excess connective tissue formation leads to muscular fibrosis. Related with an impairment of regenerative capacity after 1α,25$(OH)_2D_3$ administration at BW dose, vimentin protein expression was significantly increased. The presence of muscle fibrosis could be related to the action of 1α,25$(OH)_2D_3$ that acts as a suppressor of myogenin and EbMHC protein expression. Indeed, administration of activated 7-dehydrocholesterol via subcutaneous administration to rats increased prolyl-4-hydroxylase-β expression for 4 and 14 days following contusion suggesting an excessive deposition of extracellular matrix protein after vitamin D_3 treatment (Stratos *et al*., 2013).

Angiogenesis is crucial for skeletal muscle regeneration in order to increase blood supply and nutrient delivery to regenerating muscle. Garcia *et al*. (2013) reported two pro-angiogenic growth factors (VEGF-A and FGF-1) were increased while myogenic and/or angiogenic inhibitors (FGF-2 and TIMP-3) were decreased in C2C12 myoblasts treated with 1α,25$(OH)_2D_3$. These results suggest that 1α,25$(OH)_2D_3$ could enhance angiogenesis *in vitro*. However, the effect of 1α,25$(OH)_2D_3$ at both administrated doses on angiogenesis during muscle regeneration *in vivo* was not detected. These results may imply that the potential effect of 1α,25$(OH)_2D_3$ *in vitro* was not sufficient to promote angiogenesis during skeletal muscle regeneration.

Conclusions

In conclusion, regenerative muscle could be the target of vitamin D_3 action *in vivo* as it expresses VDR and vitamin D_3 metabolizing enzymes (CYP24A1 and CYP27B1) proteins during skeletal muscle regeneration. Increased VDR and CYP24A1 protein expression in response to a high dose of $1\alpha,25(OH)_2D_3$ suggests a local regulation of $1\alpha,25(OH)_2D_3$ in regenerative muscle. Decreased satellite cell differentiation, delayed regenerative muscle fiber formation, and increased muscular fibrosis were evident when $1\alpha,25(OH)_2D_3$ was intramuscularly administered at BW dose. However, protein synthesis signaling, fiber type composition, and angiogenesis in regenerative muscle were not affected by $1\alpha,25(OH)_2D_3$ administration at any dose investigated. The novelty of this work is the finding of non-calcemic functions of $1\alpha,25(OH)_2D_3$ on regenerative capacity and muscular fibrosis during skeletal muscle regeneration. The results of the present study provide a significant contribution to the field regarding knowledge of the physiological functions of the bioactive form of vitamin D_3 and vitamin D_3 metabolizing enzymes on the regenerative process of skeletal muscle.

References

1. **Bischoff-Ferrari HA, Borchers M, Gudat F, Durmuller U, Stahelin HB, Dick W**. Vitamin D receptor expression in human muscle tissue decreases with age. *J Bone Miner Res* 19: 265-269, 2004.
2. **Bischoff HA, Borchers M, Gudat F, Duermueller U, Theiler R, Stahelin HB, Dick W**. In situ detection of 1,25-dihydroxyvitamin D3 receptor in human skeletal muscle tissue. *Histochem J* 33: 19-24, 2001.
3. **Bloemberg D, Quadrilatero J**. Rapid determination of myosin heavy chain expression in rat, mouse, and human skeletal muscle using multicolor immunofluorescence analysis. *PloS one* 7: e35273, 2012.
4. **Endo I, Inoue D, Mitsui T, Umaki Y, Akaike M, Yoshizawa T, Kato S, Matsumoto T**. Deletion of vitamin D receptor gene in mice results in abnormal skeletal muscle development with deregulated expression of myoregulatory transcription factors. *Endocrinology* 144: 5138-5144, 2003.
5. **Garcia LA, Ferrini MG, Norris KC, Artaza JN**. 1,25(OH)(2)vitamin D(3) enhances myogenic differentiation by modulating the expression of key angiogenic growth factors and angiogenic inhibitors in C(2)C(12) skeletal muscle cells. *J Steroid Biochem Mol Biol* 133: 1-11, 2013.
6. **Garcia LA, King KK, Ferrini MG, Norris KC, Artaza JN**. 1,25(OH)2vitamin D3 stimulates myogenic differentiation by inhibiting cell proliferation and modulating the expression of promyogenic growth factors and myostatin in C2C12 skeletal muscle cells. *Endocrinology* 152: 2976-2986, 2011.
7. **Ge Y, Wu AL, Warnes C, Liu J, Zhang C, Kawasome H, Terada N, Boppart MD, Schoenherr CJ, Chen J**. mTOR regulates skeletal muscle regeneration in vivo through kinase-dependent and kinase-independent mechanisms. *Am J Physiol Cell Physiol* 297: C1434-1444, 2009.
8. **Girgis CM, Clifton-Bligh RJ, Mokbel N, Cheng K, Gunton JE**. Vitamin D signaling regulates proliferation, differentiation, and myotube size in C2C12 skeletal muscle cells. *Endocrinology* 155: 347-357, 2014.

9. **Girgis CM, Mokbel N, Cha KM, Houweling PJ, Abboud M, Fraser DR, Mason RS, Clifton-Bligh RJ, Gunton JE**. The vitamin D receptor (VDR) is expressed in skeletal muscle of male mice and modulates 25-hydroxyvitamin D (25OHD) uptake in myofibers. *Endocrinology* 155: 3227-3237, 2014.
10. **Hawke TJ, Garry DJ**. Myogenic satellite cells: physiology to molecular biology. *J Appl Physiol (1985)* 91: 534-551, 2001.
11. **Khuituan P, Teerapornpuntakit J, Wongdee K, Suntornsaratoon P, Konthapakdee N, Sangsaksri J, Sripong C, Krishnamra N, Charoenphandhu N**. Fibroblast growth factor-23 abolishes 1,25-dihydroxyvitamin D(3)-enhanced duodenal calcium transport in male mice. *Am J Physiol Endocrinol Metab* 302: E903-913, 2012.
12. **Lips P**. Vitamin D physiology. *Prog Biophys Mol Biol* 92: 4-8, 2006.
13. **Makanae Y, Ogasawara R, Sato K, Takamura Y, Matsutani K, Kido K, Shiozawa N, Nakazato K, Fujita S**. Acute bout of resistance exercise increases vitamin D receptor protein expression in rat skeletal muscle. *Exp Physiol* 100: 1168-1176, 2015.
14. **Mauro A**. Satellite cell of skeletal muscle fibers. *J Biophys Biochem Cytol* 9: 493-495, 1961.
15. **Melcon G, Kozlov S, Cutler DA, Sullivan T, Hernandez L, Zhao P, Mitchell S, Nader G, Bakay M, Rottman JN, Hoffman EP, Stewart CL**. Loss of emerin at the nuclear envelope disrupts the Rb1/E2F and MyoD pathways during muscle regeneration. *Hum Mol Genet* 15: 637-651, 2006.
16. **Okuno H, Kishimoto KN, Hatori M, Itoi E**. 1alpha,25-dihydroxyvitamin D(3) enhances fast-myosin heavy chain expression in differentiated C2C12 myoblasts. *Cell Biol Int* 36: 441-447, 2012.
17. **Olsson K, Saini A, Stromberg A, Alam S, Lilja M, Rullman E, Gustafsson T**. Evidence for vitamin D receptor expression and direct effects of 1alpha,25(OH)D in human skeletal muscle precursor cells. *Endocrinology* en20151685, 2015.
18. **Pojednic RM, Ceglia L, Lichtenstein AH, Dawson-Hughes B, Fielding RA**. Vitamin D receptor protein is associated with interleukin-6 in human skeletal muscle. *Endocrine* 49: 512-520, 2015.

19. **Pojednic RM, Ceglia L, Olsson K, Gustafsson T, Lichtenstein AH, Dawson-Hughes B, Fielding RA**. Effects of 1,25-dihydroxyvitamin D3 and vitamin D3 on the expression of the vitamin d receptor in human skeletal muscle cells. *Calcif Tissue Int* 96: 256-263, 2015.

20. **Prosser DE, Jones G**. Enzymes involved in the activation and inactivation of vitamin D. *Trends Biochem Sci* 29: 664-673, 2004.

21. **Relaix F, Zammit PS**. Satellite cells are essential for skeletal muscle regeneration: the cell on the edge returns centre stage. *Development* 139: 2845-2856, 2012.

22. **Salles J, Chanet A, Giraudet C, Patrac V, Pierre P, Jourdan M, Luiking YC, Verlaan S, Migne C, Boirie Y, Walrand S**. 1,25(OH)2-vitamin D3 enhances the stimulating effect of leucine and insulin on protein synthesis rate through Akt/PKB and mTOR mediated pathways in murine C2C12 skeletal myotubes. *Mol Nutr Food Res* 57: 2137-2146, 2013.

23. **Samuel S, Sitrin MD**. Vitamin D's role in cell proliferation and differentiation. *Nutr Rev* 66: S116-124, 2008.

24. **Seale P, Sabourin LA, Girgis-Gabardo A, Mansouri A, Gruss P, Rudnicki MA**. Pax7 is required for the specification of myogenic satellite cells. *Cell* 102: 777-786, 2000.

25. **Shi X, Garry DJ**. Muscle stem cells in development, regeneration, and disease. *Genes Dev* 20: 1692-1708, 2006.

26. **Srikuea R, Zhang X, Park-Sarge OK, Esser KA**. VDR and CYP27B1 are expressed in C2C12 cells and regenerating skeletal muscle: potential role in suppression of myoblast proliferation. *Am J Physiol Cell Physiol* 303: C396-405, 2012.

27. **Stratos I, Li Z, Herlyn P, Rotter R, Behrendt AK, Mittlmeier T, Vollmar B**. Vitamin D increases cellular turnover and functionally restores the skeletal muscle after crush injury in rats. *Am J Pathol* 182: 895-904, 2013.

28. **Wang TT, Tavera-Mendoza LE, Laperriere D, Libby E, MacLeod NB, Nagai Y, Bourdeau V, Konstorum A, Lallemant B, Zhang R, Mader S, White JH**. Large-scale in silico and microarray-based identification of direct 1,25-dihydroxyvitamin D3 target genes. *Mol Endocrinol* 19: 2685-2695, 2005.

29. **Wang Y, Becklund BR, DeLuca HF**. Identification of a highly specific and versatile vitamin D receptor antibody. *Arch Biochem Biophys* 494: 166-177, 2010.

30. **Wang Y, DeLuca HF**. Is the vitamin d receptor found in muscle? *Endocrinology* 152: 354-363, 2011.

31. **Wang Y, Zhu J, DeLuca HF**. Where is the vitamin D receptor? *Arch Biochem Biophys* 523: 123-133, 2012.

Acknowledgements

This research project was supported by 1) Thailand Research Fund (TRF), Office of the Higher Education Commission, and Mahidol University (MRG5680061 to RS) and 2) Faculty of Science, Mahidol University (to RS). Gratefully acknowledge supporting from the Olympus Bioimaging Center at Faculty of Science, Mahidol University, Prof. Chumpol Pholpramool for kindly gifting the mouse C2C12 cell line and initial suggestions on developing this project, and Kanokwan Suhatcho and Narut Leerasantana for technical assistance.

Output จากโครงการวิจัยที่ได้รับทุนจาก สกว.

Manuscript ได้ถูก submit ไปที่วารสาร Journal of Applied Physiology (Q1, IF = 3.056) โดยมีหัวหน้าโครงการวิจัยเป็น First Author และ Corresponding Author (Manuscript ID JAPPL-01018-2015) ตามเอกสารแนบ

Title

Effects of intramuscular administration of $1\alpha,25(OH)_2D_3$ during skeletal muscle regeneration on regenerative capacity, muscular fibrosis, and angiogenesis

หมายเหตุ ไฟล์ Manuscript ที่ได้ทำการ submit ไปที่วารสาร Journal of Applied Physiology ได้ถูกใส่ไว้ใน CD ประกอบรายงานฉบับสมบูรณ์เรียบร้อยแล้ว

December 1st, 2015

Editor
Journal of Applied Physiology

Dear Editor,

We wish to submit our manuscript entitled **"Effects of intramuscular administration of 1α,25(OH)$_2$D$_3$ during skeletal muscle regeneration on regenerative capacity, muscular fibrosis, and angiogenesis"** for publication as a research article in Journal of Applied Physiology. This study investigated the action of bioactive form of vitamin D$_3$ [1α,25(OH)$_2$D$_3$] on regenerative process of skeletal muscle. The significant findings of our work are: 1) Regenerative muscle expressed VDR and vitamin D$_3$ metabolizing enzyme (CYP24A1 and CYP27B1) proteins which suggest the local metabolism of vitamin D$_3$ in skeletal muscle during regenerative process; 2) Intramuscular administration of 1α,25(OH)$_2$D$_3$ at dose 1 μg/kg relative to muscle wet weight (MW) and mouse body weight (BW) to regenerative muscle had a dose-dependent effect on regenerative capacity and muscular fibrosis but not angiogenesis; 3) Decreased resident muscle stem cell (satellite cell) differentiation, delayed regenerative muscle fiber formation, and increased muscular fibrosis were evident when 1α,25(OH)$_2$D$_3$ was intramuscularly administered at BW dose. However, protein synthesis signaling, fiber type composition, and angiogenesis in regenerative muscle were not affected by 1α,25(OH)$_2$D$_3$ administration at any dose investigated.

The novelty of this work is the finding of non-calcemic functions of 1α,25(OH)$_2$D$_3$ on skeletal muscle regeneration. The results of the present study provide a significant contribution to the field regarding knowledge of the physiological functions of the bioactive form of vitamin D$_3$ and vitamin D$_3$ metabolizing enzymes on the regenerative process of skeletal muscle.

This manuscript has not been submitted for publication in any other journals.

Sincerely yours,

Ratchakrit Srikuea, Ph.D.

Department of Physiology
Faculty of Science, Mahidol University, Bangkok 10400, Thailand
Tel: +66 22015518
Fax: +66 23547154
Email: ratchakrit.sri@mahidol.ac.th

JAPPL-01018-2015 Manuscript Received

itorres@the-aps.org

Sent: Wednesday, December 02, 2015 8:39 AM
To: Ratchakrit Srikuea
Cc: ratchakrit@hotmail.com

Dear Dr. Srikuea:

On 1st Dec 2015, the manuscript record, JAPPL-01018-2015, a Research Article. entitled "Effects of intramuscular administration of 1α,25(OH)2D3 during skeletal muscle regeneration on regenerative capacity, muscular fibrosis, and angiogenesis" by Ratchakrit Srikuea and Muthita Hirunsai has been sent to the Editor-in Chief for assignment.

If any author has not seen this work, or was not aware of the submission, please contact Iliana Torres in the APS office, itorres@the-aps.org.

Thank you for submitting to the journal.

Sincerely,

Editorial Staff

The American Physiological Society - Receipt	
Invoice #	JAPPL-01018-2015-PRS
Transaction #	AU1FDD17A12D
Description	Journal of Applied Physiology Submission Payment - JAPPL-01018-2015
Bill Date	December 1, 2015 8:39:19 pm
Payment Date	December 1, 2015 8:44:54 pm
Amount Due	$50.00
Amount Received	$50.00
Credit Card	MasterCard XXXXXXXXXXX3270
Name	RATCHAKRIT
Address	109 Petchkasem Rd. Bangkae Bangkok 10160 Thailand
Phone	+66918904263
Email	ratchakrit.sri@mahidol.ac.th

Effects of intramuscular administration of 1α,25(OH)$_2$D$_3$ during skeletal muscle regeneration on regenerative capacity, muscular fibrosis, and angiogenesis

Ratchakrit Srikuea [1], Muthita Hirunsai [2]

[1] Department of Physiology, Faculty of Science, Mahidol University, Bangkok 10400, Thailand

[2] Department of Biopharmacy, Faculty of Pharmacy, Srinakharinwirot University, Nakornayok 26120, Thailand

Running head: Effects of 1α,25(OH)$_2$D$_3$ on skeletal muscle regeneration

Address for correspondence:

Ratchakrit Srikuea, Ph.D.

Department of Physiology

Faculty of Science, Mahidol University, Bangkok 10400, Thailand

Tel: +66 22015518

Fax: +66 23547154

Email: ratchakrit.sri@mahidol.ac.th

Abstract

The recent discovery of the vitamin D receptor (VDR) in regenerating muscle raises the question regarding the action of vitamin D_3 on skeletal muscle regeneration. To investigate the action of vitamin D_3 on this process, tibialis anterior (TA) muscle of male C57BL/6 mice (10 weeks of age) was injected with 1.2% $BaCl_2$ to induce extensive muscle injury. The bioactive form of vitamin D_3 [1α,25$(OH)_2D_3$] was administered daily via intramuscular injections during regenerative phase (day 4-7 post-injury). Two doses of 1α,25$(OH)_2D_3$ at 1 μg/kg muscle wet weight (MW) and mouse body weight (BW) were investigated. Muscle samples were collected on day 8 post-injury to examine proteins related to vitamin D_3 metabolism (VDR, CYP24A1, and CYP27B1), satellite cell differentiation and regenerative muscle fiber formation (myogenin and EbMHC), protein synthesis signaling (Akt, p70 S6K1, 4E-BP1, and myostatin), fiber type composition (fast and slow MHCs), fibrous formation (vimentin), and angiogenesis (CD31). Administration of 1α,25$(OH)_2D_3$ at MW and BW doses increased VDR in regenerative muscle. Increased CYP24A1 and vimentin expression accompany decreased myogenin and EbMHC expression at the BW dose of 1α,25$(OH)_2D_3$. However, there was no change in CYP27B1, Akt, p70 S6K1, 4E-BP1, myostatin, fast and slow MHCs, or CD31 expression at any dose investigated. Taken together, there was a dose-dependent effect of 1α,25$(OH)_2D_3$ on skeletal muscle regeneration. Administration of 1α,25$(OH)_2D_3$ at BW dose resulted in decreased satellite cell differentiation, delayed regenerative muscle fiber formation, and increased muscular fibrosis. However, protein synthesis signaling, fiber type composition, and angiogenesis were not affected by 1α,25$(OH)_2D_3$ administration.

Keywords:

vitamin D_3, intramuscular injection, muscle regeneration, muscular fibrosis, angiogenesis

Introduction

Vitamin D_3 (cholecalciferol) is a steroid hormone that is essential for calcium homeostasis (12). Furthermore, a broad range of physiological non-calcemic functions of vitamin D_3 have been reported i.e., controlling cell proliferation, differentiation, and apoptosis (23). The metabolism of vitamin D_3 from precursor to its bioactive form to initiate its action on the target tissue requires multiple steps. Briefly, synthesis of vitamin D_3 occurs in the skin after the vitamin D_3 precursor (7-dehydrocholesterol) is exposed to sun light to form cholecalciferol. Cholecalciferol is hydroxylated in the liver to form 25(OH)D_3 (calcidiol). 25(OH)D_3 is further hydroxylated via 1-α hydroxylase, a cytochrome P450 containing-hydroxylase encoded by *cyp27b1* gene, in the kidney to produce the bioactive form of vitamin D_3, 1α,25$(OH)_2D_3$ (calcitriol). The concentration of 1α,25$(OH)_2D_3$ is regulated by the action of the vitamin D_3 catabolizing enzyme, which is encoded by *cyp24a1* gene, to convert 1α,25$(OH)_2D_3$ to the inactive metabolite calcitroic acid (20).

The action of 1α,25$(OH)_2D_3$ requires binding to the vitamin D receptor (VDR) in order to initiate downstream cascades and modulate gene transcription. VDR is localized as a nuclear receptor and acts as a transcription factor that recognizes cognate vitamin D response elements (VDREs) in more than 3,000 target genes in the mouse genome (28). In addition to calcemic regulatory genes, myogenic regulatory genes (Myf5, MyoD, myogenin, and myostatin) (4, 6, 8) and muscle phenotypic genes (myosin heavy chain; MHC isoform) (4, 6, 16) were modulated in responses to 1α,25$(OH)_2D_3$ treatment. The action of 1α,25$(OH)_2D_3$ on skeletal muscle cells and tissue was supported by the presence of VDR protein in a mouse muscle cell line (C2C12) (6, 8, 26), rodent skeletal muscle (4, 13, 26, 27), human primary myoblasts (17, 19), and human skeletal muscle (1, 2, 18). Moreover, two major enzymes regulating vitamin D_3 metabolism, CYP27B1 and CYP24A1, were also expressed in C2C12 cells and mouse primary myotubes (9). Taken together, expression of the VDR and vitamin D_3 metabolizing enzymes in skeletal muscle suggest the possible local regulation of vitamin D_3 on this extrarenal tissue.

The presence of VDR protein in regenerative muscle, as demonstrated by immunohistochemistry (26) and Western blot analysis (27), raised a major question regarding to the potential role of $1\alpha,25(OH)_2D_3$ on the regulation of skeletal muscle regenerative capacity. Skeletal muscle regeneration is a self-repairing process following muscle injury. This process involves the activity of resident skeletal muscle stem cells (satellite cells) that are located between the basement membrane and basal lamina of muscle fibers (14). Satellite cells are unipotent and can differentiate to form muscle fibers in addition to self-renewal (21). Under normal conditions, satellite cells are quiescent but can become active, proliferating and differentiating after injury to repair damaged muscle fibers or generate new muscle fibers (10). After activation, satellite cells express transcription factors that can be used to identify the stages of their activity, i.e. MyoD, Myf5, Myf6 (activation, proliferation, and differentiation) and myogenin (differentiation) (25). Currently, the satellite cell population can be determined by the expression of specific transcription factor; Pax7 (24). The central nuclei derived from satellite cell fusion in regenerating muscle fibers are a hallmark of muscle regeneration. These newly formed muscle fibers after muscle injury can be characterized by the expression of embryonic myosin heavy chain (EbMHC) (15).

The efficiency of the regenerative process requires sufficient myoblast-derived satellite cell number, effectiveness of myoblast fusion and differentiation, and a rapid increase in the rate of protein synthesis. The suppressive effects of $1\alpha,25(OH)_2D_3$ on myogenic cells have been reported in various studies on myoblast proliferation (6, 8, 26) and myotube formation (6, 8). Although its effect leads to a decrease in myotube number, an increase in myotube size *in vitro* has been reported (6, 8). In addition, treatment with $1\alpha,25(OH)_2D_3$ in combination with insulin and leucine increased the phosphorylation of Akt/mTOR pathway suggesting an anabolic effect in skeletal muscle cells (22). An impaired muscle fiber regenerative response occurs when mTOR is inhibited after muscle injury (7); however, the direct effect of $1\alpha,25(OH)_2D_3$ on Akt/mTOR pathway activation in regenerative muscle has not been

investigated. To our knowledge, only one investigation reported an effect of vitamin D_3 on muscle regeneration using a crush injury model (27). Administration of activated 7-dehydrocholesterol via subcutaneous administration to the rats immediately after contusion induced-muscle injury leads to partial restoration of muscle function. However, VDR protein expression and satellite cell activity did not changes in response to activated 7-dehydrocholesterol administration. Furthermore, an investigation on the direct action of the bioactive form of vitamin D_3, $1\alpha,25(OH)_2D_3$, on skeletal muscle regeneration has not been investigated.

Connective tissue formation and angiogenesis act as contributing factors to determine skeletal muscle regenerative capacity. Increased fibroblast proliferation and collagen production after activated 7-dehydrocholesterol administration has been demonstrated (27). However, a single dose of activated 7-dehydrocholesterol immediately after muscle injury leads to an increased serum $25(OH)D_3$ that suppressed $1\alpha,25(OH)_2D_3$ serum level. This leaves the direct action of $1\alpha,25(OH)_2D_3$ on regulation of connective tissue formation/muscular fibrosis in regenerative muscle still unanswered. Moreover, the effect of $1\alpha,25(OH)_2D_3$ on pro-angiogenic growth factors and angiogenic inhibition was recently discovered (5). Treatment of $1\alpha,25(OH)_2D_3$ to C2C12 myoblasts increased vascular endothelial growth factor A (VEGF-A) and fibroblast growth factor-1 (FGF-1) while suppressing FGF-2 and tissue inhibitor of matrix metalloproteinases-3 (TIMP-3). However, this study was conducted *in vitro* demonstrating a need to clarify $1\alpha,25(OH)_2D_3$ action on angiogenesis during skeletal muscle regeneration *in vivo*.

Taken together, the aim of this study was to investigate the direct action of $1\alpha,25(OH)_2D_3$ on regenerative capacity, muscular fibrosis, and angiogenesis during skeletal muscle regeneration.

Materials and Methods

Animals

Adult male C57BL/6 mice were obtained from the National Laboratory Animal Centre, Salaya, Nakhon Pathom, Thailand. All animal procedures were performed in accordance with institutional guidelines for the care and use of laboratory animals as approved by the Ethics Committee on the Use of Experimental Animals, Faculty of Science, Mahidol University, Thailand (Protocol no. MUSC56-005-267).

$BaCl_2$-induced muscle injury

C57BL/6 mice (10 weeks of age) were anesthetized by inhalation with isoflurane gas prior injury induction. Left and right tibialis anterior (TA) muscles were injected intramuscularly with 50 µl of 1.2% $BaCl_2$ dissolved in sterile PBS to induce extensive muscle injury.

Intramuscular 1α,25$(OH)_2D_3$ administration

Mice were randomly assigned in to one of three groups (n=6/group): control group, injury + 1α,25$(OH)_2D_3$ (dose 1 µg/kg relative to TA muscle wet weight; MW) group, and injury + 1α,25$(OH)_2D_3$ (dose 1 µg/kg relative to mouse body weight; BW) group. Two doses of 1α,25$(OH)_2D_3$ were used in this study to determine the dose dependent effect of 1α,25$(OH)_2D_3$ on skeletal muscle regenerative capacity, muscular fibrosis, and angiogenesis. 1α,25$(OH)_2D_3$ (Cayman Chemical Inc., 71820) was administered daily via intramuscular injection to the left injured TA muscle on days 4-7 post-injury. The right injured TA served as contralateral injured muscle and was administrated a vehicle treatment. The administration period of 1α,25$(OH)_2D_3$ represents the phase of muscle regeneration that involves satellite cell differentiation, rapid increases in protein synthesis, regenerative muscle fiber formation, extracellular matrix remodeling, and revascularization.

Muscle wet weight/body weight ratio

On day 8 post-injury, injured TA muscles from either vehicle- or 1α,25$(OH)_2D_3$-administrated were dissected and weighed using digital weight scale to within ± 0.001 mg (Mettler Toledo, MS204S). Immediately after dissection, excess fluid was removed with filter paper. TA muscle wet weight (mg) was measured, normalized to mouse body weight (g), and recorded as muscle wet weight to body weight ratio.

Western blot analysis

Muscle samples were homogenized in ice-cold homogenizing buffer containing 50 mM Tris pH 7.5, 150 mM NaCl, 1 mM EDTA, 1% Triton X-100 supplemented with protease inhibitor cocktail (Sigma, P8340) (1:100) and phosphatase inhibitor cocktail (Calbiochem, 524625) (1:100). Muscle homogenates were centrifuged at 1,500 g for 10 min at 4^{o}C to separate cytosolic and myofibrillar fractions. The cytosolic fraction was further centrifuged at 10,000 g for 10 min at 4^{o}C and the supernatant portion was collected. To remove debris in myofibrillar fraction, pellets were suspended in the same ice-cold homogenizing buffer and centrifuged at 1,500 g for 10 min × 3 (4°C). Thereafter, the insoluble pellet was re-suspended with 0.5 M NaOH in 50 mM Tris-HCl, pH 7.5. Protein concentrations were determined by BCA assay in triplicate measurements. Under a reducing condition, 40 μg of cytosolic protein and 10 μg myofibrillar protein fractions containing sample buffer solution were denatured by heating at 60^{o}C for 10 min. The protein samples were loaded into SDS-polyacrylamide gel (5% stacking and 8-10% separating gels), and then transferred to a PVDF membrane (Millipore, IPVH-00010). The membrane was blocked with 5% non-fat milk (Bio-Rad, 1706404XTU), and probed with primary antibodies. The cytosolic proteins were incubated overnight with the following primary antibodies; VDR (D-6) (Santa Cruz Biotechnology sc-13133, 1:200), CYP24A1 (Santa Cruz Biotechnology SC-66851, 1:200), CYP27B1 (Santa Cruz Biotechnology SC-67261, 1:200), myogenin (Santa Cruz Biotechnology SC-12732, 1:200), myostatin (Santa Cruz Biotechnology SC-393335, 1:200), vimentin (Santa Cruz Biotechnology

SC-32322, 1:200), CD31 (Abcam ab28364, 1:500), phospho-p70 S6K1 Thr389 (Cell signaling 9206, 1:1,000), p70 S6K1 (Cell signaling 2708, 1:1,000), phospho-4E-BP1 (Cell signaling 9451, 1:1,000), 4E-BP1 (Cell signaling 9644, 1:1,000), phospho-Akt Ser473 (Cell signaling 4060, 1:1,000), and Akt Ser473 (Cell signaling 2967, 1:2,000). However, the myofibrillar proteins were incubated with the following primary antibodies including fast MHC (Abcam ab91506, 1:2,000), slow MHC (Abcam ab11083, 1:2,000), and EbMHC (Santa Cruz Biotechnology SC-53091, 1:500). Particularly, fast MHC and slow MHC antibodies also applied with cytosolic protein fraction to determine soluble pool of MHCs. Thereafter, the membrane was incubated with appropriate horseradish peroxidase (HRP) conjugated secondary antibodies. Protein bands were visualized with chemiluminescence HRP detection reagent (Millipore, WBLUR0100) and exposed to CL-XPosure film (Thermo Scientific, PIE34090). Band density was analyzed with ImageJ software version 1.44p [National Institutes of Health (NIH), Bethesda, MD]. Cytosolic protein expression was normalized to GAPDH (Millipore AB2302, 1:5,000), except phospho-p70 S6K1 Thr389, phospho-4E-BP1, and phospho-Akt Ser473 which were normalized to their total proteins. Myofibrillar protein expression was normalized with amount of loading protein as determined by Ponceau S staining.

Histological analysis

The frozen muscle samples were sectioned at 10 μm thickness with cryostat (Leica, Model CM1850). To determine cross-sectional area (CSA) of regenerative muscle fibers, the muscle sections were stained with hematoxylin and eosin to visualize the presence of central nucleated regenerative muscle fibers that represents the hallmark of muscle regeneration. Representative images were taken at 200× magnification with Olympus microscope BX53 (Olympus, Japan). Six images were randomly captured using cellSens Dimension version 1.81 software (Olympus, Japan) for quantitative analysis. Regenerative muscle fiber CSA was quantified using ImageJ software version 1.44p.

Immunohistochemical analysis

The serial sections at 10 μm thickness were used to investigate the changes of VDR, CYP24A1, CYP27B1, ATP synthase (complex V) subunit alpha (OxPhos) (Invitrogen, 1IV13-45-9240), Pax7 (R&D systems MAB1675), myogenin, EbMHC, fast MHC, slow MHC, vimentin, and CD31 protein expression using immunofluorescence staining. All subsequent steps were performed at room temperature except as noted. Briefly, VDR, CYP24A1, CYP27B1, ATP synthase (complex V) subunit alpha (OxPhos), Pax7, myogenin, and vimentin-stained sections were pre-fixed with 4% paraformaldehyde (PFA) from 10 min. In contrast, CD31-stained sections were pre-fixed with ice-cold acetone for 10 min while fast MHC, slow MHC, and EbMHC-stained section were unfixed at this step. For nuclear localization proteins (VDR, Pax7, and myogenin), the sections were permeabilized with 0.5% Triton X-100 for 5 min. Then, the sections were blocked with mouse IgG blocking reagent (Vector Labs, MKB-2213) for 1 h followed with 10% normal goat serum (Invitrogen, PCN5000) for 1 h. Primary antibodies were incubated overnight at 4^{o}C and dilution used for immunohistochemical analysis were listed as follows: mouse monoclonal VDR (D-6) (1:50), rabbit polyclonal VDR (H-81) (1:50), rabbit polyclonal CYP24A1 (1:50), rabbit polyclonal CYP27B1 (1:50), mouse monoclonal ATP synthase (complex V) subunit alpha (OxPhos) (1:200), mouse monoclonal myogenin (1:50), rabbit polyclonal fast MHC (1:1,000), mouse monoclonal slow MHC (1:2,000), mouse monoclonal EbMHC (1:100), mouse monoclonal vimentin (1:100), and rabbit polyclonal CD31 (1:100). Rabbit polyclonal laminin antibody (Sigma L9393, 1:400) was used to visualize regenerative muscle fiber structure. Thereafter, the sections were incubated with goat anti-mouse Alexa 568 (Invitrogen A-11004, 1:500) and goat anti-rabbit Alexa 488 (Invitrogen A-11008, 1:500) for 1 h in the dark. Fast MHC, slow MHC, and EbMHC-stained sections were post-fixed with 4% PFA for 10 min. All stained sections were mounted with anti-fade containing DAPI (Vector Labs, H-1200). Representative images were taken at 100×, 200×, or 400× magnification with Olympus microscope BX53 (Olympus,

Japan). Six to eight images were randomly captured at 200× magnification using cellSens Dimension version 1.81 software (Olympus, Japan) for quantitative analysis. Myogenin-positive nuclei counting and quantitative expression analysis of EbMHC, vimentin, and CD31 protein were performed using ImageJ software version 1.44p.

Cell Culture

The C2C12 mouse muscle cell line (Source: The American Type Culture Collection, CRL-1772) was used in this study. This cell line has been widely used to test the myogenic differentiation capacity that represents satellite cell differentiation during skeletal muscle regeneration *in vivo*. Briefly, C2C12 myoblasts were cultured with growth medium (DMEM + 10% fetal bovine serum) in 6-well plate at a starting density 5×10^4 cells/well. When cell density reached approximately 70% confluency, growth medium was replaced with differentiation medium (DMEM + 2% horse serum) to activate cell fusion and differentiation to form myotubes. At this step, differentiation medium was supplemented with $1\alpha,25(OH)_2D_3$ at final concentrations of 0.1, 1, and 10 nM and refreshed daily for 4 days to test the direct effect of $1\alpha,25(OH)_2D_3$ on myogenic cell differentiation and myotube formation. The changes of myogenin and EbMHC protein expression was investigated with immunocytochemistry. In another set of experiment, C2C12 myoblasts were seeded at density 2.5×10^4 cells/well and cultured with growth medium in 12-well plate for 24 h. Thereafter, cells were treated with $1\alpha,25(OH)_2D_3$ at final concentration 10 nM for 24 h to determine VDR and CYP24A1 protein expression and localization. The mitochondrial compartment of the treated C2C12 myoblasts was localized with ATP synthase (complex V) subunit alpha (OxPhos).

Immunocytochemistry

Briefly, cells were fixed with 4% PFA for 10 min and permeabilized with 0.1% Triton X-100 for 5 min. The permeabilization step was performed specifically for nuclear localization protein staining (VDR and myogenin proteins). Cells were blocked with 10% normal goat serum for 30 min and incubated with primary antibodies as follows: VDR (D-6) (1:100),

CYP24A1 (1:100), ATP synthase (complex V) subunit alpha (OxPhos) (1:200), myogenin (1:100), EbMHC (1:200) for 1 h. Cells were incubated simultaneously with goat anti-mouse Alexa 568 (1:500) and goat anti-rabbit Alexa 488 (1:500) for 1 h in the dark. Nuclei were counterstained with DAPI (Invitrogen, 1:1,000) for 5 min and a temporary mounting medium (20% PBS + 80% glycerol) was applied. Representative images were captured at either 100× or 200× magnification with Olympus microscope IX83 (Olympus, Japan). Images for quantitative analysis were randomly captured at 100× magnification. The quantitative analysis of myogenin positive nuclei and EbMHC protein expression was performed using cellSens Dimension version 1.81 software.

Statistical Analysis

Data are presented as mean and standard error of the mean (mean ± SEM). Normal distribution and homogeneity of variance were determined using Shapiro-Wilk test and Levene's test, respectively. Significant differences among groups were analyzed with either one-way ANOVA with Tukey's post hoc test or Kruskal-Wallis with Dunn's multiple comparison test where appropriate. Data are analyzed with SPSS version 18.0.0, and the level of statistical significance was set with α level of $p<0.05$.

Results

Effect of consecutive intramuscular administrations on muscle wet weight to body weight ratio

Muscle wet weight to body weight ratio was determined to evaluate whether consecutive intramuscular administration of either vehicle or $1\alpha,25(OH)_2D_3$ at both MW and BW doses during the regenerative phase (day 4-7 post-injury) has an effect on muscle edema that may impact skeletal muscle regenerative capacity. The experimental diagram for consecutive intramuscular administration of either vehicle or $1\alpha,25(OH)_2D_3$ is illustrated in

Fig. 1A. The results demonstrated that the TA muscle wet weight to mouse body weight ratio significantly decreased during skeletal muscle regeneration in vehicle-administrated (1.54±0.05 mg/g BW), 1α,25$(OH)_2D_3$ administrated at MW dose (1.58±0.02 mg/g BW) and BW dose (1.57±0.08 mg/g BW) compared to control group (1.81±0.02 mg/g BW) (p<0.05) (Fig. 1B). Irrespective of treatment (vehicle- or 1α,25$(OH)_2D_3$-administration), the muscle wet weight to body weight ratios were not significant different. These data suggest that muscle edema was not apparent after consecutive intramuscular administration of either vehicle or 1α,25$(OH)_2D_3$ at both MW and BW doses during skeletal muscle regeneration.

VDR protein was expressed in regenerative muscle fibers and satellite cells

To determine if skeletal muscle regenerative capacity could be modulated by 1α,25$(OH)_2D_3$, VDR protein expression in regenerative muscle fibers and satellite cells was verified using the highly sensitive VDR antibody, VDR (D-6) (31). First, we demonstrated that regenerative muscle fibers expressed VDR protein as determined by immunostaining with the mouse VDR (D-6) antibody (Fig. 2A). Since regenerative muscle fiber formation is depended on the function of satellite cells, we further determined whether satellite cells are a target of 1α,25$(OH)_2D_3$ in regenerative muscle. Counterstaining with both mouse Pax7 antibody and a rabbit VDR (H-81) antibody that was previously reported to detect VDR protein expression in regenerative muscle fibers (26) was performed (Fig. 2B). The results revealed that in addition to regenerating muscle fibers, satellite cells also expressed VDR protein. Furthermore, the specificity of VDR staining in regenerative muscle with rabbit VDR (H-81) antibody was verified with mouse VDR (D-6) antibody (Fig. 2C).

Intramuscular administration of 1α,25$(OH)_2D_3$ into regenerative muscle increased VDR protein expression

Since VDR protein was expressed in regenerating muscle fibers and satellite cells, this suggests a possible role of 1α,25$(OH)_2D_3$ in regulating muscle regenerative capacity. Therefore, intramuscular administration of 1α,25$(OH)_2D_3$ during skeletal muscle regeneration

was investigated. Two relative doses of 1α,25(OH)$_2$D$_3$ (1 μg/kg relative to TA muscle wet weight (MW) and mouse body weight (BW)) were administrated for 4 consecutive days during days 4-7 post-injury (regenerative phase). Western blot analysis using VDR (D-6) antibody revealed that VDR protein was expressed at a barely detectable level in control compared to regenerative muscle (Fig. 2D). VDR protein expression was significantly increased 5.6±1.7-fold during muscle regeneration in vehicle-administrated group (p<0.05) and further increased in response to 1α,25(OH)$_2$D$_3$ administration at MW dose (8.1±2.2-fold) and BW dose (9.9±3.1-fold) (p<0.01) when compared to control group (Fig. 2D; two set of samples were illustrated). These results suggest that intramuscular administration of 1α,25(OH)$_2$D$_3$ during muscle regeneration enhanced VDR protein expression in regenerative muscle.

Intramuscular administration of 1α,25(OH)$_2$D$_3$ during muscle regeneration increased CYP24A1 but not CYP27B1 protein expression

To understand the regulation of vitamin D$_3$ during skeletal muscle regeneration, we sought to determine the effect of intramuscular administration of 1α,25(OH)$_2$D$_3$ on alterations in vitamin D$_3$ metabolizing enzymes in regenerative muscle. It is known that 1α,25(OH)$_2$D$_3$ concentration is regulated by two vitamin D$_3$ regulating enzymes, including CYP24A1 and CYP27B1. In general, excess 1α,25(OH)$_2$D$_3$ can be converted to its catabolite form 1α,24,25(OH)$_2$D$_3$ via CYP24A1 enzyme in which 1α,24,25(OH)$_2$D$_3$ is less active and has a lower affinity for VDR binding. In contrast, CYP27B1 functions to increase 1α,25(OH)$_2$D$_3$ synthesis from 25(OH)D$_3$ in both renal and extrarenal tissue. In the present study, Western blot analysis revealed that administration of 1α,25(OH)$_2$D$_3$ at BW dose significantly increased CYP24A1 protein expression by 1.5±0.2-fold compared to control group (p<0.05) while no significant difference was detected at MW dose (Fig 3A). Immunohistochemical analysis revealed that CYP24A1 protein was expressed in regenerative muscle and its localization was present at both regenerative muscle fibers and the extracellular matrix. Interestingly, CYP24A1 protein was co-localized with VDR protein in the central nuclei of regenerative muscle fibers

(Fig. 3B). This result suggests the possible local regulation of $1\alpha,25(OH)_2D_3$ during skeletal muscle regeneration to regulate the concentration of $1\alpha,25(OH)_2D_3$. The specific nuclear localization of CYP24A1 protein in regenerative muscle fibers was further clarified in mouse C2C12 myoblasts. Results clearly demonstrate that CYP24A1 is mainly expressed in the nuclei of myoblasts which co-localized with VDR protein after $1\alpha,25(OH)_2D_3$ treatment (Fig. 3C; upper panel). Furthermore, CYP24A1 protein was expressed at low levels in mitochondrial compartment as determined by counterstaining with ATP synthase (complex V) subunit alpha (OxPhos) to show mitochondrial localization (Fig. 3C; lower panel). In contrast to CYP24A1, CYP27B1 protein expression was not changed in response to either vehicle or $1\alpha,25(OH)_2D_3$ administration at MW and BW doses (Fig. 3D). In addition, CYP27B1 protein was expressed mainly in mitochondrial compartment of the regenerative muscle fibers and extracellular matrix (Fig. 3E).

Skeletal muscle regenerative capacity in responses to intramuscular administration of $1\alpha,25(OH)_2D_3$

- **Decreased regenerative muscle fiber CSA**

H&E-stained sections illustrated the presence of small regenerative muscle fibers in $1\alpha,25(OH)_2D_3$ administrated groups at both MW and BW doses compared to control group (Fig. 4A). The number of regenerative muscle fiber size <600 μm^2 significantly increased in $1\alpha,25(OH)_2D_3$ administration at BW dose compared to vehicle group (49±10 fibers vs. 251±53 fibers, $p<0.01$) (Fig. 4B). To support this notion, the CSA histogram revealed a leftward shift of regenerative muscle fiber CSA size <600 μm^2 in $1\alpha,25(OH)_2D_3$ administration at BW dose compared to vehicle group (Fig. 4C).

- **Decreased satellite cell differentiation and regenerative muscle fiber formation**

Following the observation of increased number of regenerative muscle fibers <600 μm^2, we investigated the expression level of proteins related to satellite cell differentiation (myogenin) that are required for developing nascent myotubes during skeletal muscle

regeneration. Myogenin positive nuclear localization in regenerative muscle fibers was illustrated in Fig. 5A (arrows). The qualitative expression of myogenin positive nuclei in control, vehicle-, and 1α,25$(OH)_2D_3$- administrated groups at MW and BW doses were demonstrated in Fig. 5B. The quantitative analysis from immunohistochemical staining revealed a significant decrease in myogenin positive nuclei/field during skeletal muscle regeneration in 1α,25$(OH)_2D_3$-administrated group at BW dose compared to vehicle-administrated group (8±1 vs. 14±2 positive nuclei/field) (p<0.05) (Fig. 5C). This result was confirmed by Western blot analysis with a suppressive of myogenin protein expression after 1α,25$(OH)_2D_3$ administration at BW dose (Fig. 5D). In addition, results from the *in vitro* study of C2C12 myotubes (Fig. 5E) supported *in vivo* results that myogenin protein expression was significantly decreased to 59.6±3.5% after 1α,25$(OH)_2D_3$ treatment at high dose (10 nM) compared to vehicle-treated (p<0.05) (Fig. 5F).

To further clarify that the suppression of satellite cell differentiation led to an impairment in skeletal muscle regeneration, we examined EbMHC protein expression that is required for de novo fiber formation. EbMHC protein localization and expression in regenerative muscle fibers was illustrated in Fig. 6A (arrows). Qualitative expression of EbMHC protein in control, vehicle-, and 1α,25$(OH)_2D_3$- administrated groups at MW and BW doses were demonstrated in Fig. 6B. EbMHC protein expression was significantly suppressed after intramuscular administration of 1α,25$(OH)_2D_3$ at BW dose compared to vehicle-administrated as determined by quantitative expression analysis (3.9±1.1vs. 8.6±1.7%) (p<0.05) (Fig. 6C). These results were confirmed by Western blot analysis that demonstrate a suppressive effect on EbMHC protein expression after 1α,25$(OH)_2D_3$ administration at BW dose (Fig. 6D). Furthermore, treatment of C2C12 myotubes with 1α,25$(OH)_2D_3$ led to a dose-dependent suppression of EbMHC protein expression (Fig. 6E-F). The quantitative analysis revealed significantly decreased EbMHC protein expression to 42.4±1.9% after C2C12 myotubes were treated with 10 nM 1α,25$(OH)_2D_3$ compared to the vehicle-treated group

(p<0.001) (Fig. 6F). Taken together, these data suggest that intramuscular administration of 1α,25$(OH)_2D_3$ at BW dose led to impaired muscle regenerative capacity via suppression of satellite cell differentiation and EbMHC protein expression.

- **No change in regenerative muscle protein synthesis and myostatin expression**

To determine whether 1α,25$(OH)_2D_3$ affects muscle protein synthesis during skeletal muscle regeneration, we examined its effect on the expression of p70 S6K1, 4E-BP1, and Akt that represent a major protein synthesis pathway in skeletal muscle tissue. Western blot analysis demonstrated that phosphorylated protein/total protein levels of p70 S6K1 (Fig. 7A), 4E-BP1 (Fig. 7B), and Akt (Fig. 7C) were not significantly different in either administered condition (vehicle- or 1α,25$(OH)_2D_3$-administration). To support this notion, there was also no difference in expression of mature myostatin protein compared between vehicle- and 1α,25$(OH)_2D_3$ administrated groups (Fig. 7D). These results suggest that an impairment of regenerative muscle capacity originated from the suppression of satellite cell differentiation and regenerative muscle fiber formation rather than decreased muscle protein synthesis.

- **No fiber type transition**

Recent studies in cell culture provided evidence that 1α,25$(OH)_2D_3$ treatment induced increased type II muscle fibers (16). Here, we investigated whether intramuscular administration of 1α,25$(OH)_2D_3$ could alter regenerative muscle fiber phenotype. The fiber type distribution of mouse TA muscle between control and regenerative muscle were illustrated in Fig. 8A. The expression of fast fibers was higher than slow fibers in both normal and regenerative TA muscles. The results demonstrated no significant increase in fast fiber phenotype in any administrated doses of 1α,25$(OH)_2D_3$ in both myofibrillar (Fig. 8B) and supernatant protein fractions (Fig. 8C). In contrast, there was a tend to increase slow MHC in regenerative muscle after administration of 1α,25$(OH)_2D_3$ at BW dose in myofibrillar protein fraction (Fig. 8B). However, slow MHC protein expression was almost undetectable in supernatant protein fraction (Fig. 8C).

- **Increased connective tissue formation**

Extracellular matrix remodeling is an essential factor during skeletal muscle regeneration to provide the connective tissue support. Delayed muscle regeneration could lead to an increase in fibrous tissue formation. Connective tissue formation was significantly increased during skeletal muscle regeneration and further increased when 1α,25$(OH)_2D_3$ at BW dose was intramuscularly administered as determined by vimentin protein expression (a marker of muscular fibrosis) (Fig. 9A). Quantitative analysis revealed an approximate 4-fold increase in vimentin protein expression during skeletal muscle regeneration compared to control. Moreover, vimentin protein expression was significantly increased after 1α,25$(OH)_2D_3$ administration at BW dose compared to vehicle group (18.7±2.6% vs. 12.6±1.0%) (p<0.05) (Fig. 9B). The expressions of vimentin protein in control and regenerative muscle with either vehicle or 1α,25$(OH)_2D_3$ administrated at both MW and BW doses was confirmed with Western blot analysis (Fig. 9C).

- **No change of capillary density**

Revascularization is required during skeletal muscle regeneration to deliver nutrients and oxygen supply for functional recovery. Immunostaining of CD31, an endothelial cell marker that used to determine angiogenesis was illustrated in Fig. 9D. In control muscle, the percentage of CD31 area expression was approximately 3.1±0.2% and increased to 4.3±0.2%, 4.5±0.2%, and 4.5±0.5% during skeletal muscle regeneration after administrations of vehicle and 1α,25$(OH)_2D_3$ at MW and BW doses, respectively. However, there was no significant difference between vehicle- and 1α,25$(OH)_2D_3$-administrated groups (Fig. 9E). CD31 protein expression in control, vehicle- and 1α,25$(OH)_2D_3$-administrated groups was confirmed with Western blot analysis (Fig. 9F).

Discussion

In the present study, we examined the action of the bioactive form of vitamin D_3 [1α,25$(OH)_2D_3$] via intramuscular administration during skeletal muscle regeneration. The significant findings of our work are: 1) regenerative muscle expressed VDR and vitamin D_3 metabolizing enzyme (CYP24A1 and CYP27B1) proteins which suggest the local metabolism of vitamin D_3 in skeletal muscle during regenerative process; 2) an increased VDR protein expression in regenerative muscle after intramuscular administration of 1α,25$(OH)_2D_3$ was verified with VDR (D-6) antibody. This antibody was reported as highly sensitive antibody to detect VDR protein expression in skeletal muscle tissue; 3) intramuscular administration of 1α,25$(OH)_2D_3$ at MW and BW doses into regenerative muscle had a dose-dependent effect on skeletal muscle regenerative capacity and muscular fibrosis but not angiogenesis.

Expression of VDR protein is currently under debated and contradictory results have been reported in normal skeletal muscle. Western blot analysis using VDR (D-6), which has the highest sensitivity to VDR, to verify VDR protein expression was undetectable (30) and detectable (9) in whole muscle lysate. Moreover, VDR protein was expressed in normal skeletal muscle with immunohistochemistry using VDR (D-6) antibody (9), but this evidence has not been reported in the other investigations (31). Although, VDR protein was barely detectable in normal skeletal muscle, it was substantially expressed and localized in regenerative muscle fibers during skeletal muscle regeneration using VDR (H-81) antibody (26). In the present study, we further confirmed that VDR protein was expressed during skeletal muscle regeneration using highly sensitive VDR (D-6) antibody (29). Both VDR (D-6) and VDR (H-81) antibodies were raised against identical amino acids 344-424 of VDR of human origin, except the host species of VDR (D-6) was mouse monoclonal and VDR (H-81) was rabbit polyclonal. The specificity of VDR (H-81) was verified with VDR (D-6) antibody on its ability to detect VDR protein in regenerative muscle using immunohistochemical

analysis. The results confirmed the expression of VDR protein in the central nuclei of regenerative muscle fibers can be detected with both VDR (H-81) and VDR (D-6) antibodies.

Skeletal muscle regeneration is the self-repairing process after muscle injury in which the regenerative capacity relies on the function of satellite cells (10). However, whether endogenous VDR protein is expressed in satellite cells is currently unknown. Here, we demonstrated that satellite cells expressed VDR protein during skeletal muscle regeneration as demonstrated by the co-localization of Pax7 and VDR proteins. This finding suggests the possible direct action of vitamin D_3 on myogenesis during the regenerative process and further extends the knowledge on VDR protein expression in regenerative muscle (26). To support this notion, the presence of endogenous VDR protein expression was reported in the nucleus of C2C12 myoblasts (6, 8, 26) and primary myotubes isolated from skeletal muscle fibers (9) suggesting satellite cells could be the source of VDR after skeletal muscle injury.

The intramuscular administration of $1\alpha,25(OH)_2D_3$ was performed in this study to verify the direct action of $1\alpha,25(OH)_2D_3$ at the injured site. The beneficial effect of intramuscular administration of the bioactive form of vitamin D_3 was the ability to control the concentration of $1\alpha,25(OH)_2D_3$ at the administered site, maximize the interaction of $1\alpha,25(OH)_2D_3$ to its receptor, and reduce the undesired systemic effect to the other tissues. In this study, two doses of $1\alpha,25(OH)_2D_3$ with consecutive administration during skeletal muscle regeneration were investigated to clarify the dose dependent effect of $1\alpha,25(OH)_2D_3$. The results demonstrated that intramuscular administration of $1\alpha,25(OH)_2D_3$ at both MW and BW doses significantly increase VDR protein expression in regenerative muscle. The effective dose which increased VDR protein expression was similar to the systemic dose (1 μg/kg BW) that is used to investigate calcemic function of $1\alpha,25(OH)_2D_3$ in the duodenum (a vitamin D_3 sensitive tissue) (11). However, VDR protein expression was slightly increased (1.8-fold) in the BW dose administration compared to MW dose. This result raised the possibility that regenerative

457 muscle has a local control of vitamin D_3 metabolism to regulate the response to high
458 concentration of 1α,25$(OH)_2D_3$.

459 *In vitro* study in primary myotubes revealed that when the cells were treated with
460 1α,25$(OH)_2D_3$, CYP24A1 mRNA expression was significantly increased as a dose dependent
461 manner in response to 1α,25$(OH)_2D_3$ treatments (9). In the current investigation, CYP24A1
462 protein expression was increased after 1α,25$(OH)_2D_3$ was administrated at BW dose suggesting
463 the local regulation of 1α,25$(OH)_2D_3$ concentration *in vivo*. The increase in CYP24A1 possibly
464 decreased the toxicity of high concentration of 1α,25$(OH)_2D_3$ to regenerative muscle. Besides
465 CY24A1 protein expression, we investigated the expression level of CYP27B1 protein, a
466 vitamin D_3 regulating enzyme, which was previously reported to be expressed in regenerative
467 muscle (26). 1α,25$(OH)_2D_3$ administration at both MW and BW doses did not change
468 CYP27B1 protein level. This result could imply that the regulation of this enzyme was less
469 affected by 1α,25$(OH)_2D_3$ concentration *in vivo*. In contrast, the regulation of CYP27B1
470 protein was dependent on the level of 25$(OH)D_3$ as demonstrated by luciferase reporter assays
471 studied in both C2C12 myoblasts (8) and primary myotubes (9).

472 Impairments in muscle regenerative capacity were demonstrated after 1α,25$(OH)_2D_3$
473 administration at BW dose as CSA analysis revealed an significant increase in regenerating
474 muscle fibers with a size <600 μm^2. This suppressive effect of 1α,25$(OH)_2D_3$ on skeletal
475 muscle regeneration could involve either decrease satellite cell differentiation that led to
476 impaired regenerative muscle fiber formation or suppression of protein synthesis signaling in
477 regenerative muscle. Here, administration of 1α,25$(OH)_2D_3$ at BW dose induced a significant
478 decrease in proteins related to satellite cell differentiation (myogenin) and regenerative muscle
479 fiber formation (EbMHC) during skeletal muscle regeneration. Suppression of these two
480 proteins after 1α,25$(OH)_2D_3$ treatment in C2C12 myotubes *in vitro* supported the finding *in*
481 *vivo*. These data suggest that satellite cell differentiation and regenerative muscle formation
482 could be impaired after high concentrations of 1α,25$(OH)_2D_3$ are administered. However, the

major pathway of skeletal muscle protein synthesis was not affected by 1α,25$(OH)_2D_3$ administration. Phosphorylation of Akt, P70 S6K1, and 4E-BP1 proteins relative to their total protein expressions were not altered. Moreover, myostatin protein expression during skeletal muscle regeneration was not influenced by 1α,25$(OH)_2D_3$ administration. Taken together, these results suggest that 1α,25$(OH)_2D_3$ could interfere with the process of muscle stem cell differentiation that leads to impaired regenerative muscle fiber formation rather than suppressing protein synthesis signaling in regenerative muscle.

Although mouse TA muscle is a majority of fast muscle fibers (>99%) (3), we observed a tend to increase slow MHC protein expression with no significant change of fast MHC when 1α,25$(OH)_2D_3$ was administrated at BW dose compared to vehicle-administrated. These data are in contrast to the previous reported that fast MHC expression was increased in differentiated C2C12 myoblasts after 1 nM of 1α,25$(OH)_2D_3$ treatment (16). This discrepancy may rely on the aspect that differentiated C2C12 myoblasts in cultured do not contain all the characteristics of regenerating muscle fibers. Moreover, lacking nerve innovation and interaction between growth factors during the regenerative phase are limitations in an investigation of fiber type transition in the culture system. Therefore, this limitations may lead to the differential response of fiber type transition after 1α,25$(OH)_2D_3$ administration *in vivo* vs. *in vitro* studies.

Full recovery of skeletal muscle regeneration requires the balance between regenerating muscle fibers and connective tissue formation where excess connective tissue formation leads to muscular fibrosis. Related with an impairment of regenerative capacity after 1α,25$(OH)_2D_3$ administration at BW dose, vimentin protein expression was significantly increased. The presence of muscle fibrosis could be related to the action of 1α,25$(OH)_2D_3$ that acts as a suppressor of myogenin and EbMHC protein expression. Indeed, administration of activated 7-dehydrocholesterol via subcutaneous administration to rats increased prolyl-4-hydroxylase-β

508 expression for 4 and 14 days following contusion suggesting an excessive deposition of
509 extracellular matrix protein after vitamin D_3 treatment (27).

510 Angiogenesis is crucial for skeletal muscle regeneration in order to increase blood
511 supply and nutrient delivery to regenerating muscle. Two pro-angiogenic growth factors
512 (VEGF-A and FGF-1) were increased while myogenic and/or angiogenic inhibitors (FGF-2
513 and TIMP-3) were decreased in C2C12 myoblasts treated with $1\alpha,25(OH)_2D_3$. These results
514 suggest that $1\alpha,25(OH)_2D_3$ could enhance angiogenesis *in vitro* (5). However, we did not
515 detect the effect of $1\alpha,25(OH)_2D_3$ at both administrated doses on angiogenesis during muscle
516 regeneration *in vivo*. These results may imply that the potential effect of $1\alpha,25(OH)_2D_3$ *in vitro*
517 was not sufficient to promote angiogenesis during skeletal muscle regeneration.

518 In conclusion, regenerative muscle could be the target of vitamin D_3 action *in vivo* as it
519 expresses VDR and vitamin D_3 metabolizing enzymes (CYP24A1 and CYP27B1) proteins
520 during skeletal muscle regeneration. Increased VDR and CYP24A1 protein expression in
521 response to a high dose of $1\alpha,25(OH)_2D_3$ suggests a local regulation of $1\alpha,25(OH)_2D_3$ in
522 regenerative muscle. Decreased satellite cell differentiation, delayed regenerative muscle fiber
523 formation, and increased muscular fibrosis were evident when $1\alpha,25(OH)_2D_3$ was
524 intramuscularly administered at BW dose. However, protein synthesis signaling, fiber type
525 composition, and angiogenesis in regenerative muscle were not affected by $1\alpha,25(OH)_2D_3$
526 administration at any dose investigated. The novelty of this work is the finding of non-calcemic
527 functions of $1\alpha,25(OH)_2D_3$ on regenerative capacity and muscular fibrosis during skeletal
528 muscle regeneration. The results of the present study provide a significant contribution to the
529 field regarding knowledge of the physiological functions of the bioactive form of vitamin D_3
530 and vitamin D_3 metabolizing enzymes on the regenerative process of skeletal muscle.

Acknowledgements: This research project was supported by 1) Thailand Research Fund (TRF), Office of the Higher Education Commission, and Mahidol University (MRG5680061 to RS) and 2) Faculty of Science, Mahidol University (to RS). Authors gratefully acknowledge supported from the Olympus Bioimaging Center at Faculty of Science, Mahidol University. We thank Prof. Chumpol Pholpramool for kindly gifting the mouse C2C12 cell line and initial suggestions on developing this project. We also thank Kanokwan Suhatcho and Narut Leerasantana for technical assistance. Proofreading of the manuscript by Assistant Professor Dr. Christopher Fry is appreciated.

Disclosure: No conflicts of interest, financial or otherwise, are declared by the author(s).

Author Contributions: R.S. conception and design of research; R.S. M.H. performed experiments; R.S. M.H. analyzed data; R.S M.H. interpreted results of experiments; R.S. prepared figures; R.S. drafted manuscript; R.S M.H. edited and revised manuscript; all authors approved final version of manuscript

546 **Figure Captions**

547 **Fig. 1 Experimental diagram and muscle wet weight to body weight ratio.** (A)
548 Experimental diagram for consecutive intramuscular administration of 1α,25$(OH)_2D_3$ during
549 skeletal muscle regeneration. Vehicle and 1α,25$(OH)_2D_3$ at MW and BW doses were
550 administered daily via intramuscular injections during day 4 to 7 post-injury. This
551 administration period represents the regenerative phase. (B) TA muscle wet weight was
552 normalized to mouse body weight and plotted as control, vehicle-administrated, and
553 1α,25$(OH)_2D_3$ MW and BW doses administrated groups (n=6/group), *p<0.05 compared to
554 control group. 1α,25$(OH)_2D_3$ (MW) and (BW) represent dose at 1 μg/kg relative to TA muscle
555 wet weight and mouse body weight, respectively.

556

557 **Fig. 2 Localization of VDR protein in regenerative muscle and the response to**
558 **intramuscular administration of 1α,25$(OH)_2D_3$**. (A) Expression of VDR protein in central
559 nuclei of regenerative muscle fibers using VDR (D-6) antibody, arrows indicate VDR-positive
560 nuclei. Representative images were captured at 400× magnification with scale bars 20 μm. (B)
561 VDR protein was expressed and localized in the nucleus of satellite cells (Pax7 positive nuclei)
562 as determined by co-localization of VDR (H-81) and Pax7 proteins (arrows). (C) The
563 specificity of VDR (D-6) vs. VDR (H-81) to detected VDR protein in regenerative muscle was
564 verified. Representative images of B-C were captured at 200× magnification (cropped) with
565 scale bars 20 μm and 10 μm, respectively. (D) Western blot analysis revealed VDR protein
566 expression in control, vehicle-administrated, and 1α,25$(OH)_2D_3$ at MW and BW doses
567 administrated groups. GAPDH was used as a loading control. *p<0.05, **p<0.01 compared to
568 control group (n=6/group). 1α,25$(OH)_2D_3$ (MW) and (BW) represent dose at 1 μg/kg relative
569 to TA muscle wet weight and mouse body weight, respectively.

Fig. 3 Expression of vitamin D_3 metabolizing enzymes in response to intramuscular administration of 1α,25(OH)$_2$D$_3$. (A) Western blot analysis revealed CYP24A1 protein expression in control, vehicle-administrated, and 1α,25(OH)$_2$D$_3$ at MW and BW doses administrated groups, *p<0.05 compared to control group (n=6/group). GAPDH was used as a loading control. (B) CYP24A1 protein is localized in regenerative muscle fibers and the extracellular matrix compartment. Co-localization of CYP24A1 and VDR proteins was detected in central nuclei of regenerative muscle fibers. Representative images were captured at 400× magnification with scale bars 20 μm. (C) CYP24A1 protein was expressed predominantly in the nucleus of C2C12 myoblasts and co-localized with VDR after 1α,25(OH)$_2$D$_3$ treatment at 10 nM for 24 h. Barely overlapping with ATP synthase (complex V) subunit alpha (OxPhos) was detected in C2C12 myoblasts under the same experimental condition. Representative images were captured at 200× magnification with scale bars 100 μm. (D) Western blot analysis revealed CYP27B1 protein expression in control, vehicle-administrated, and at MW and BW doses administrated groups (n=6/group). GAPDH was used as a loading control. (E) CYP27B1 protein is predominantly localized in the mitochondrial compartment of regenerative muscle fibers (OxPhos positive-stained) and the extracellular matrix. Representative images were captured at 200× magnification (cropped) with scale bars 20 μm. 1α,25(OH)$_2$D$_3$ (MW) and (BW) represent dose at 1 μg/kg relative to TA muscle wet weight and mouse body weight, respectively.

Fig. 4 Regenerative muscle fiber size in response to in response to intramuscular administration of 1α,25(OH)$_2$D$_3$. (A) Representative H&E-stained sections from control, vehicle-administrated, and 1α,25(OH)$_2$D$_3$ at MW and BW doses administrated groups. 1α,25(OH)$_2$D$_3$ (MW) and (BW) represent dose at 1 μg/kg relative to TA muscle wet weight and mouse body weight. Small regenerative muscle fibers were observed in 1α,25(OH)$_2$D$_3$ at MW and BW doses administrated groups compared to vehicle-administrated group.

596 Representative images were captured at 200× magnification with scale bars 100 μm. (B) The
597 average number of regenerative muscle fibers size <600 μm^2 compared between control,
598 vehicle-administrated, and 1α,25$(OH)_2D_3$ at MW and BW doses administrated groups.
599 **p<0.01 compared to vehicle-administrated group (n=6/group). (C) CSA histogram revealed a
600 leftward shift of regenerative muscle fiber size <600 μm^2 in 1α,25$(OH)_2D_3$ at BW dose
601 administrated compared to vehicle-administrated groups. The total number of measured fibers
602 was 3,936 fibers for vehicle-administrated group and 4,979 fibers for 1α,25$(OH)_2D_3$ at BW
603 dose group (n=6/group).
604
605 **Fig. 5 Myogenin protein expression in responses to 1α,25$(OH)_2D_3$ administration *in vivo***
606 **and *in vitro*.** (A) Representative images for identification of differentiated satellite cells in
607 regenerative muscle. Differentiated satellite cells were identified as myogenin-positive nuclei
608 (arrows). Laminin was counterstained for visualization of regenerative muscle fibers and DAPI
609 was stained for nuclear localization. Merged image shown in the right panel. (B)
610 Representative images of myogenin positive nuclei in control, vehicle-administrated, and
611 1α,25$(OH)_2D_3$ at MW and BW doses administrated groups. Images of panels A-B were
612 captured at 200× magnification with scale bars 100 μm. (C) Quantitative analysis of myogenin
613 positive nuclei in vehicle-administrated and 1α,25$(OH)_2D_3$ at MW and BW doses
614 administrated groups (n=6/group). *p<0.05 compared to vehicle-administrated group. (D)
615 Western blot analysis revealed myogenin protein expression in control, vehicle-administrated,
616 and 1α,25$(OH)_2D_3$ at MW and BW doses administrated groups. GAPDH was used as a loading
617 control. 1α,25$(OH)_2D_3$ (MW) and (BW) represent dose at 1 μg/kg relative to TA muscle wet
618 weight and mouse body weight, respectively. (E) Representative images of myogenin-positive
619 nuclei in C2C12 myotubes that were treated with 1α,25$(OH)_2D_3$ at 0.1, 1, and 10 nM compared
620 to vehicle-treated group. Images of panel E were captured at 100× magnification with scale
621 bars 200 μm. (F) Quantitative analysis of myogenin-positive nuclei in control, vehicle-treated,

622 and 1α,25(OH)$_2$D$_3$ at 0.1, 1, and 10 nM treated groups. Six images were used for counting the
623 number of myogenin positive nuclei. *p<0.05 compared to vehicle-treated group (n= 3
624 replicate experiments).
625
626 **Fig. 6 EbMHC protein expression in responses to 1α,25(OH)$_2$D$_3$ administration *in vivo***
627 **and *in vitro*.** (A) Representative images for identification of EbMHC protein expression in
628 regenerative muscle. Newly formed regenerative muscle fibers were identified by the
629 expression of EbMHC (arrows). Laminin was counterstained for visualization of regenerative
630 muscle fibers and DAPI was stained for nuclear localization. Merged image shown in the right
631 panel. (B) Representative of EbMHC-positive fibers in control, vehicle-administrated, and
632 1α,25(OH)$_2$D$_3$ at MW and BW doses administrated groups. Images of panels A-B were
633 captured at 200× magnification with scale bars 100 μm. (C) Quantitative analysis on the
634 percentage of EbMHC protein expression in vehicle-administrated and 1α,25(OH)$_2$D$_3$ at MW
635 and BW doses administrated groups (n=6/group). *p<0.05, $^{\#}p$<0.05 compared to vehicle-
636 administrated and 1α,25(OH)$_2$D$_3$ at MW dose administrated groups, respectively. (D) Western
637 blot analysis from myofibrillar protein fraction revealed EbMHC protein expression in control,
638 vehicle-administrated, and 1α,25(OH)$_2$D$_3$ at MW and BW doses administrated groups. Ponceau
639 S was used as a loading control. 1α,25(OH)$_2$D$_3$ (MW) and (BW) represent dose at 1 μg/kg
640 relative to TA muscle wet weight and mouse body weight, respectively. (E) Representative
641 images of EbMHC protein expression in C2C12 myotubes that were treated with
642 1α,25(OH)$_2$D$_3$ at 0.1, 1, and 10 nM compared to vehicle-treated group. Images of panel E were
643 captured at 100× magnification with scale bars 200 μm. (F) Quantitative analysis of EbMHC
644 protein expression in control, vehicle-treated, and 1α,25(OH)$_2$D$_3$ at 0.1, 1, and 10 nM treated
645 groups. Twenty-five images were used for analysis of EbMHC area of expression. *p<0.05,
646 **p<0.01, ***p<0.001 compared to vehicle-treated group (n= 3 replicate experiments).

Fig. 7 Muscle protein synthesis signaling in response to intramuscular administration of 1α,25(OH)$_2$D$_3$. Western blot analysis of (A) phospho-p70 s6K1 and total p70 s6K1 (B) phospho-4E-BP1 and total 4E-BP1 (C) phospho-Akt and total Akt and (D) myostatin protein expression in control, vehicle-administrated, and 1α,25(OH)$_2$D$_3$ at MW and BW doses administrated groups. GAPDH was used as a loading control for myostatin protein expression. **p*<0.05 compared to control group (n=6/group). 1α,25(OH)$_2$D$_3$ (MW) and (BW) represent dose at 1 μg/kg relative to TA muscle wet weight and mouse body weight, respectively.

Fig. 8 Fast MHC and slow MHC protein expression in responses to intramuscular administration of 1α,25(OH)$_2$D$_3$. (A) Representative images for identification of fast MHC and slow MHC protein expression in control and regenerative muscles. Fast MHC was illustrated in green and slow MHC was illustrated in red, DAPI was stained for nuclear localization. Merged image shown in the right panel. Images were captured at 100× magnification with scale bars 200 μm. (B) Western blot analysis from myofibrillar protein fraction revealed fast MHC and slow MHC protein expression in control, vehicle-administrated, and 1α,25(OH)$_2$D$_3$ at MW and BW doses administrated groups (n=6/group). (C) Western blot analysis from cytosolic protein fraction revealed fast MHC and slow MHC protein expression in control, vehicle-administrated, and 1α,25(OH)$_2$D$_3$ at MW and BW doses administrated groups (n=6/group). Ponceau S and GAPDH were used as loading control for myofibrillar and cytosolic protein expression, respectively. 1α,25(OH)$_2$D$_3$ (MW) and (BW) represent dose at 1 μg/kg relative to TA muscle wet weight and mouse body weight, respectively.

Fig. 9 Connective tissue formation and angiogenesis in responses to 1α,25(OH)$_2$D$_3$ administration. (A) Representative images of vimentin protein expression in control, vehicle-administrated, and 1α,25(OH)$_2$D$_3$ at MW and BW doses administrated groups. (B) Quantitative analysis on the percentage of vimentin protein expression in control, vehicle-administrated, and 1α,25(OH)$_2$D$_3$ at MW and BW doses administrated groups. $^{**}p<0.01$ compared to control group; $^{\#}p<0.05$ compared to vehicle and 1α,25(OH)$_2$D$_3$ at MW dose administrated groups. (C) Western blot analysis revealed vimentin protein expression in control, vehicle-administrated, and 1α,25(OH)$_2$D$_3$ at MW and BW doses administrated groups (n=6/group). GAPDH was used as a loading control. (D) Representative images of CD31 protein expression in control, vehicle-administrated, and 1α,25(OH)$_2$D$_3$ at MW and BW doses administrated groups. (E) Quantitative analysis on the percentage of CD31 protein expression in control, vehicle-administrated, and 1α,25(OH)$_2$D$_3$ at MW and BW doses administrated groups. (F) Western blot analysis revealed CD31 protein expression in control, vehicle-administrated, and 1α,25(OH)$_2$D$_3$ at MW and BW doses administrated groups (n=6/group). GAPDH was used as a loading control. Images of panels A and D were captured at 200× magnification with scale bars 100 μm. 1α,25(OH)$_2$D$_3$ (MW) and (BW) represent dose at 1 μg/kg relative to TA muscle wet weight and mouse body weight, respectively.

686 **References**

687 1. **Bischoff-Ferrari HA, Borchers M, Gudat F, Durmuller U, Stahelin HB, Dick W**.
688 Vitamin D receptor expression in human muscle tissue decreases with age. *J Bone Miner*
689 *Res* 19: 265-269, 2004.

690 2. **Bischoff HA, Borchers M, Gudat F, Duermueller U, Theiler R, Stahelin HB, Dick W**.
691 In situ detection of 1,25-dihydroxyvitamin D3 receptor in human skeletal muscle tissue.
692 *Histochem J* 33: 19-24, 2001.

693 3. **Bloemberg D, Quadrilatero J**. Rapid determination of myosin heavy chain expression in
694 rat, mouse, and human skeletal muscle using multicolor immunofluorescence analysis.
695 *PloS one* 7: e35273, 2012.

696 4. **Endo I, Inoue D, Mitsui T, Umaki Y, Akaike M, Yoshizawa T, Kato S, Matsumoto T**.
697 Deletion of vitamin D receptor gene in mice results in abnormal skeletal muscle
698 development with deregulated expression of myoregulatory transcription factors.
699 *Endocrinology* 144: 5138-5144, 2003.

700 5. **Garcia LA, Ferrini MG, Norris KC, Artaza JN**. 1,25(OH)(2)vitamin D(3) enhances
701 myogenic differentiation by modulating the expression of key angiogenic growth factors
702 and angiogenic inhibitors in C(2)C(12) skeletal muscle cells. *J Steroid Biochem Mol Biol*
703 133: 1-11, 2013.

704 6. **Garcia LA, King KK, Ferrini MG, Norris KC, Artaza JN**. 1,25(OH)2vitamin D3
705 stimulates myogenic differentiation by inhibiting cell proliferation and modulating the
706 expression of promyogenic growth factors and myostatin in C2C12 skeletal muscle cells.
707 *Endocrinology* 152: 2976-2986, 2011.

708 7. **Ge Y, Wu AL, Warnes C, Liu J, Zhang C, Kawasome H, Terada N, Boppart MD,**
709 **Schoenherr CJ, Chen J**. mTOR regulates skeletal muscle regeneration in vivo through
710 kinase-dependent and kinase-independent mechanisms. *Am J Physiol Cell Physiol* 297:
711 C1434-1444, 2009.

8. **Girgis CM, Clifton-Bligh RJ, Mokbel N, Cheng K, Gunton JE**. Vitamin D signaling regulates proliferation, differentiation, and myotube size in C2C12 skeletal muscle cells. *Endocrinology* 155: 347-357, 2014.

9. **Girgis CM, Mokbel N, Cha KM, Houweling PJ, Abboud M, Fraser DR, Mason RS, Clifton-Bligh RJ, Gunton JE**. The vitamin D receptor (VDR) is expressed in skeletal muscle of male mice and modulates 25-hydroxyvitamin D (25OHD) uptake in myofibers. *Endocrinology* 155: 3227-3237, 2014.

10. **Hawke TJ, Garry DJ**. Myogenic satellite cells: physiology to molecular biology. *J Appl Physiol (1985)* 91: 534-551, 2001.

11. **Khuituan P, Teerapornpuntakit J, Wongdee K, Suntornsaratoon P, Konthapakdee N, Sangsaksri J, Sripong C, Krishnamra N, Charoenphandhu N**. Fibroblast growth factor-23 abolishes 1,25-dihydroxyvitamin D(3)-enhanced duodenal calcium transport in male mice. *Am J Physiol Endocrinol Metab* 302: E903-913, 2012.

12. **Lips P**. Vitamin D physiology. *Prog Biophys Mol Biol* 92: 4-8, 2006.

13. **Makanae Y, Ogasawara R, Sato K, Takamura Y, Matsutani K, Kido K, Shiozawa N, Nakazato K, Fujita S**. Acute bout of resistance exercise increases vitamin D receptor protein expression in rat skeletal muscle. *Exp Physiol* 100: 1168-1176, 2015.

14. **Mauro A**. Satellite cell of skeletal muscle fibers. *J Biophys Biochem Cytol* 9: 493-495, 1961.

15. **Melcon G, Kozlov S, Cutler DA, Sullivan T, Hernandez L, Zhao P, Mitchell S, Nader G, Bakay M, Rottman JN, Hoffman EP, Stewart CL**. Loss of emerin at the nuclear envelope disrupts the Rb1/E2F and MyoD pathways during muscle regeneration. *Hum Mol Genet* 15: 637-651, 2006.

16. **Okuno H, Kishimoto KN, Hatori M, Itoi E**. 1alpha,25-dihydroxyvitamin D(3) enhances fast-myosin heavy chain expression in differentiated C2C12 myoblasts. *Cell Biol Int* 36: 441-447, 2012.

17. **Olsson K, Saini A, Stromberg A, Alam S, Lilja M, Rullman E, Gustafsson T**. Evidence for vitamin D receptor expression and direct effects of 1alpha,25(OH)D in human skeletal muscle precursor cells. *Endocrinology* en20151685, 2015.

18. **Pojednic RM, Ceglia L, Lichtenstein AH, Dawson-Hughes B, Fielding RA**. Vitamin D receptor protein is associated with interleukin-6 in human skeletal muscle. *Endocrine* 49: 512-520, 2015.

19. **Pojednic RM, Ceglia L, Olsson K, Gustafsson T, Lichtenstein AH, Dawson-Hughes B, Fielding RA**. Effects of 1,25-dihydroxyvitamin D3 and vitamin D3 on the expression of the vitamin d receptor in human skeletal muscle cells. *Calcif Tissue Int* 96: 256-263, 2015.

20. **Prosser DE, Jones G**. Enzymes involved in the activation and inactivation of vitamin D. *Trends Biochem Sci* 29: 664-673, 2004.

21. **Relaix F, Zammit PS**. Satellite cells are essential for skeletal muscle regeneration: the cell on the edge returns centre stage. *Development* 139: 2845-2856, 2012.

22. **Salles J, Chanet A, Giraudet C, Patrac V, Pierre P, Jourdan M, Luiking YC, Verlaan S, Migne C, Boirie Y, Walrand S**. 1,25(OH)2-vitamin D3 enhances the stimulating effect of leucine and insulin on protein synthesis rate through Akt/PKB and mTOR mediated pathways in murine C2C12 skeletal myotubes. *Mol Nutr Food Res* 57: 2137-2146, 2013.

23. **Samuel S, Sitrin MD**. Vitamin D's role in cell proliferation and differentiation. *Nutr Rev* 66: S116-124, 2008.

24. **Seale P, Sabourin LA, Girgis-Gabardo A, Mansouri A, Gruss P, Rudnicki MA**. Pax7 is required for the specification of myogenic satellite cells. *Cell* 102: 777-786, 2000.

25. **Shi X, Garry DJ**. Muscle stem cells in development, regeneration, and disease. *Genes Dev* 20: 1692-1708, 2006.

26. **Srikuea R, Zhang X, Park-Sarge OK, Esser KA**. VDR and CYP27B1 are expressed in C2C12 cells and regenerating skeletal muscle: potential role in suppression of myoblast proliferation. *Am J Physiol Cell Physiol* 303: C396-405, 2012.

764 27. **Stratos I, Li Z, Herlyn P, Rotter R, Behrendt AK, Mittlmeier T, Vollmar B**. Vitamin
765 D increases cellular turnover and functionally restores the skeletal muscle after crush
766 injury in rats. *Am J Pathol* 182: 895-904, 2013.
767 28. **Wang TT, Tavera-Mendoza LE, Laperriere D, Libby E, MacLeod NB, Nagai Y,**
768 **Bourdeau V, Konstorum A, Lallemant B, Zhang R, Mader S, White JH**. Large-scale
769 in silico and microarray-based identification of direct 1,25-dihydroxyvitamin D3 target
770 genes. *Mol Endocrinol* 19: 2685-2695, 2005.
771 29. **Wang Y, Becklund BR, DeLuca HF**. Identification of a highly specific and versatile
772 vitamin D receptor antibody. *Arch Biochem Biophys* 494: 166-177, 2010.
773 30. **Wang Y, DeLuca HF**. Is the vitamin d receptor found in muscle? *Endocrinology* 152:
774 354-363, 2011.
775 31. **Wang Y, Zhu J, DeLuca HF**. Where is the vitamin D receptor? *Arch Biochem Biophys*
776 523: 123-133, 2012.

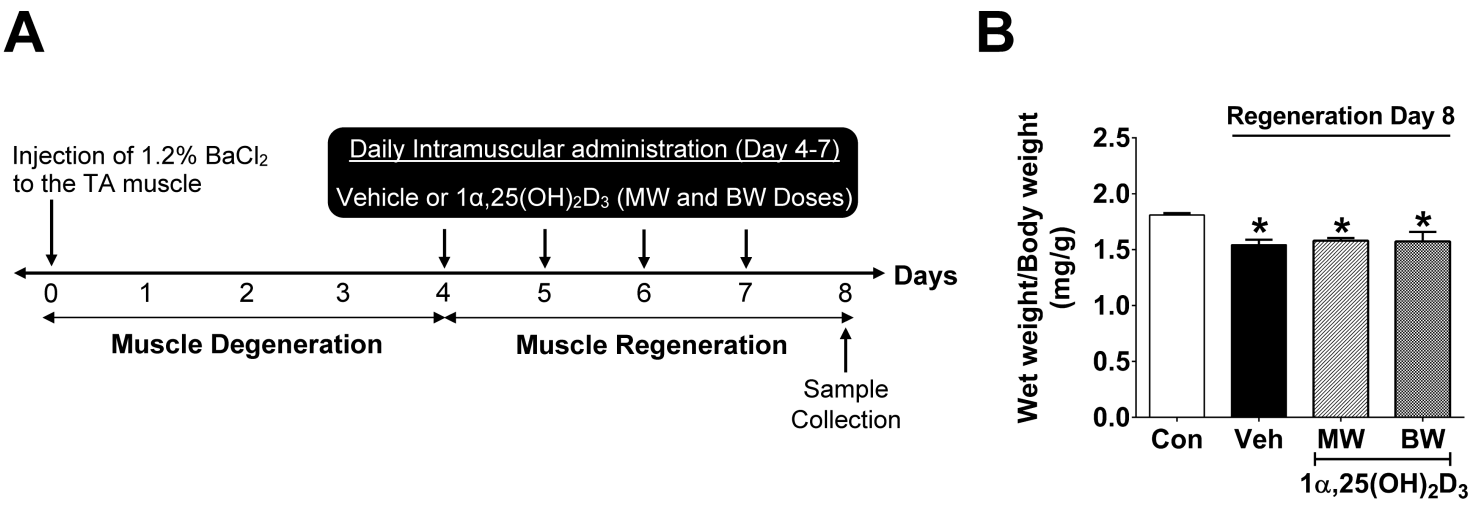
A
Injection of 1.2% BaCl2
to the TA muscle
Daily Intramuscular administration (Day 4-7)
Vehicle or 1α,25(OH)2D3 (MW and BW Doses)
0
1
2
3
4
5
6
7
8
Days
Muscle Degeneration
Muscle Regeneration
Sample
Collection
B
Regeneration Day 8
Wet weight/Body weight
(mg/g)
2.5
2.0
1.5
1.0
0.5
0.0
*
*
*
Con
Veh
MW
BW
1α,25(OH)2D3

Figure 1

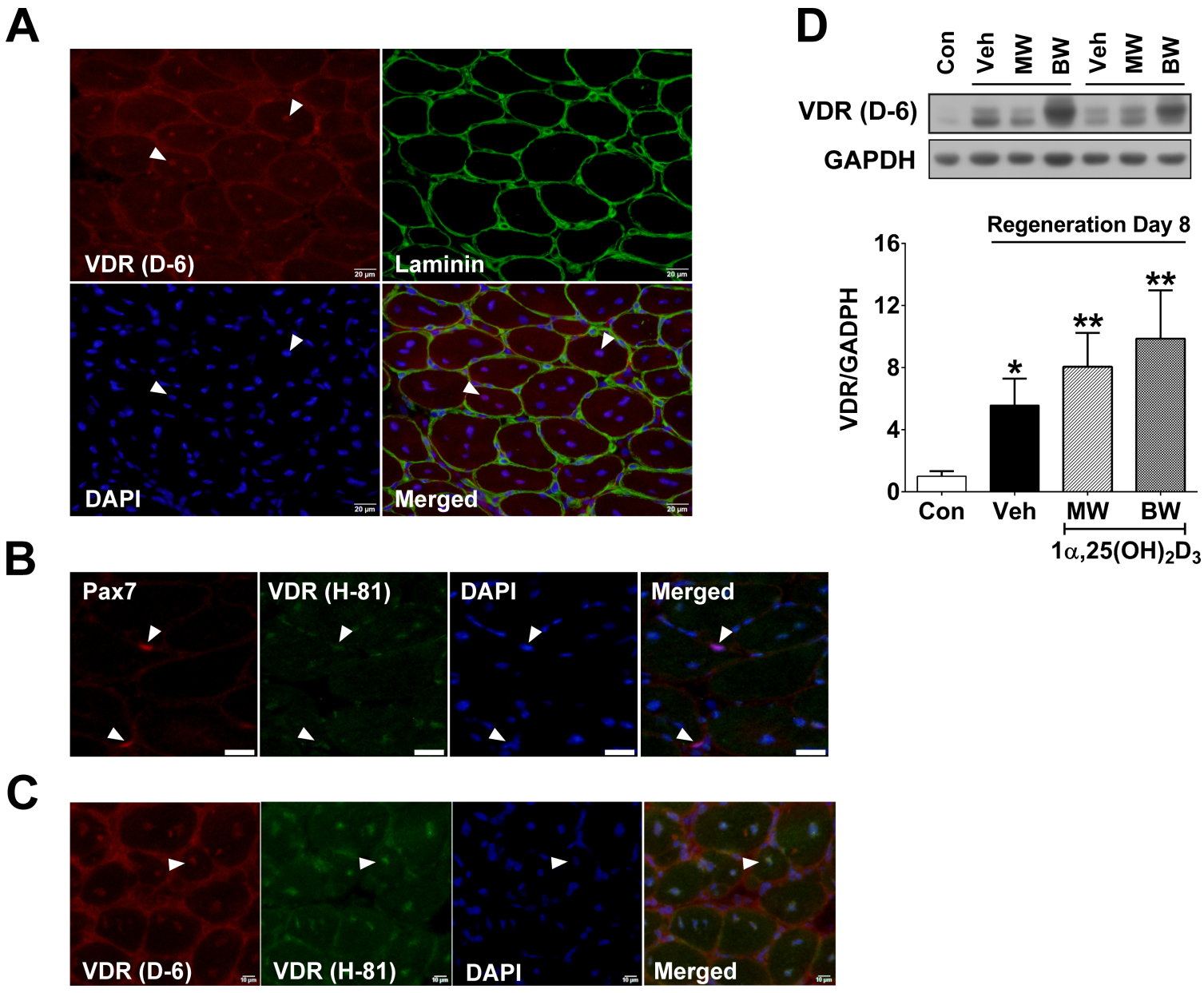
A
VDR (D-6)
Laminin
DAPI
Merged
B
Pax7
VDR (H-81)
DAPI
Merged
C
VDR (D-6)
VDR (H-81)
DAPI
Merged
D
Con
Veh
MW
BW
Veh
MW
BW
VDR (D-6)
GAPDH
Regeneration Day 8
VDR/GADPH
16
12
8
4
0
*
**
**
Con
Veh
MW
BW
1α,25(OH)2D3

Figure 2

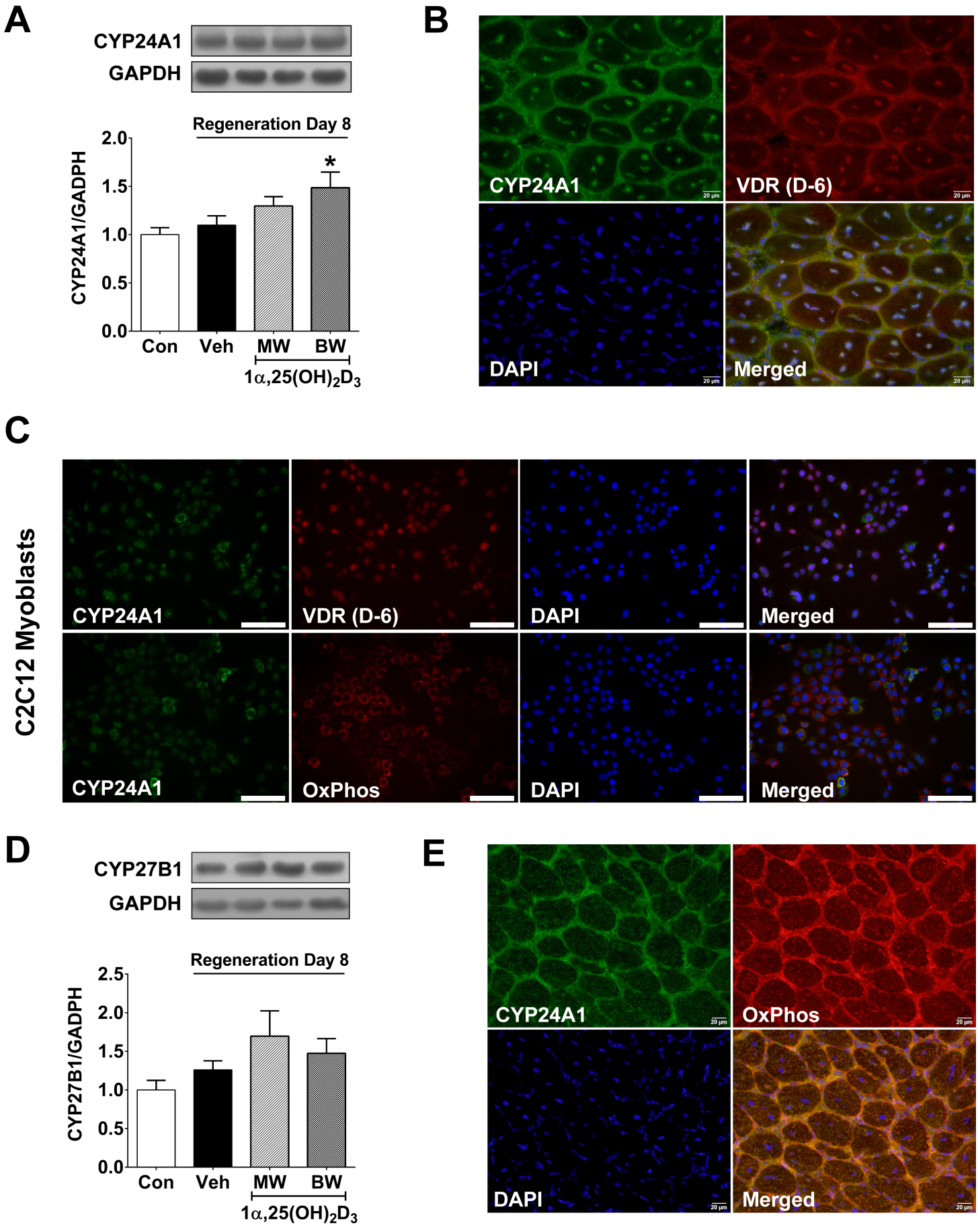
A
CYP24A1
GAPDH
Regeneration Day 8
CYP24A1/GADPH
2.0
1.5
1.0
0.5
0.0
*
Con
Veh
MW
BW
1α,25(OH)2D3
B
CYP24A1
VDR (D-6)
DAPI
Merged
C
C2C12 Myoblasts
CYP24A1
VDR (D-6)
DAPI
Merged
CYP24A1
OxPhos
DAPI
Merged
D
CYP27B1
GAPDH
Regeneration Day 8
CYP27B1/GADPH
2.5
2.0
1.5
1.0
0.5
0.0
Con
Veh
MW
BW
1α,25(OH)2D3
E
CYP24A1
OxPhos
DAPI
Merged

Figure 3

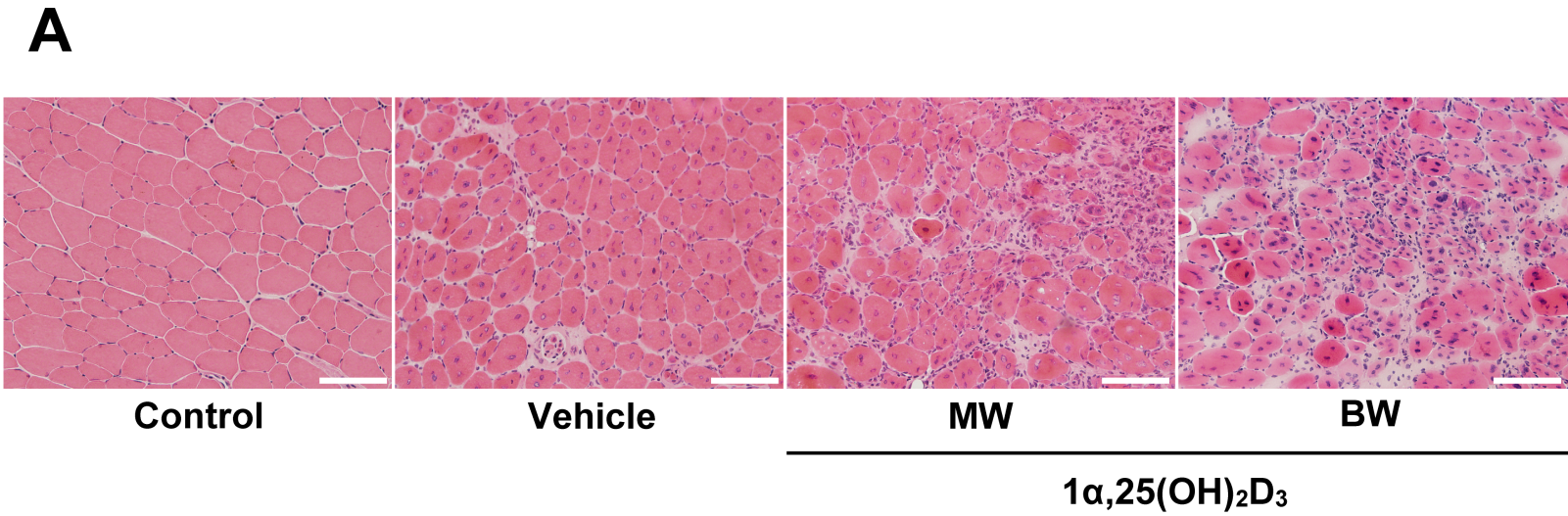
A
Control
Vehicle
MW
BW
1α,25(OH)2D3
B
Regeneration Day 8
No. Regenerative Fibers (Size<600 μm2)
400
300
200
100
0
**
Veh
MW
BW
1α,25(OH)2D3
C
1α,25(OH)2D3 (BW)
Vehicle
% of Fiber Number
30
25
20
15
10
5
0
0
300
600
900
1200
1500
1800
2100
2400
2700
3000
Regenerative Muscle Fiber CSA (μm2)

Figure 4

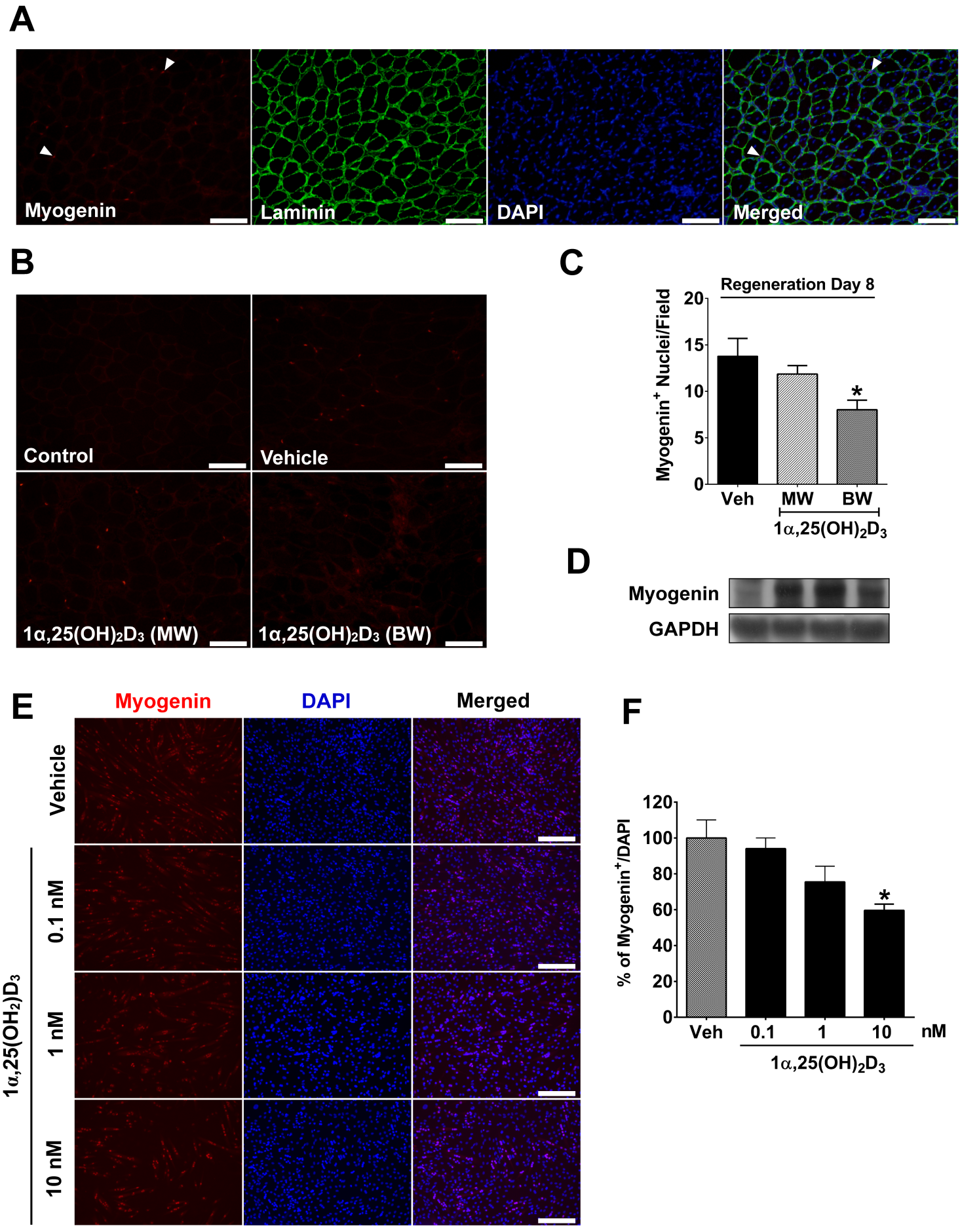
A
Myogenin
Laminin
DAPI
Merged
B
Control
Vehicle
1α,25(OH)2D3 (MW)
1α,25(OH)2D3 (BW)
C
Regeneration Day 8
Myogenin+ Nuclei/Field
20
15
10
5
0
Veh
MW
BW
*
1α,25(OH)2D3
D
Myogenin
GAPDH
E
Myogenin
DAPI
Merged
Vehicle
0.1 nM
1 nM
10 nM
1α,25(OH2)D3
F
% of Myogenin+/DAPI
120
100
80
60
40
20
0
Veh
0.1
1
10
nM
*
1α,25(OH)2D3

Figure 5

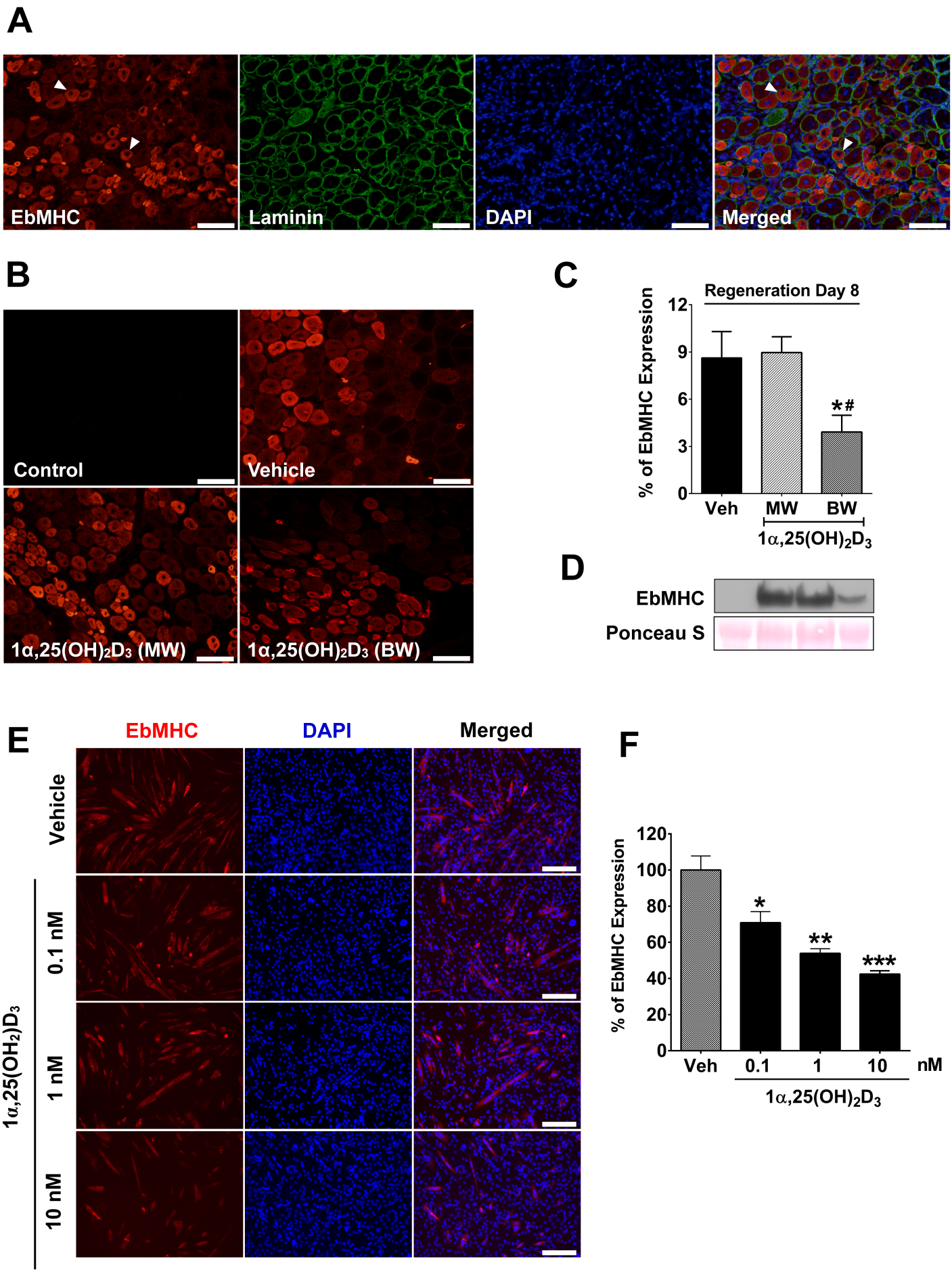
A
EbMHC
Laminin
DAPI
Merged
B
Control
Vehicle
1α,25(OH)2D3 (MW)
1α,25(OH)2D3 (BW)
C
Regeneration Day 8
% of EbMHC Expression
12
9
6
3
0
*#
Veh
MW
BW
1α,25(OH)2D3
D
EbMHC
Ponceau S
E
EbMHC
DAPI
Merged
Vehicle
0.1 nM
1 nM
10 nM
1α,25(OH2)D3
F
% of EbMHC Expression
120
100
80
60
40
20
0
*
**
***
Veh
0.1
1
10
nM
1α,25(OH)2D3

Figure 6

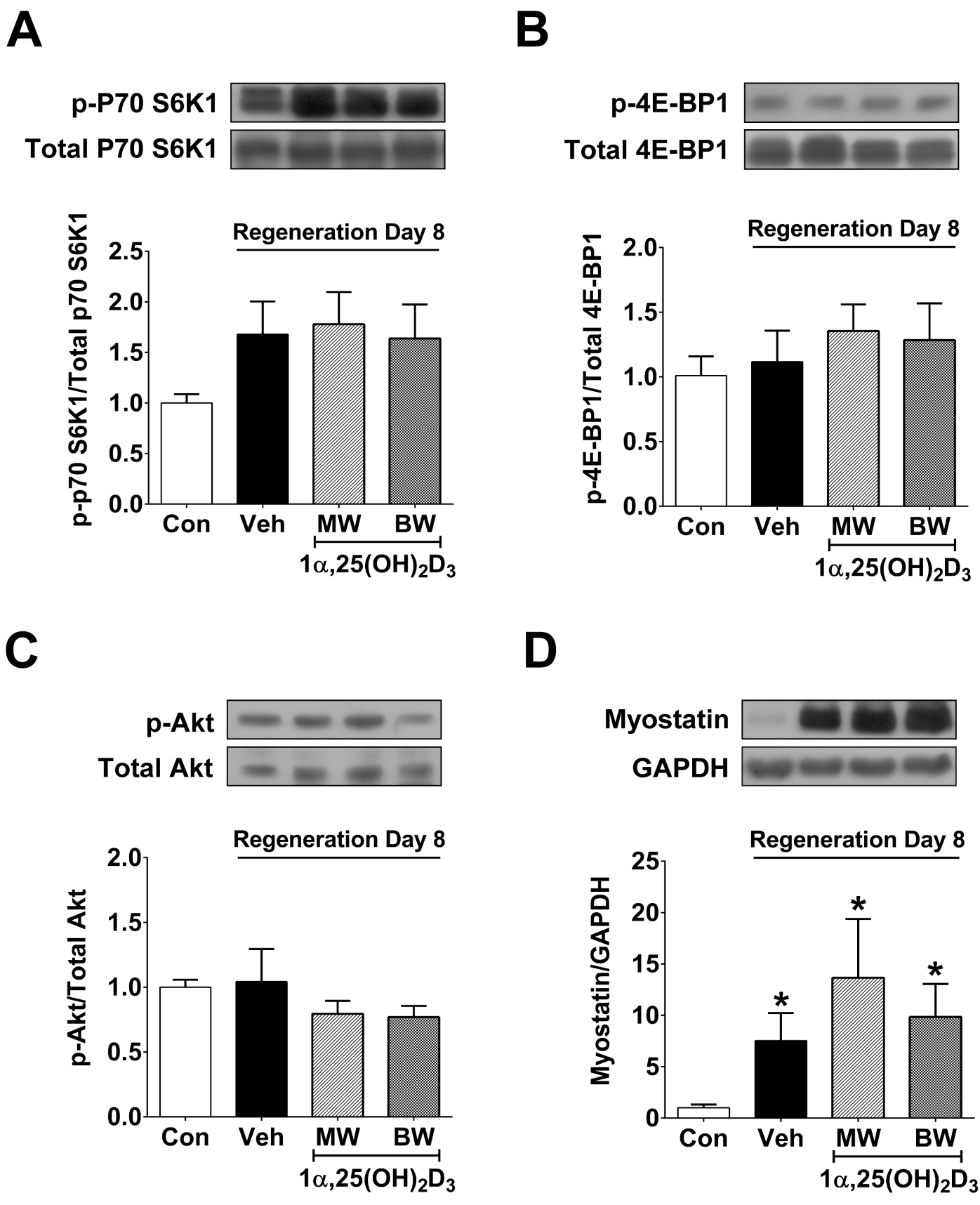
A
p-P70 S6K1
Total P70 S6K1
Regeneration Day 8
p-p70 S6K1/Total p70 S6K1
2.5
2.0
1.5
1.0
0.5
0.0
Con
Veh
MW
BW
1α,25(OH)2D3
B
p-4E-BP1
Total 4E-BP1
Regeneration Day 8
p-4E-BP1/Total 4E-BP1
2.0
1.5
1.0
0.5
0.0
Con
Veh
MW
BW
1α,25(OH)2D3
C
p-Akt
Total Akt
Regeneration Day 8
p-Akt/Total Akt
2.0
1.5
1.0
0.5
0.0
Con
Veh
MW
BW
1α,25(OH)2D3
D
Myostatin
GAPDH
Regeneration Day 8
Myostatin/GAPDH
25
20
15
10
5
0
*
*
*
Con
Veh
MW
BW
1α,25(OH)2D3

Figure 7

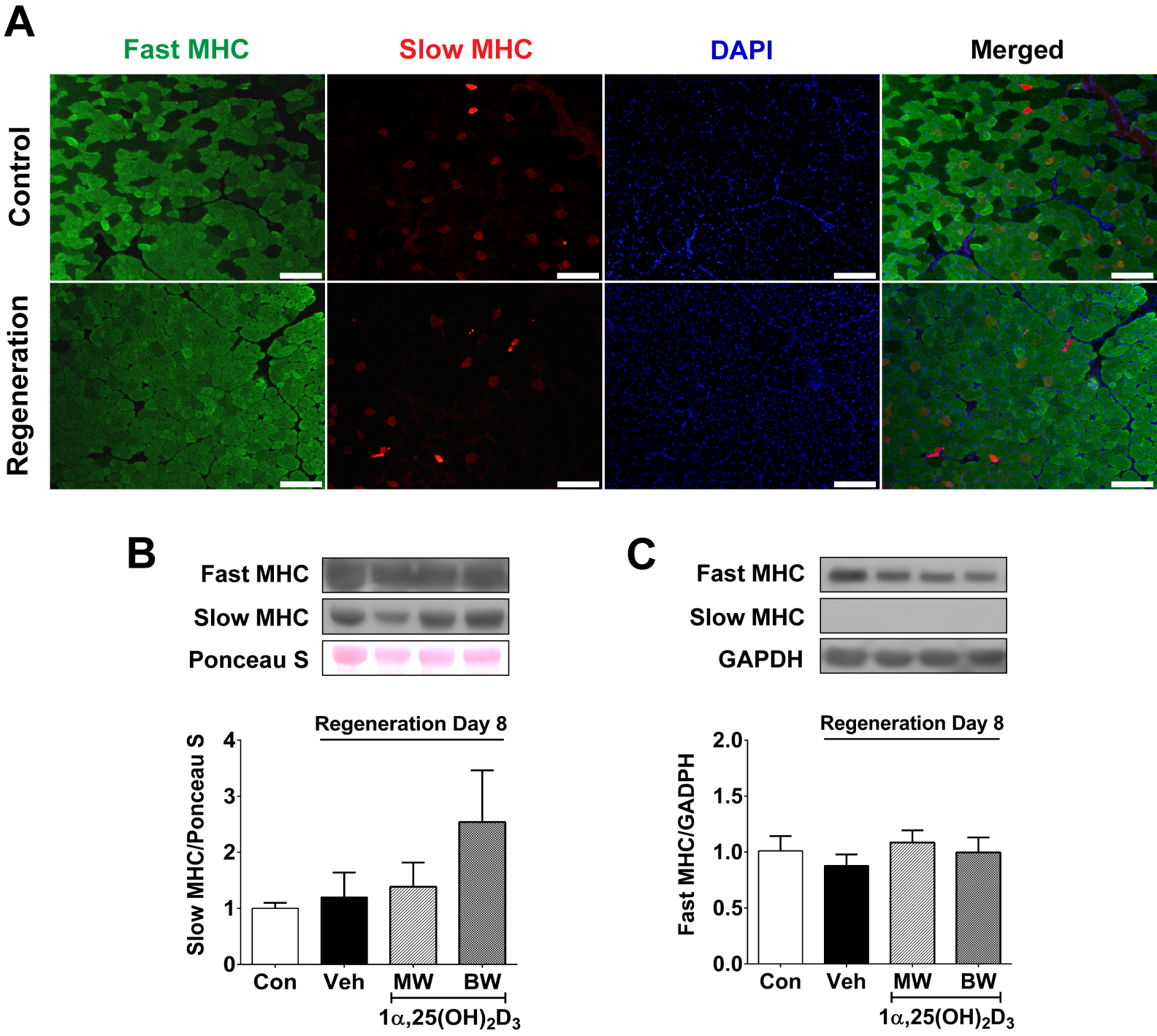
A
Fast MHC
Slow MHC
DAPI
Merged
Control
Regeneration
B
Fast MHC
Slow MHC
Ponceau S
Regeneration Day 8
Slow MHC/Ponceau S
0
1
2
3
4
Con
Veh
MW
BW
1α,25(OH)2D3
C
Fast MHC
Slow MHC
GAPDH
Regeneration Day 8
Fast MHC/GADPH
0.0
0.5
1.0
1.5
2.0
Con
Veh
MW
BW
1α,25(OH)2D3

Figure 8

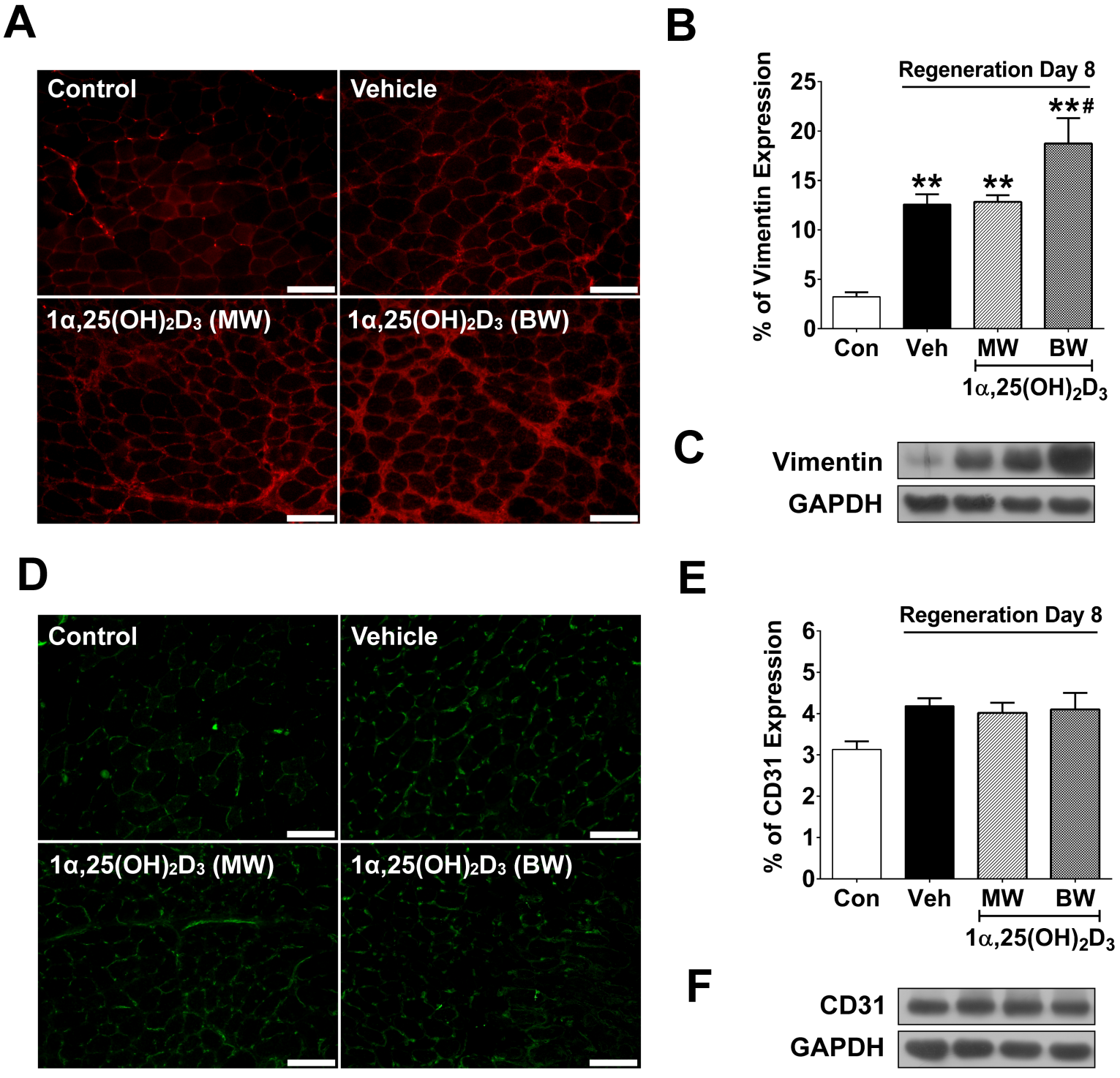
A
Control
Vehicle
1α,25(OH)2D3 (MW)
1α,25(OH)2D3 (BW)
B
Regeneration Day 8
% of Vimentin Expression
25
20
15
10
5
0
**
**
**#
Con
Veh
MW
BW
1α,25(OH)2D3
C
Vimentin
GAPDH
D
Control
Vehicle
1α,25(OH)2D3 (MW)
1α,25(OH)2D3 (BW)
E
Regeneration Day 8
% of CD31 Expression
6
5
4
3
2
1
0
Con
Veh
MW
BW
1α,25(OH)2D3
F
CD31
GAPDH

Figure 9